

# Open Research Online

---

The Open University's repository of research publications and other research outputs

## High Resolution Gene Expression Analysis in the Human Retina

### Thesis

How to cite:

Trifunović, Dragana (2008). High Resolution Gene Expression Analysis in the Human Retina. PhD thesis The Open University.

For guidance on citations see [FAQs](#).

© 2008 The Author

Version: Version of Record

---

Copyright and Moral Rights for the articles on this site are retained by the individual authors and/or other copyright owners. For more information on Open Research Online's data [policy](#) on reuse of materials please consult the policies page.

---

[oro.open.ac.uk](http://oro.open.ac.uk)



ProQuest Number: 13837705

All rights reserved

INFORMATION TO ALL USERS

The quality of this reproduction is dependent upon the quality of the copy submitted.

In the unlikely event that the author did not send a complete manuscript and there are missing pages, these will be noted. Also, if material had to be removed, a note will indicate the deletion.



ProQuest 13837705

Published by ProQuest LLC (2019). Copyright of the Dissertation is held by the Author.

All rights reserved.

This work is protected against unauthorized copying under Title 17, United States Code  
Microform Edition © ProQuest LLC.

ProQuest LLC.  
789 East Eisenhower Parkway  
P.O. Box 1346  
Ann Arbor, MI 48106 – 1346

## **Abstract**

Inherited retinal disorders are characterized by a remarkable genetic heterogeneity; so far, over 160 genes have been identified as responsible for this kind of diseases. Nevertheless, it is believed that the total number of retinal disease genes is much higher than what is currently known. Central to the first part of this PhD thesis was to identify new candidate genes for retinal disorders. The approach used to achieve this goal was based on *in silico* prediction of genes with exclusive or predominant retinal expression in human retina, followed by experimental verification of their predicted expression by both RT-PCR and RNA *in situ* hybridization. The work carried out for this part of the thesis provided a list of new candidate disease genes for inherited retinal disorders.

The second part of this PhD project aimed at the generation of a high resolution gene expression atlas of retinitis pigmentosa (RP) genes in human and murine retina. RP is one of the leading causes of visual handicap in the world population. The study of the disease mechanisms and the development of efficient therapeutic approaches have mostly relied on the availability of animal models for this condition, so far. Nevertheless, little information is available about the RNA expression profiles of RP genes in the human retina. To overcome this lack of information, I generated the first gene expression atlas of 34 known RP genes in human and murine retinas. Differences observed in the expression patterns of some genes in human and mouse will open new perspectives on the function of these genes and on their putative roles in disease pathogenesis.

## Table of contents

<b>ABSTRACT</b> .....	<b>I</b>
<b>TABLE OF CONTENTS</b> .....	<b>II</b>
<b>LIST OF FIGURES AND TABLES</b> .....	<b>V</b>
<b>ABBREVIATIONS</b> .....	<b>VIII</b>
<b>INTRODUCTION</b> .....	<b>1</b>
1.1 THE EYE AND THE RETINA.....	2
1.2 THE PHOTORECEPTORS .....	5
1.2.1 Phototransduction .....	7
1.2.2 The visual cycle pathway.....	10
1.3 INHERITED RETINAL DISEASES .....	12
1.3.1 Retinitis pigmentosa .....	13
1.3.1.1 Clinical aspects.....	13
1.3.1.2 Genetics of RP.....	16
1.4 NEW APPROACHES TO IDENTIFY ADDITIONAL RETINAL DISEASE GENES .....	23
1.5 FUNCTIONAL CHARACTERIZATION OF RETINAL DISEASE GENES.	27
1.6 AIMS OF THE THESIS.....	30
<b>MATERIALS AND METHODS</b> .....	<b>33</b>
2.1 BIOINFORMATIC ANALYSIS .....	34
2.1.1 <i>In silico</i> identification of human EST clusters predominantly expressed in retina.....	34
2.1.2 Identification and annotation of protein domains .....	34

---

2.2 SAMPLE PREPARATION .....	35
2.2.1 Genomic DNA extraction .....	35
2.2.2 RNA extraction .....	35
2.2.3 Synthesis of cDNA .....	36
2.2.4 Treatment of human and mouse eye bulbs .....	37
2.2.5 Hematoxylin/Eosin Staining .....	38
2.3 EXPRESSION STUDIES.....	38
2.3.1 Reverse Transcriptase Polymerase Chain Reaction RT-PCR.....	38
2.3.2 RNA in situ hybridization .....	39
2.3.2.1 Synthesis of cRNA probes .....	39
2.3.2.2 Transformation of <i>E.coli</i> with plasmid DNA.....	43
2.3.2.3 Isolation of plasmid DNA from <i>E.coli</i> .....	43
2.3.2.4 Linearization of the plasmids .....	44
2.3.2.4 In vitro cRNA transcription .....	44
2.3.2.5 RNA in situ hybridization on cryostat sections .....	45
2.3.3 Immunofluorescence .....	46
2.4 MUTATION ANALYSIS .....	47
2.4.1 Sample preparation for DHPLC analysis.....	47
2.4.2 DHPLC analysis .....	48
2.4.3 DNA sequence analysis .....	48
<b>RESULTS.....</b>	<b>49</b>
3.1 IDENTIFICATION OF PUTATIVE NOVEL HUMAN GENES WITH PREDOMINANT RETINAL EXPRESSION .....	50
3.1.1 In silico identification of human EST clusters predominantly expressed in retina .....	50

---

3.1.2 Expression studies of selected human cDNA clusters by RT-PCR ..	66
3.1.3 Expression studies of the selected human cDNA clusters by RNA in situ hybridization.....	71
3.1.4 Mutation analysis of the cDNA cluster Hs.131130 (KCNV2) .....	84
<b>3.2 GENERATION OF AN RP GENE EXPRESSION ATLAS .....</b>	<b>85</b>
3.2.1 CNGB1, USH2A and FSCN2 are expressed across all retinal cell layers.....	92
3.2.2 RNA in situ hybridization expression profiles of the RGR, RLBP1 and CA4 genes.....	98
3.2.3 RPGR and PAP1 genes show prevalent expression in human photoreceptors .....	102
<b>DISCUSSION .....</b>	<b>105</b>
4.1 IDENTIFICATION OF HUMAN GENES WITH PREDOMINANT RETINAL EXPRESSION.....	106
4.2 GENERATION OF THE RP GENE EXPRESSION ATLAS.....	115
<b>REFERENCES .....</b>	<b>124</b>
<b>ACKNOWLEDGMENTS .....</b>	<b>145</b>

## List of figures and tables

Figure 1. Schematic view of the human eye anatomy .....	3
Figure 2. 3-D block portion of human retina .....	4
Figure 3. Schematic diagram of rod and cone photoreceptor cells.....	6
Figure 4. Details of phototransduction in rod photoreceptors .....	9
Figure 5. Diagram showing all the proteins involved in the visual cycle in rod photoreceptors and RPE .....	10
Figure 6. Visual field of a healthy person compared to that of a retinitis pigmentosa patient .....	14
Figure 7. Ophthalmoscopic findings observed in RP .....	15
Figure 8. Electroretinogram measurements .....	16
Figure 9. Mutation prevalence of RP genes .....	17
Figure 10. Schematic view of rod photoreceptor cell with annotated functions of the genes known to cause isolated form of RP .....	19
Figure 11. Schematic outline of the strategy undertaken to identify new candidate genes for human retinal dystrophies .....	51
Figure 12. Example of a Unigene query for EST clusters with restricted expression in human eye cDNA libraries.....	52
Figure 13. Examples of the RT-PCR analysis performed for the selected thirty cDNA clusters.....	67
Figure 14. Optimization of the procedure for the handling of human eye sections for RNA in situ hybridization experiments.....	74
Figure 15. Expression analysis of clusters Hs.21162 and Hs.433492.....	78
Figure 16. Expression analysis of clusters Hs.449884 and Hs.33102.....	79
Figure 17. Expression analysis of clusters Hs.131130 and Hs.69749.....	81



---

Figure 18. Expression analysis of clusters Hs.295015 and Hs.221513.....	83
Figure 19. Evaluation of the possible influence of post-mortem time on RNA ISH findings in the human eye.....	88
Figure 20. RT-PCR analysis of MERTK expression. ....	89
Figure 21. Examples of genes with similar RNA ISH expression patterns in human and murine eyes.....	90
Figure 22. Schematic view of the information accessible from the RP gene expression atlas database ( <a href="http://www.tigem.it/RPexp/">http://www.tigem.it/RPexp/</a> ) for each analyzed gene .....	91
Figure 23. Localization of CNGB1, USH2A, and FSCN2 mRNA in human and mouse retinas.....	93
Figure 24. NRL expression profile .....	95
Figure 25. Expression profiles of Cngb1, Fscn2 and Ush2A genes in wild type and mutant mouse retinas.....	97
Figure 26. Expression profiles of RGR, RLBP1 and CA4 genes .....	99
Figure 27. RLBP1 protein localization in human retina.....	101
Figure 28. RPGR and PAP1 mRNA distribution .....	103
Table 1. Information about eye donors.....	37
Table 2. List of the primers used for RT-PCR analysis, annealing temperatures for each primer pair and size of the obtained products.....	39
Table 3. Information about the source used to obtain cDNA templates, template size and RNA ISH hybridization temperature used for each analyzed gene .....	40
Table 4. List of the oligonucleotide primer pairs for the KCNV2 mutation analysis .....	47

*Table 5. List of all the EST clusters retrieved from the Unigene database ..... 54*

*Table 6. cDNAs selected for experimental validation of predominant retinal  
expression by RT-PCR..... 68*

*Table 7. RT-PCR and RNA ISH expression analysis of the selected fifteen  
cDNA clusters in human retina ..... 75*

*Table 8. Summary of the RNA in situ hybridization expressions in human and  
mouse retinas..... 86*

---

## **Abbreviations**

AMD age-related macular degeneration

bp base pairs

CD cone dystrophy

cGMP cyclic guanosine monophosphate

DHPLC denaturing high performance liquid chromatography

DIG digoxigenin

dNTP deoxyribonucleotide triphosphate

DTT dithiothreitol

ERG electroretinogram

ESTs expressed sequence tags

GCL ganglion cell layer

GDP guanosine diphosphate

GTP guanosine triphosphate

INL inner nuclear layer

IS inner segment

LB Luria broth

LCA Leber congenital amaurosis

mRNA messenger RNA

MUT mutant

ONL outer nuclear layer

OS outer segment

PBS phosphate buffered saline

PFA paraformaldehyde

PR photoreceptors

RNA ISH RNA *in situ* hybridization

RNA ribonucleic acid

RP retinitis pigmentosa

RPE retinal pigment epithelium

RT-PCR reverse transcriptase-polymerase chain reaction

WT wild type

# *Introduction*

---

## 1.1 THE EYE AND THE RETINA

The eye is perhaps the most important sensory organ for humans and vision is by far the most complex of the senses. This is due to the fact that vision must handle demands such as: transduction of light stimuli to neural impulses, binocular and more distant depth perception, and color discrimination.

The structure of the human eye (Figure 1) can be divided into three main layers or tunics whose names reflect their basic functions: the fibrous tunic, the vascular tunic, and the nervous tunic. The fibrous tunic, also known as the *tunica fibrosa oculi*, is the outer layer of the eyeball consisting of the cornea and sclera. It consists of dense connective tissue filled with collagen to both protect the inner components of the eye and maintain its shape. The vascular tunic, also known as the *tunica vasculosa oculi*, is the middle vascularized layer, which includes the iris, ciliary body, and choroids. The iris sits between the anterior chamber and the posterior chamber in the front part of the eye. These chambers contain the aqueous humour, which is important for nourishing the lens and the cornea. The lens is a clear, flexible structure responsible for sharpening of the image at the retina and is connected to the ciliary body that contains the ciliary muscles. Functions of the ciliary body are represented by the production of aqueous humor and by an important contribution in the control of the accommodation by changing the shape of the lens. The vitreous humour is a jelly-like substance that fills the back portion of the eye behind the lens. Besides helping the eye to keep its shape, this clear gel transmits light to the back of the eye. The choroid contains blood vessels that supply the retinal cells with necessary oxygen and remove the waste products of respiration. The nervous tunic, also known as the *tunica nervosa oculi*, is the inner sensory structure, which includes the retina.

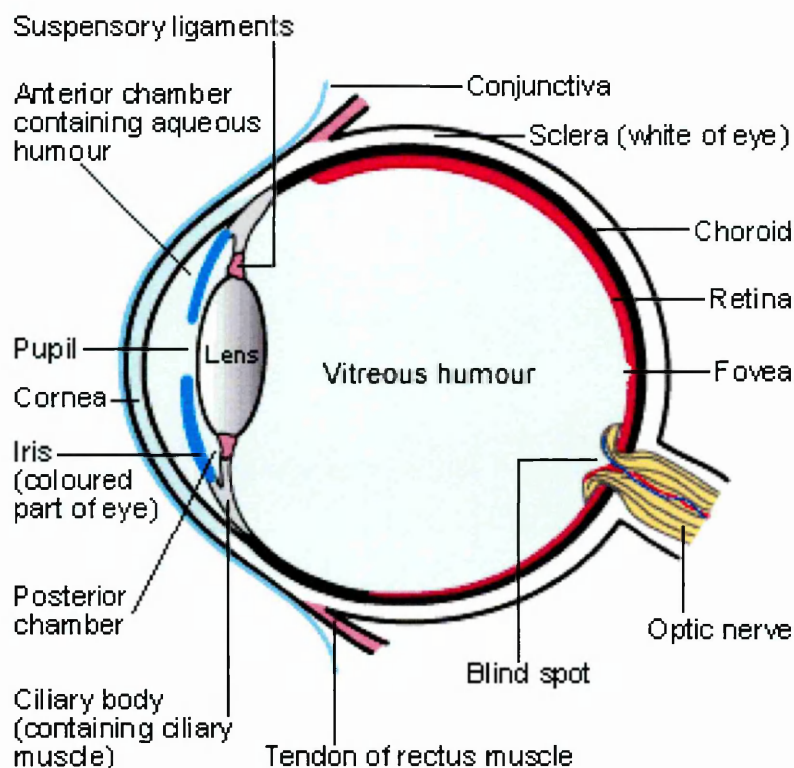


**Figure 1. Schematic view of the human eye anatomy.**

Retina is a highly organized eye compartment where light transduction into neural impulses takes place. Due to the complexity of this process, retinal cells give rise to a variety of neuronal cell types that are involved in the transmission of the nervous stimuli to the brain. Retina is composed of seven classes of cells: photoreceptor cells (rods and cones), bipolar cells, horizontal cells, amacrine cells, Müller glia cells and retinal ganglion cells and they are organized in six layers each of which is responsible for a certain function (Figure 2). The outermost layer is the retinal pigment epithelium (RPE), which is situated between the choroid and the photoreceptors. RPE is involved in the phagocytosis of the outer segment of photoreceptor cells and in the chromophore regeneration (see below). RPE cells are pigmented and therefore play a function in preventing light scattering.

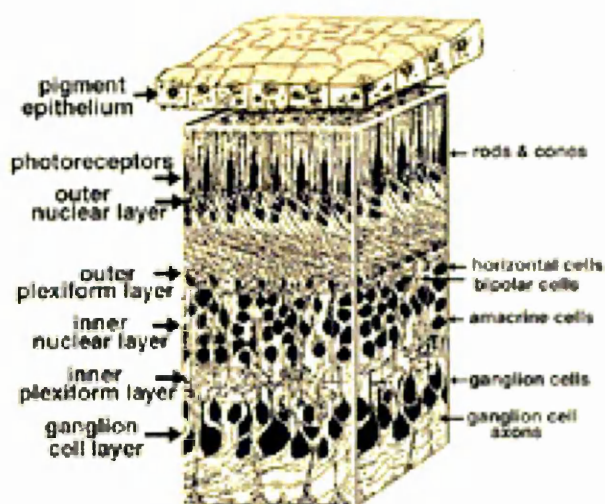


**Figure 2. 3-D block portion of human retina** (from <http://webvision.med.utah.edu>). Diagram depicting retinal cell types organized in layers either composed by cell bodies or by cell processes.

The second layer, the photoreceptor layer, comprises the photoreceptors, where the photoreceptor cell bodies form the outer nuclear layer (ONL). At the synaptic terminals of photoreceptors, in a region called the outer plexiform layer (OPL), light-induced signals are transferred from rods and cones to bipolar and horizontal cells. Cell bodies of these neurons together with Müller glia and amacrine cells form the structure called the inner nuclear layer (INL). Horizontal cells provide lateral interaction in the OPL and aid in signal processing. One type of rod bipolar cells and at least 10 different types of cone bipolar cells transfer light-induced signals to the ganglion cells at the inner plexiform layer (IPL), which also comprises dendrites of amacrine cells and ganglion cells. Amacrine cells are inhibitory interneurons, and about 40 different morphological types are described even though the function of the majority of subtypes is still not clear. Müller cells are the main glial cells of the retina. They form architectural support structures stretching radially across the entire thickness of the retina and set the limits of the retina at the outer and inner limiting membranes, respectively. The ganglion cell layer (GCL) forms the innermost



retinal layer. Ganglion cell dendrites collect the signals of bipolar and amacrine cells and transmit these signals through their axons to the visual centers of the brain<sup>1</sup>. Axons of the different ganglion cells of the retina converge at the level of the optic disc and exit the eye bulb to form the optic nerve.

## **1.2 THE PHOTORECEPTORS**

Perception of light initiates in the highly specialized retinal cells called photoreceptors. Photoreceptors are polarized retinal neurons with the unique property of transforming physical signals (photons of light) first into biochemical messages and then into action potentials “perceived” by specialized brain structures (visual cortex). Photoreceptors contain four distinct compartments: *a*) the outer segment (OS), *b*) a thin cilium, which connects the outer to the *c*) inner segment (IS), a cell body containing the nuclei and the cytoplasm and *d*) a short axon connecting the photoreceptor cell to interneurons (Figure 3). The OS consists of an array of flat membranous disks, in which the phototransduction cascade occurs, whereas the IS contains most of the photoreceptor metabolic machinery, including the endoplasmic reticulum, the Golgi apparatus, and the mitochondria. Cellular components and metabolites are exchanged and/or transported between the IS and OS through the narrow connecting cilium<sup>2</sup>. The connecting cilium of photoreceptor cells is the only intercellular link between the morphologically, functionally and biochemically different compartments of the inner and outer segment. The cilium plays an important role in the organization and the function of photoreceptor cells, namely in delivery and turnover of enzymes and substrates of the visual transduction cascade, and the photosensitive membranes of the outer segment. The protein components of the cilium participate in the intracellular transport through the cilium, in the outer

segment disk morphogenesis and in the maintenance of discrete membrane domains<sup>3</sup>.

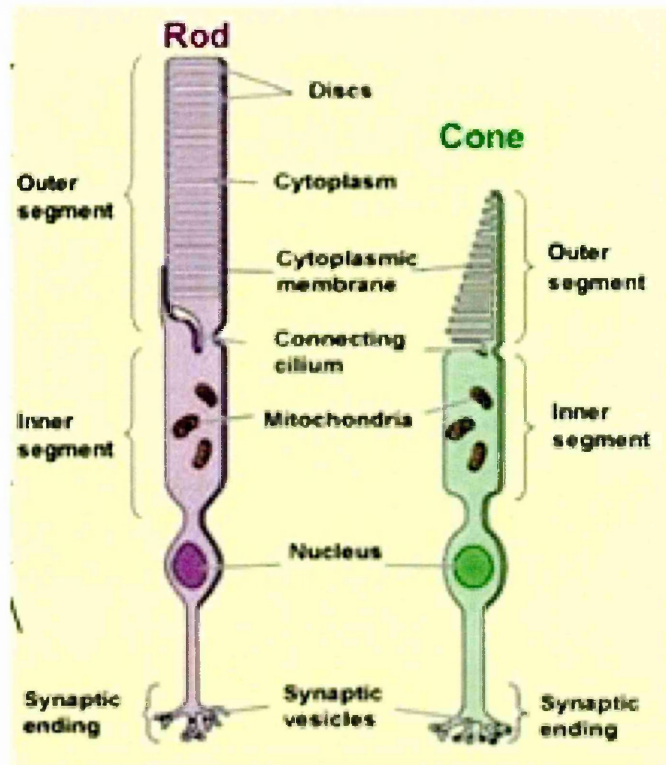


**Figure 3. Schematic diagram of rod and cone photoreceptor cells.**

There are two types of photoreceptor cells in the human retina: rods and cones. Rods represent about 95% of photoreceptor cells in the human retina and are responsible for sensing contrast, brightness and motion, while fine resolution, spatial resolution and color vision are perceived by cones. Humans have three types of cones that contain different visual pigments and are referred as blue, green, and red, or, respectively, short, medium and long wavelength sensitive cones. In the human retina, the majority of cones are concentrated in the central part of the macula (called fovea), which is the retinal structure characterized by the highest density of cone photoreceptors.

### 1.2.1 Phototransduction

As already mentioned, transduction of absorbed light into electrical signal that is eventually perceived as sight, takes place within photoreceptor cells via a complex molecular process called phototransduction. Within rod cells, phototransduction initiates with the absorption of light by rhodopsin. Rhodopsin is the photopigment that accounts for 85% of the total amount of rod outer segment proteins<sup>4</sup>. It is composed of a protein backbone, termed rod-specific opsin, a seven transmembrane G-protein-coupled receptor, bound to the light-sensitive chromophore 11-*cis*-retinal<sup>5</sup>. The absorption of a single photon by the chromophore (11-*cis*-retinal) induces a rhodopsin conformational change. The chromophore undergoes photoisomerization to all-*trans* retinal, inducing a correspondent change in the opsin from its inactive to its active conformation<sup>5</sup>. The active form, known as Metarhodopsin II, subsequently catalyzes the activation of the G-protein transducin<sup>6</sup>. Transducin is a multisubunit peripheral membrane protein consisting of three subunits:  $\alpha$ ,  $\beta$  and  $\gamma$ . The  $\alpha$  subunit contains a binding site for GTP or GDP and a catalytic site for the hydrolysis of bound GTP. The  $\alpha$  subunit is associated with  $\beta$ , and  $\gamma$  subunits when GDP is bound (the inactive dark state), whereas they are separate when GTP is bound (the light-activated state). In the dark, nearly all of the transducin molecules are in the inactive state, bound to GDP. Following illumination inactive transducin encounters Metarhodopsin II within disc membranes. Metarhodopsin II induces the release of GDP from transducin and allows GTP to enter. Metarhodopsin II-transducin-GTP then dissociates into transducin  $\alpha$  subunit-GTP, transducin  $\beta$  and  $\gamma$  subunits, and Metarhodopsin II. GTP bound to  $\alpha$  subunit carries the excitation signal to *PDE* (see below), and Metarhodopsin II is free again to catalyze another round of GTP-GDP exchange<sup>7</sup>. During this stage, the signal is

amplified by the activation of hundreds of transducin molecules by a single activated rhodopsin. The free alpha subunit of transducin, stimulates cyclic guanosine monophosphate phosphodiesterase (*PDE*). Similarly to transducin, the phosphodiesterase consists of  $\alpha$ ,  $\beta$  and two  $\gamma$  subunits. The  $\alpha$  and  $\beta$  catalytic subunits of *PDE* are kept inhibited in the dark by the  $\gamma$  subunits. Upon activation of *PDE*,  $\gamma$  subunits dissociate thus enabling the activation of the catalytic subunits to hydrolyze cyclic guanosine monophosphate (cGMP)<sup>8</sup>. The resulting decrease in cGMP concentration closes the cGMP-gated cation channels (*CNG*) in the photoreceptor plasma membrane<sup>9</sup>. In the dark, these channels actively transport sodium and calcium ions into the cell, while other channels maintain a continuous efflux of sodium maintaining a depolarized status. Closure of the channels, in response to light, disrupts the influx, while the efflux of sodium and calcium continues undisturbed. The decline in sodium concentration leads to hyperpolarization of the entire cell membrane, which results in decreased release of the neurotransmitter (glutamate) at the synaptic terminal<sup>10</sup>. The processes involved are schematically shown in Figure 4.

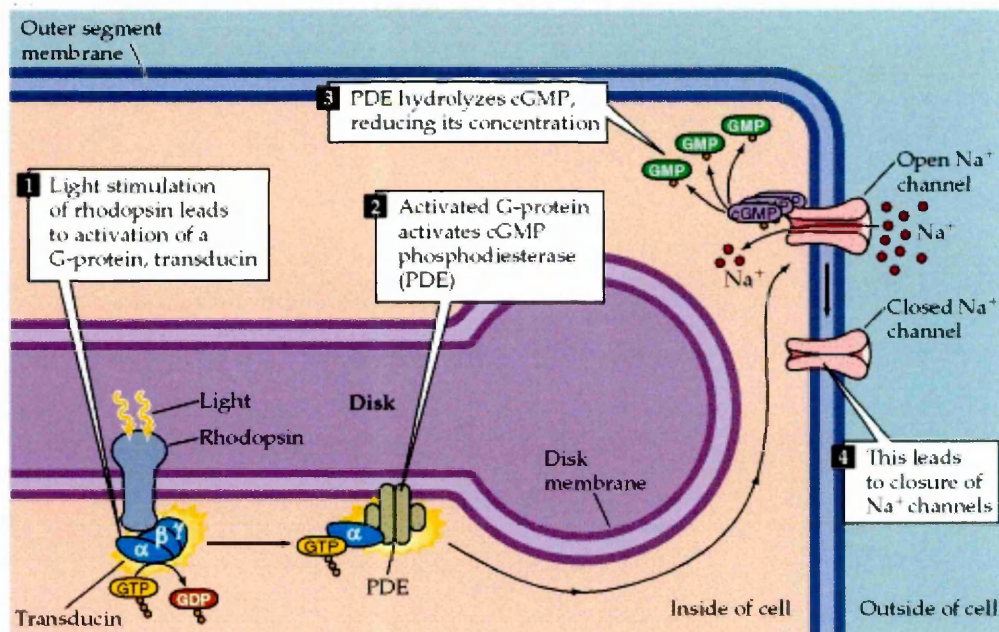


**Figure 4. Details of phototransduction in rod photoreceptors** (from Purves et al., *Neuroscience*, 2001).

The decline in calcium concentration mediates the recovery of the photoreceptor cell after a bleach of light. This is as important for maintaining sensitivity in vision as the cell's ability to respond to a single photon. Deactivation of rhodopsin starts with its phosphorylation by rhodopsin kinase and is followed by the capture of rhodopsin by the protein arrestin<sup>9</sup>. The arrestin-binding prevents further activation of transducin and releases the all-*trans*-retinal from rhodopsin. The concentration of cGMP within the cell is restored by the increased synthesis of cGMP by a retinal guanylate cyclase (*RetGC*). These pathways are triggered by the decline in the intracellular calcium concentration and mediated by a family of calcium-binding proteins, including recoverin and guanylyl cyclase activating protein (*GCAP*). The calcium-bound recoverin inhibits the activity of rhodopsin kinase<sup>11</sup>. Sustained phototransduction depends on replenishing the 11-*cis* retinal lost as a result of light activation of the visual pigments. Recycling of the vitamin A analogs (11-*cis*

retinal) takes place between the photoreceptor cells and the RPE, in a process called visual cycle<sup>12</sup>.

### 1.2.2 The visual cycle pathway

Absorption of a photon of light by rhodopsin causes isomerisation of the chromophore from 11-*cis*-retinal to all-*trans*-retinal. In order to restore light sensitivity of rhodopsin, all-*trans*-retinal must be converted back to 11-*cis*-retinal through a multistep pathway called visual cycle (Figure 5). Visual cycle initiates in the photoreceptor cells, precisely in the inner surface of the rod disks membrane, with the release of all-*trans*-retinal which is subsequently transferred to the cytoplasmic surface of the disks by the retina-specific ATP-binding cassette transporter (*ABCA4*)<sup>13, 14</sup>.

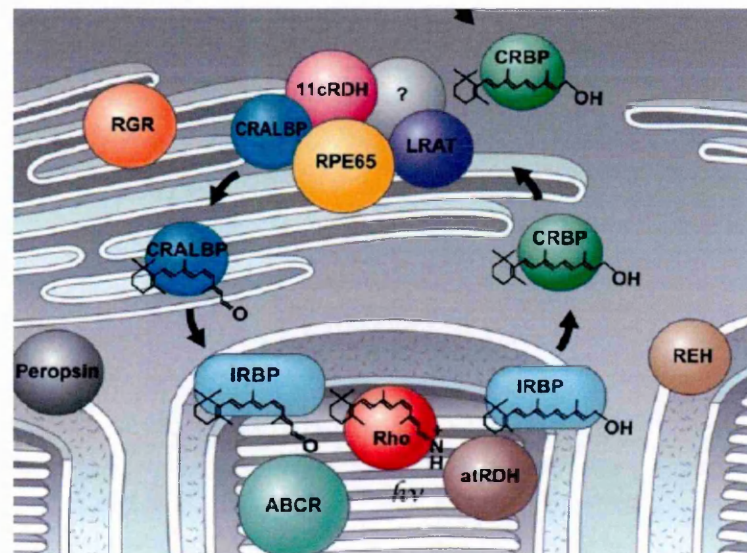


**Figure 5. Diagram showing all the proteins involved in the visual cycle in rod photoreceptors and RPE (from Thompson and Gal, Progress in retinal and eye research, 2001).**

In the photoreceptor cytoplasm, all-*trans* retinal is reduced by an all-*trans* retinol dehydrogenase (*RDH*) from the family of short chain acyl-CoA dehydrogenase/reductase(s) and the resulting all-*trans* retinol is transported

across the subretinal space to the RPE<sup>15</sup>. All-*trans* retinol is also supplied to the RPE by the choroidal vasculature, entering the RPE in a receptor-mediated process involving recognition of a serum retinol-binding protein/transthyretin (RBP/TTR) complex<sup>16</sup>. Within the RPE, all-*trans* retinol is bound to the cellular retinal binding protein (CRBP)<sup>17</sup>. The conversion of vitamin A to 11-*cis* retinal requires at least three enzymes associated with the RPE smooth endoplasmic reticulum, as well as *RPE65*, a unique RPE-specific protein. The first enzyme, lecithin retinol acyltransferase (*LRAT*), esterifies all-*trans* retinol to phosphatidylcholine in the lipid bilayer to form all-*trans* retinyl esters<sup>18</sup>. The second enzyme, retinoid isomerase, generates the 11-*cis* double bond in the aliphatic side chain. This enzyme is also referred to as isomerohydrolase, as it has been proposed to catalyze the concerted hydrolysis of all-*trans* retinyl ester and the isomerization to 11-*cis* retinol<sup>19</sup>. *RPE65* is also required for the isomerization reaction<sup>20</sup>, but it has not been shown to have intrinsic isomerase activity. The third enzyme, 11-*cis* retinol dehydrogenase (*11cisRDH*), encoded by the *RDH5* gene, converts 11-*cis* retinol to the final product 11-*cis* retinal<sup>21</sup> in a reaction that is accelerated by the presence of the cellular retinaldehyde-binding protein (*CRALBP*)<sup>22</sup>. Alternatively, 11-*cis* retinol can be esterified and stored in the RPE as 11-*cis* retinyl esters. The 11-*cis* retinal exits the RPE, traverses the subretinal space, and enters the photoreceptor outer segments where it combines with the opsin protein to form the visual pigments. Alternatively, 11-*cis*-retinal could be produced by direct photoisomerization of all-*trans*-retinal with the help of retinal G-protein-coupled receptor protein (*RGR*) in RPE and Müller cells<sup>11, 20, 21</sup>.

---

### **1.3 INHERITED RETINAL DISEASES**

The complex retinal structure, and signaling network which includes numerous neurotransmitters, neuromodulators, phototransduction proteins, transcription factors, etc., lead to a wide range of targets for potential events that may cause pathogenic changes in its function. According to some estimates<sup>23</sup> the eye is the fourth most common system affected by genetic diseases in man. At the same time, genetic eye diseases, both monogenic and genetically complex, comprise the commonest causes of blindness in children and adults in the developed world<sup>24</sup>. Among all the different eye diseases, retinal disorders are especially relevant. In the industrialized world, the most common diseases involving the retina are diabetic retinopathy, glaucoma, and age-related macular degeneration (AMD), which together affect a high percentage of the population<sup>25</sup>. Each of these diseases has both genetic and non-genetic components but they can be overall considered as multifactorial disorders. Compared to complex diseases, simple monogenic retinal diseases, i.e., diseases in which mutations in a single gene are responsible for the observed phenotype, are less frequent, tend to have an earlier onset and a more severe clinical course and are generally untreatable. Due to these characteristics, together with the possibility of exploiting genetic approaches to understand disease mechanisms that can be transferred to the more complex disorders, the scientific community devoted considerable research efforts in the past twenty years to the study of the molecular basis of retinal monogenic disorders, in spite of their relative lower frequencies versus complex diseases. Overall, there are more than 100 different forms of inherited retinal dystrophies, either isolated or syndromic, as listed in the online database of human genetic diseases (Online Mendelian Inheritance in Man-OMIM). Retinitis pigmentosa is by far the most



studied inherited retinal disease and represents an example of the remarkable genetic heterogeneity connected with retinal dystrophies.

### **1.3.1 Retinitis pigmentosa**

#### **1.3.1.1 Clinical aspects**

Retinitis pigmentosa (RP) is one of the leading causes of inherited visual handicap in the working population with a prevalence of 1:3500<sup>26</sup>, while a congenital form of retinal dystrophy, Leber congenital amaurosis (LCA), is the most prevalent cause of hereditary visual handicap in children<sup>27</sup>. The term retinitis pigmentosa is used to describe a set of hereditary retinal diseases that feature degeneration of primarily rod and subsequently cone photoreceptors. From a clinical point of view, it is a highly variable disorder starting from the age of onset, with some patients developing symptomatic visual loss in childhood and others remaining asymptomatic until mid-late adulthood. The most frequently observed clinical pattern is represented by, initially, difficulties in dark adaptation and night blindness (usually in the adolescence) and loss of mid-peripheral visual field in young adulthood. As the disease advances, RP patients lose far peripheral vision, subsequently develop tunnel vision (Figure 6), and finally lose also the central vision, usually by the age of sixty years<sup>28</sup>.

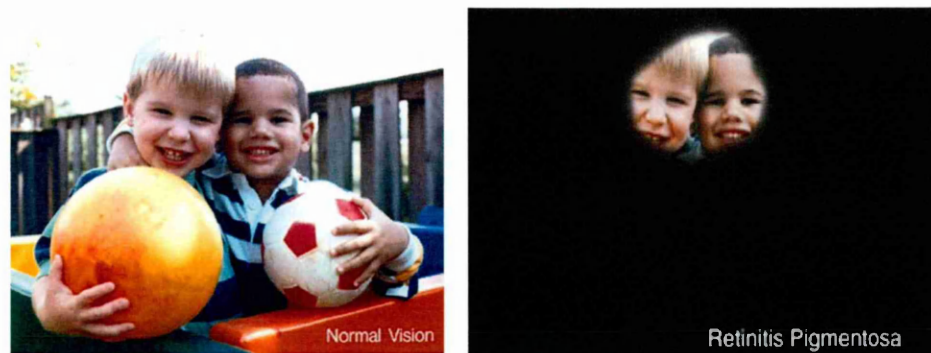


**Figure 6. Visual field of a healthy person compared to that of a retinitis pigmentosa patient** (from <http://webvision.med.utah.edu/>).

Clinically, RP patients are diagnosed based on three main abnormalities: atrophy and pigmentary changes of the retina and the RPE, abnormal electroretinogram (ERG) and attenuation of the retinal vasculature and changes to the optic nerve head<sup>29</sup>. The pigmentary changes remain a common factor in RP diagnoses. Typically, these result from the release of pigment by degenerating cells in the retinal pigment epithelium. The pigment granules accumulate in perivascular clusters, known as “bone-spicule formations” due to their morphological appearance, in the neural retina. Consequently, early in the disease, the pigmented posterior pole of the eye, the fundus, develops a granular appearance. This is followed by the development of bone-spicule pigmentary deposits overlying the depigmented fundus<sup>30</sup> (as shown in Figure 7).

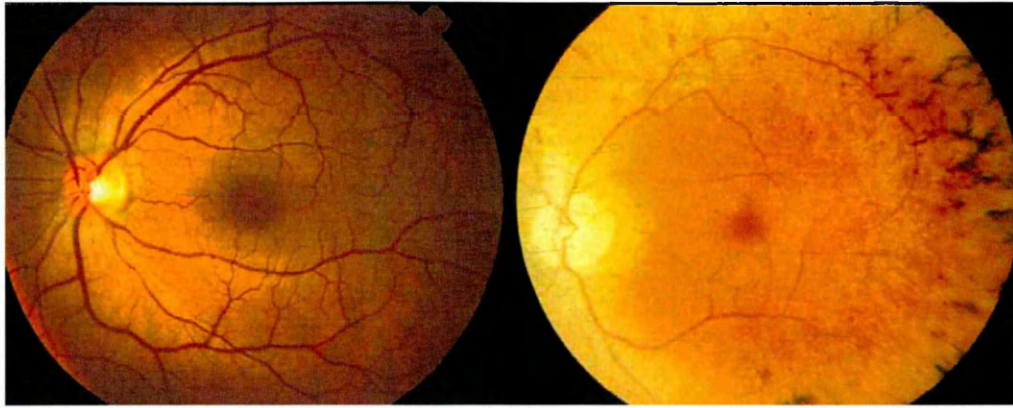


**Figure 7. Ophthalmoscopic findings observed in RP.** Fundus oculi examination of a healthy individual (left) and of a patient with retinitis pigmentosa (right).

In the image of the diseased eye, optic-disc pallor, attenuated retinal arterioles, and peripheral intraretinal pigment deposits in a bone-spicule configuration are seen (from Hartong, D.T. et al., 2006).

Electroretinogram is the main tool for diagnosis and classification of retinitis pigmentosa. In this procedure, photoreceptor cells are either dark adapted (scotopic ERG) or adapted to a specific level of light (photopic ERG), and then stimulated with a brief flash of light. The summed electrical response of the retina is recorded extraocularly with a contact lens electrode. The scotopic ERG selectively measures the response of the rod photoreceptor cells, while the photopic ERG measures that of the cones. In typical RP, the rod loss manifests initially as alterations (decreased amplitude) of the scotopic ERG and shows a proportional loss of the photoreceptor cell and post-photoreceptor components of the ERG<sup>29</sup> (Figure 8).

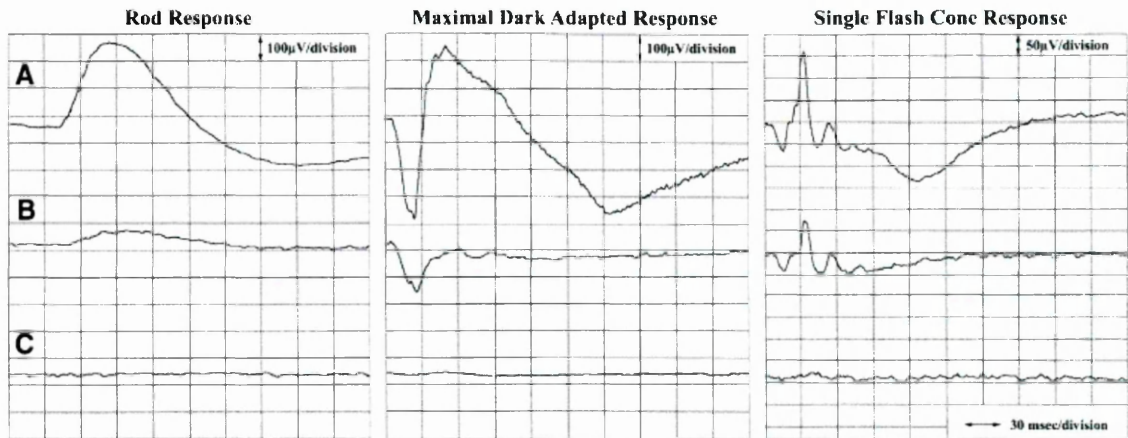


**Figure 8. Electretinogram measurements.**

ERG measurements of rod-isolated, combined rod and cone responses in dark adapted state and cone response in light-adapted state from normal individual (A), a patient with moderately advanced RP (B) and a patient with advanced RP (C) (from Farrar J. et al., 2002).

### 1.3.1.2 Genetics of RP

Retinitis pigmentosa can be inherited in all the main modes of inheritance, i.e., autosomal dominant (about 15-25% of cases), autosomal recessive (5-20%), X-linked (5-15%) and mitochondrial<sup>29, 31</sup>. However, the majority of patients (50%) are apparently sporadic. Schematic classification of all the RP genes divided by the mode of inheritance with annotated approximate contribution to the disease is shown in Figure 9. In most cases, patients with retinitis pigmentosa have no associated systemic or extraocular abnormalities. Nevertheless, there are multisystem diseases, such as Usher and Bardet-Biedl syndromes, in which RP is accompanied by symptoms in other tissues and organs. Usher's syndrome, in which retinitis pigmentosa is associated with hearing impairment, is the most frequent syndromic form of RP<sup>32</sup>, while in Bardet-Biedl syndrome, retinitis pigmentosa is associated with obesity, cognitive impairment, polydactyly, hypogonadism, and renal disease<sup>33</sup>. As mentioned previously, a remarkable

feature of retinitis pigmentosa is its high genetic heterogeneity: so far, more than 50 genes responsible for non-syndromic forms have been mapped (RetNet: <http://www.sph.uth.tmc.edu/Retnet/>). And what is even more astonishing is the functional diversity of the types of gene that have been implicated in retinal degeneration.

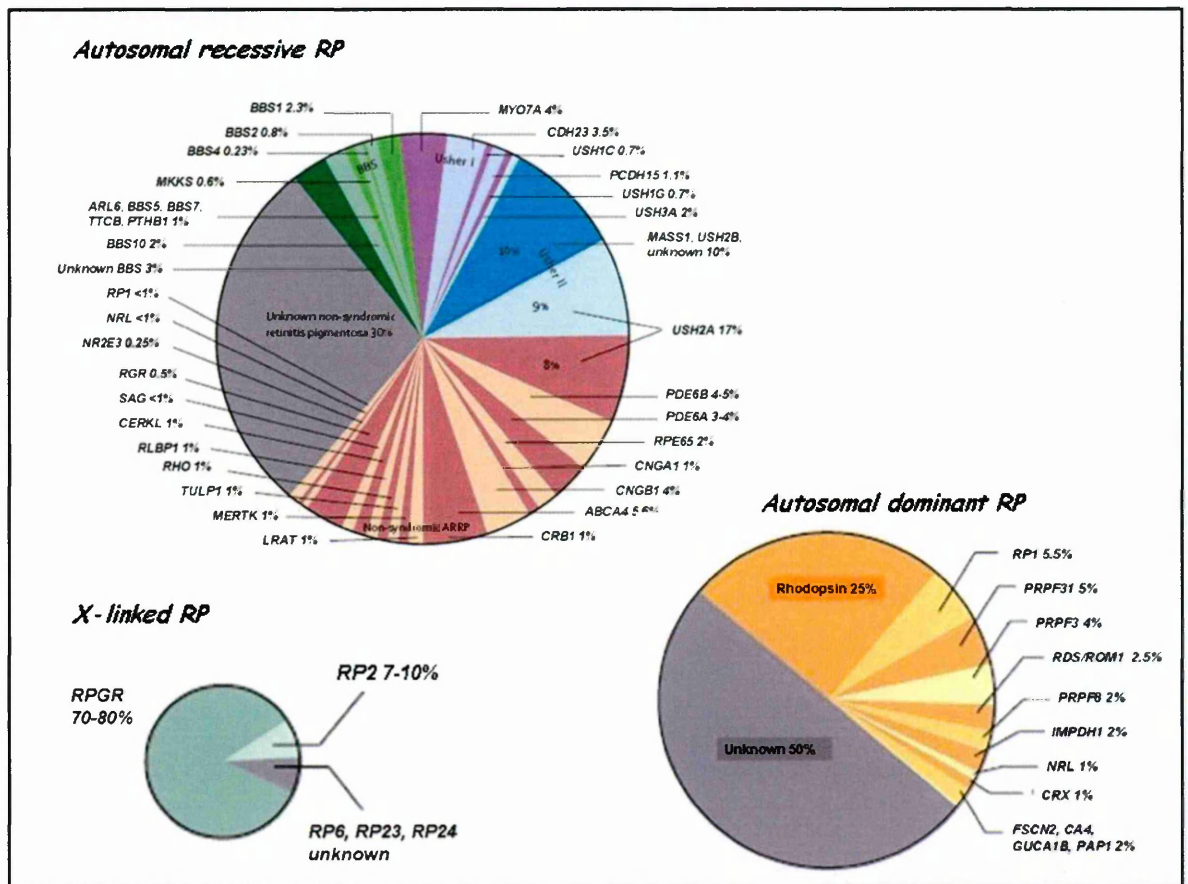


**Figure 9. Mutation prevalence of RP genes.**

Diagrams listing all currently known RP genes, including those responsible for Usher and Bardet-Biedl syndromes, divided by their patterns of inheritance and showing their relative contribution to retinitis pigmentosa in the human population (from Hartong D et al., 2006.).

The currently known RP genes can be classified based on their predicted functional activities, in the following groups: members of the phototransduction cascade, members of the visual cycle pathway, transcription factors, splicing factors, photoreceptor structural proteins, genes involved in protein folding or trafficking and pH balance (as schematically depicted in Figure 10).

### 1.) Phototransduction Cascade:

As mentioned earlier, the signal transduction pathway in the eye transforming light into an electrical signal is known as phototransduction cascade. It is a highly complex process involving a number of genes, which are well characterized, although the possibility exists that additional regulatory proteins remain to be discovered. Almost all of the proteins participating in phototransduction have been shown to be associated with different kinds of inherited retinal degeneration diseases. The first gene to be discovered was rhodopsin (*RHO*) which was cloned and mapped in 1984<sup>34</sup>. Since then, more than 100 different mutations in *RHO* have been identified, accounting for approximately 30% of all autosomal dominant retinitis pigmentosa<sup>24</sup>. In addition to *RHO*, other phototransduction genes have been shown to be responsible for different human retinal diseases, including alpha and beta subunits of phosphodiesterase (*PDE6A*, *PDE6B*)<sup>35, 36</sup>, cyclic nucleotide gated cation channel (*CNG*)<sup>37</sup> and arrestin (*SAG*)<sup>38</sup>. Besides these genes directly involved in phototransduction cascade, two other genes which are indirectly involved in the process are also shown to be mutated in the RP, guanylate cyclase activating protein 1B (*GUCA1B*)<sup>39</sup> and inosine monophosphate dehydrogenase 1 (*IMPDH1*)<sup>40</sup>. *GUCA1B* activates guanylate cyclase in the low  $Ca^{2+}$  concentration after photobleaching in order to increase cGMP concentration<sup>41</sup>, while *IMPDH1*

is responsible for the production of guanine nucleotides within photoreceptor cells<sup>42</sup>.

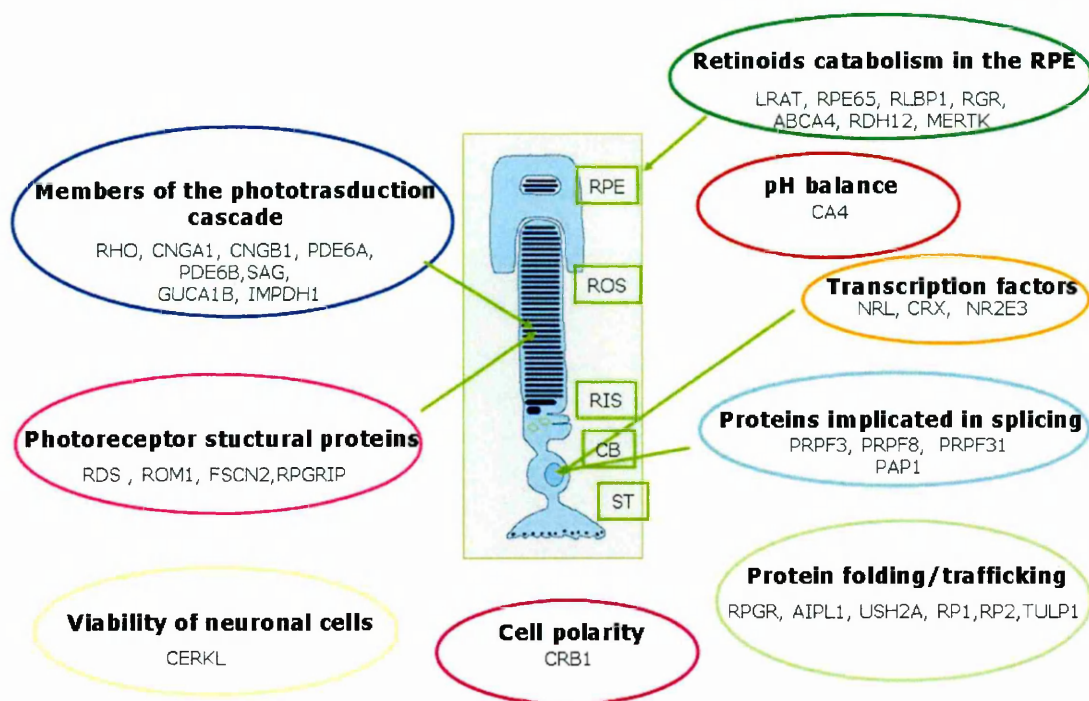


**Figure 10. Schematic view of rod photoreceptor cell with annotated functions of the genes known to cause isolated form of RP.**

RPE-retinal pigment epithelium, OS-rod outer segment, IS-rod inner segment, CB-cell body, ST-synaptic terminus.

## 2.) Visual cycle:

The second common group of genes mutated in RP comprises those encoding proteins of the visual cycle. It has been shown that the following members of the visual cycle pathway are mutated in RP:

-*ABCA4*<sup>43, 44</sup>, which accounts for about 5-6% of recessive RP;

-*RLBP1*<sup>45</sup>, *RPE65*<sup>46, 47</sup>, *RGR*<sup>48</sup> and *LRAT*<sup>49</sup> all involved in recessive forms of RP or Leber congenital amaurosis, with *RLBP1* and *LRAT* accounting for 1% of cases, *RGR* for 0,5 % and *RPE65* for 2%<sup>28</sup> (see Figure 9).

Another gene indirectly involved in the visual cycle pathway is the c-mer protooncogene receptor tyrosine kinase (*MERTK*), which is responsible for phagocytosis of the shed photoreceptor outer segments and was also shown to cause recessive RP<sup>50</sup>.

### 3.) Photoreceptor Structure:

Three genes important for maintenance of the highly organized photoreceptor structure were found to be mutated in RP, so far: *RDS*, *RPGRIP*, and *FSCN2*. Peripherin (*RDS*) is a membrane glycoprotein in the disc rim region of the rod and cone outer segment with an important function in discs assembly, orientation and stability<sup>51</sup> and when mutated causes dominant RP. The RPGR-interacting protein (*RPGRIP*), responsible for Leber congenital amaurosis<sup>52</sup> is a structural component of the ciliary axoneme with a suggested role in disk morphogenesis<sup>53</sup>. In 2001 Wada et al. identified a mutation in the retinal fascin homolog 2 (*FSCN2*) in all fourteen patients from four Japanese families with autosomal recessive RP<sup>54</sup>. Fascin is an actin-bundling protein with a putative function in regulation of outer segment disk morphogenesis and photoreceptor shortening<sup>55</sup>. Nevertheless, Zhang et al. subsequently showed that the same *FSCN2* mutation is not associated with hereditary retinal degeneration in Chinese individuals putting into question whether or not *FSCN2* is indeed an RP causing gene<sup>56</sup>.

### 4.) Transcription factors:

Several transcription regulatory proteins are essential for ocular development<sup>23</sup>,<sup>57</sup> but few of them are expressed specifically in the retina. So far, only three transcription factor genes, *CRX*, *NRL* and *NR2E3*, have been found to cause



retinal diseases in humans. *NRL* and *CRX*, which synergistically control expression of photoreceptor cell-specific genes<sup>58</sup>, are known to be mutated in RP<sup>59, 60</sup>. The mutations appear both to interfere with photoreceptor cell development and, much later in life, with photoreceptor survival<sup>58-64</sup>. Recently, also *NR2E3* was shown to be mutated in autosomal dominant RP<sup>65</sup>. It was suggested that *NR2E3* may be involved in regulating the expression of rod photoreceptor-specific genes and may play a role in transcriptional regulatory network(s) during rod differentiation<sup>66</sup>.

#### 5.) Splicing factors:

Interestingly, some genes for retinitis pigmentosa encode proteins that are essential for life. Recently it has been found that the ubiquitously expressed pre-mRNA splicing factors *PRPF3*, *PRPF31*, *PRPF8*, and *PAP1* are involved in the pathogenesis of RP<sup>67-70</sup>. These genes encode components of the spliceosome, a vital complex that excises introns from primary RNA transcripts. These proteins are highly conserved in eukaryotes ranging from mammals to yeast, so the fact that mutations in these factors are detrimental only for rods leading to RP without apparently affecting the function of other tissues and organs in patients is particularly intriguing. While for *PRPF31* haploinsufficiency appears to be the cause of the disease<sup>71</sup>, mutations in *PRPF3* shows a photoreceptor specific dominant effect<sup>72</sup>.

#### 6.) Genes involved in protein folding/trafficking:

The retina is an actively metabolic organ and undergoes a significant extent of intracellular trafficking, therefore it is reasonable to speculate that mutations in genes involved in protein trafficking or protein folding may be harmful. So far,

five genes involved in such functions were found to be mutated in RP (*AiPL1*, *RPGR*, *USH2A*, *RP1* and *RP2*). The aryl-hydrocarbon interacting protein-like 1 (*AiPL1*) is probably involved in protein maturation or translocation of multiprotein complexes in the retina<sup>73, 74</sup> and, similarly, the putative function of the retinitis pigmentosa guanosine triphosphatase (GTPase) regulator (*RPGR*) is in protein trafficking regulation<sup>75, 76</sup>. Usherin 2A (*USH2A*) is an extracellular matrix type protein and is involved in protein-protein interaction<sup>77</sup>. The *RP1* gene is responsible for morphogenesis of photoreceptors outer segment and protein transport<sup>78</sup>, while the suggested role of *RP2* is in cell signaling or vesicular transport<sup>79</sup>.

Several other genes with functions different from the ones mentioned so far can cause retinitis pigmentosa. Ceramide kinase-like protein (*CERKL*) plays an essential role in cell survival and apoptosis<sup>80</sup>, while the crumbs homolog 1 (*CRB1*) is believed to be responsible for cell polarity<sup>81</sup>. The tubby-like protein1 (*TULP1*) is responsible for recessive RP, but its function is still unknown, although there are suggestions that it may be involved in actin cytoskeletal functions such as protein trafficking<sup>82</sup>. Another gene with apparently no retina specific role, i.e., the carbonic anhydrase 4 (*CA4*) was found to be mutated in patients with RP. *CA4* is important for the pH balance maintenance, and therefore mutations in *CA4* may lead to photoreceptor malfunctioning since the phototransduction cascade is modulated by pH changes<sup>83</sup>.

---

## **1.4 NEW APPROACHES TO IDENTIFY ADDITIONAL RETINAL DISEASE GENES**

The remarkable genetic heterogeneity of inherited retinal disorders such as retinitis pigmentosa underscores the complexity inherent to the identification of all its genetic causes. As already mentioned, in the past couple of decades, great effort has been put into the determination of the causes that lead to retinal dysfunction, and nowadays there are over 190 genes identified as responsible for different inherited retinal disorders<sup>84</sup>. However out of 190 mapped genes only 130 have been identified so far (RetNet: <http://www.sph.uth.tmc.edu/Retnet/>). Additionally, it is widely believed that the total number of retinal disease genes is higher than what is currently known<sup>85</sup>. In order to have more chances of devising successfully therapeutic treatments for retinal diseases, it is necessary to have a comprehensive knowledge of all the genetic causes responsible for these diseases. Until a few years ago, the most successful strategy for retinal disease gene identification was represented by positional cloning. Positional cloning identifies a disease gene based on no other information about the gene except its chromosomal location. The procedure is based on mapping the disease as closely as possible in affected families by linkage analysis, followed by identification of candidate genes localized in the critical region and mutation analysis in patients. The completion of the Human Genome Project and all the related achievements, such as *a*) the complete sequencing of the human genome as well as of the genomes of several model organisms (the mouse above all) and the *b*) selective sequencing of transcribed sequences mainly represented by the Expressed Sequence Tag (EST) effort, to cite only a few, has completely revolutionized the approaches aimed at disease gene identification. The era of high-throughput cDNA

sequencing was initiated in 1991<sup>86</sup>. The basic strategy involved random selection of cDNA clones and single, automated, sequencing reads from one or both ends of their inserts<sup>87</sup>. The term EST was introduced to refer to this new class of sequence, which is characterized by being short (typically about 400–600 bases) and relatively inaccurate (around 2% sequencing error). The use of single-pass sequencing was an important aspect of making the approach cost effective. In most cases, there was no initial attempt to identify or characterize the clones. Instead, they were identified using only the small bit of sequence data obtained, comparing it to the sequences of known genes and other ESTs. However, as a consequence of such a low specific approach, many clones were redundant with others already sampled and a smaller number represented various sorts of contaminants or cloning artifacts. Despite their fragmentary and inaccurate nature, ESTs have so far represented an invaluable resource for the discovery of new genes, particularly those involved in human disease processes<sup>88</sup>.

One of the novel approaches to identify candidate genes for retinal diseases is to pinpoint genes with exclusive or predominant retinal expression. The rationale behind this approach lays in the fact that in the absence of biological clues, disease gene candidacy is often assessed by expression profiling, whereby genes expressed specifically or preferentially in the tissue(s) affected by the disorder are prioritized for screening. Expression profiling has been particularly successful in ophthalmic genetics, in part because more than half of the cloned genes associated with retinal phenotypes are specifically or preferentially expressed in the retina<sup>89</sup> (RetNet: <http://www.sph.uth.tmc.edu/Retnet/>). So high is this correlation between tissue specificity and clinical phenotype that the mining of genes with exclusive or

predominant expression profiles is considered to be an important tool for identification of retinal disease genes. Indeed, different research groups have used both bioinformatics tools and molecular methods for the identification of genes with enriched expression in photoreceptors and RPE<sup>89-95</sup>. For example, Lord-Grignon et al.<sup>90</sup> took advantage of the Digital Differential Display (DDD) approach to compare the abundance of EST transcripts from whole-eye and retinal libraries with non-neuronal libraries, selecting the transcripts enriched in eye-derived libraries. DDD is a computational method that allows comparative analysis of the frequency of individual ESTs among pools of cDNA libraries. By this approach, the authors identified twenty-seven potentially novel highly represented ESTs in the retina. Retinal expression of the selected ESTs was confirmed by RT-PCR comparing the presence of the cDNAs in embryonic optic vesicle and adult retina to an entire embryo minus optic vesicle and adult liver. Cellular expression of the EST shown to be predominantly expressed in retina was assessed by RNA *in situ* hybridization on mouse retina. This analysis revealed that out of twenty uncharacterized ESTs, thirteen turned out to have a cell-specific mRNA distribution within the retina, with eight showing predominant expression in photoreceptors and/or RPE. Human orthologues for four photoreceptors/RPE enriched ESTs mapped within distinct cytogenetic intervals containing uncloned retinal disease genes. On the other hand, Blackshaw et al.<sup>95</sup> used serial analysis of gene expression (SAGE) to generate retinal libraries, followed by Northern blotting and RNA *in situ* hybridization on mouse retina to verify retina enriched transcripts. SAGE is a method for comprehensive analysis of gene expression patterns. Three principles underlie the SAGE methodology: a) a short sequence tag (10-14bp) contains sufficient information to uniquely identify a transcript provided that the tag is obtained from a unique

position within each transcript, *b*) sequence tags can be linked together to form long serial molecules that can be cloned and sequenced, *c*) quantitation of the number of times a particular tag is observed provides the expression level of the corresponding transcript. This approach enabled the authors to identify 264 uncharacterized genes that were specific to or highly enriched in rods. *In silico* mapping of the human orthologs of genes identified revealed that 86 of them mapped within intervals containing uncloned retinal disease genes, representing 37 different loci. The two above described approaches for the identification of novel retinal disease genes were performed on mouse retina. Similarly, combination of *in silico* and experimental analysis was also used to identify ESTs predominantly expressed in the human retina<sup>89, 92, 94</sup>. For example, Sohocki et al.<sup>92</sup> have identified novel retina/pineal-expressed EST clusters by exploiting the TIGR Human Gene Index database. The TIGR Human Gene Index database lists assembled clusters of ESTs, arising from the same transcript, and organizes these clusters according to tissue expression. The rationale behind the identification of pineal/retinal ESTs lays in the fact that the retina and pineal gland both originate embryologically from the most anterior region of the neural plate, the diencephalon. Development and differentiation of these organs are also related as many developmental genes, such as the homeobox genes *XRX1* and *CRX*, have expression patterns limited to the developing retina and pineal gland. Furthermore, mammalian pinealocytes are evolutionarily related to photoreceptor cells and express a selective group of “retinal proteins” that are involved in the phototransduction cascade. The pineal/retinal specifically expressed ESTs identified by Sohocki et al.<sup>92</sup> were experimentally confirmed by PCR on an adult retina cDNA library. Using the

described approach, the authors identified seven novel candidate genes for known retinal diseases.

Despite the fact that many retinal dystrophy disease genes have been identified so far using the approaches described above, there is almost no information about the cellular expression of novel candidate disease genes in the human retina since most of the high resolution expression studies so far were carried out in the mouse retina<sup>95</sup>.

### **1.5 FUNCTIONAL CHARACTERIZATION OF RETINAL DISEASE GENES**

In order to better understand the genetic basis and molecular mechanisms of retinal degeneration and to develop therapeutic strategies, numerous animal models have been generated<sup>96</sup>. Animal models do represent a very powerful tool in modern biology to study human diseases. Typically, these models are generated by knocking out or by overexpressing, in the selected organism, the gene to analyze, depending on the mutation mechanism. The majority of the animal models used in eye research are murine models, mainly due to the fact that mice are easily handled from an experimental point of view, have relatively short life span and their genes usually share high percentage of sequence identity with the corresponding human genes. Nonetheless, some notable differences between the human and the murine retina may hamper the transfer of the knowledge gained from mouse models to patients. For example, mice, like most nocturnal animals, do not have cone-rich areas for visual acuity such as the fovea<sup>97</sup>. Due to this, macular disorders, such as age related macular degeneration, which is a major cause of blindness in elderly<sup>98</sup>, cannot be studied in murine models. Thus, differences in distribution of rods and cones in human and mouse retina may be an obstacle in transferring observations

derived from mouse models to humans. In addition, only two types of cones are present in the murine retina, short and middle wavelength cones, while the human retina contains also long wavelength cones. More importantly, not all mouse models show the same phenotype as patients with the same gene lesion. For example human patients with dominant RP or Leber congenital amaurosis caused by mutation in the *IMPDH1* gene show a more severe disorder than a mouse model with a mutation in the orthologous murine gene<sup>42</sup>. Hence, to design efficient therapeutic approaches for RP and other eye diseases, it is essential to have detailed information about the expression of RP genes in the human retina. This is especially important in the cases when gene therapy may be applicable. The eye has a combination of features that make it ideally suited as a target organ for gene therapy.

Gene therapy is a technique for correcting defective genes responsible for disease development by several approaches: *a)* a normal gene may be inserted into a nonspecific location within the genome to replace a nonfunctional gene in recessive diseases<sup>99, 100</sup>; *b)* an abnormal gene could be swapped for a normal gene through homologous recombination, a technique not developed yet for in vivo therapy; *c)* wild type and mutant alleles of the affected genes can be silenced and a wild type allele, not sensitive to the silencing method, can be supplied<sup>101</sup> in dominant diseases and also *d)* a therapeutic/trophic factor can be delivered in the affected tissue (bFGF, CNTF in the retina). A carrier system, such as viruses, must be used to deliver the therapeutic gene to the patient's target cells. The highly compartmentalized anatomy of the eye facilitates accurate delivery of viral particles to specific tissues under direct visualization using microsurgical techniques. This enables precise targeting of the therapeutic gene at target sites within the eye bulb while minimizing systemic



dissemination and the unwanted systemic effects. Additionally, due to the ocular anatomical barriers and a unique immune environment, the eye presents a degree of protection from immune responses directed against vector antigens that might cause inflammation and limit transgene expression<sup>102</sup>. Since efficient vector-mediated retinal gene therapy is largely dependent on the site of expression of the therapeutic gene, detailed knowledge on the precise localization of the mutated gene is absolutely required. Unfortunately, to date, little information is available about the expression patterns of RP genes at the cellular level in the human retina and all the current knowledge is inferred through studies in the mouse. When using only the mouse models to study pathogenesis of human retinal disorders, some problems may arise when therapeutic strategies will be transferred to the man due to the already mentioned notable differences between the human and murine retina. Due to the above mentioned differences between murine and human retina, having the information about the expression profiles of both known retinal disease genes and putative new candidate genes in human retina is crucial for future progress of eye disease treatment. The general importance of providing information regarding the expression patterns of retinal genes is even more emphasized by the fact that the previously reported generation of RNA ISH gene expression atlases was very beneficial also for a better understanding of non-retinal diseases. For example, the generation of a human chromosome 21 gene expression atlas<sup>103</sup> was an important step towards the understanding of gene function and of the pathogenetic mechanisms involved in Down's syndrome. Similarly, an expression atlas of connexin genes<sup>104</sup> provided an valuable source of information concerning this group of genes involved in several different diseases such as hearing, dermatological and peripheral nerve disorders.

## **1.6 AIMS OF THE THESIS**

The main goal of the research described in this thesis was to perform systematic gene expression studies in the human retina. Two main aims have been the focus of these studies: the first was the identification of new candidates for human retinal disorders, and the second was to provide information about the expression profiles in the human retina of known genes underlying retinal disorders. To this purpose, I undertook three steps:

- 1. I screened the publicly available human EST databases to identify novel transcripts specifically or preferentially expressed in the human retina;*
- 2. I determined the expression profiles of novel or poorly characterized genes identified in step 1 in order to use this information to ascribe a possible role in the retina and define whether they may represent candidates for eye inherited disorders and*
- 3. I performed expression studies in the human and murine retina of already known genes responsible for retinal inherited disorders (retinitis pigmentosa).*

The research performed in the first part of the thesis was driven by the evidence that about 50% of RP patients do not have mutations in known retinal dystrophy genes. Therefore there is a need to identify new candidate genes to be screened for mutation in these cases. In order to define a gene as candidate for retinal disorder, I chose to look for genes preferentially expressed in the retina because most of the genes linked to these diseases show such a characteristic. For this reason, I focused on cellular localization in human retina of the genes selected by the combination of *in silico* prediction of exclusive or predominant retinal expression followed by experimental validation of their

expression profiles. In order to identify new candidate genes for retinal disorders, new human transcripts with predominant retinal expression were identified by *in silico* approaches. The newly-identified transcripts underwent experimental validation of their *in silico* predicted retinal expression. As a first step, reverse transcriptase-polymerase chain reaction (RT-PCR) on human retina RNA as well as on RNA derived from other tissues was performed. This type of analysis was essential to validate the *in silico* prediction of identified genes with exclusive or predominant retinal expression, i.e. only genes confirmed by RT-PCR were considered for expression studies by RNA *in situ* hybridization (RNA ISH). These studies were followed by RNA ISH experiments to obtain expression profile at the cellular level to pinpoint the most interesting genes for further characterization. Finally, mutation analysis on a collection of Italian LCA and RP patients was performed for one selected candidate gene.

The second part of my PhD project focused on the determination of the expression profiles for genes known to cause retinitis pigmentosa. To overcome the lack of high-resolution expression data of genes mutated in RP in the human retina, I carried out a systematic analysis of the expression patterns of RP genes by RNA *in situ* hybridization both in human and mouse eye sections. Generation of an RNA expression atlas of RP genes in both species provides a comparative analysis of a given RP gene of interest or of a group of RP genes thus facilitating a more efficient translation of the knowledge gained from mouse models to patients. To this purpose, I undertook the following steps: selection of all known RP genes to be studied; design and preparation of the appropriate gene templates to perform RNA *in situ* hybridization studies on human and murine adult eyes; careful optimization of the handling procedure for the human eye in order to obtain a well preserved histology and reliable hybridization

results; RNA *in situ* hybridization analysis of RP genes both in human and mouse retina; additional experimental validation of some expression profiles and finally, collection of the results in the form of an atlas. This study generated a publicly available RP gene expression atlas database and revealed interesting differences in the expression profiles of some of the analyzed RP genes in human compared to mouse retina and with respect to previously published data.

# *Materials and methods*

## **2.1 BIOINFORMATIC ANALYSIS**

### **2.1.1 *In silico* identification of human EST clusters predominantly expressed in retina**

Clusters of Expressed Sequence Tags and/or other cDNAs showing predominant expression in the eye when compared to other tissues were retrieved from the Unigene database (<http://www.ncbi.nlm.nih.gov/entrez/query.fcgi?db=unigene>). This database enables to perform searches for cDNA clusters, from a particular organism, that are enriched for ESTs derived from libraries constructed from a particular tissue. Therefore, in order to identify human cDNAs that, based on their EST representation, are predicted to have a predominant expression in the eye, I queried the database using the following combination of query terms: 9606[taxid] AND Eye[restricted] where "9606" is the identifier for *Homo sapiens*. The retrieved cDNA sequences of each cluster were assembled using the CAP server ([http://www.infobiogen.fr/services/analyseq/cgi-bin/cap\\_in.pl](http://www.infobiogen.fr/services/analyseq/cgi-bin/cap_in.pl)) to obtain consensus sequences. In order to determine the genomic locations as well as the relation of these clusters to already known genes, each cluster-specific consensus sequence(s) was mapped to the human genome using the BLAT algorithm available at the Human Genome Browser server (<http://genome.ucsc.edu/cgi-bin/hgBlat>).

### **2.1.2 Identification and annotation of protein domains**

The identification and annotation of protein domains and the analysis of protein domain architectures was performed by using the web-based tool Simple Modular Architecture Research Tool-SMART (<http://smart.embl-heidelberg.de/>).

## **2.2 SAMPLE PREPARATION**

### **2.2.1 Genomic DNA extraction**

Mouse tail tips and human blood were incubated over night at 55°C in lysis buffer (50mM Tris.HCl pH7.5, 100mM EDTA pH8, 100mM NaCl, 1%SDS with 1.0 mg/ml Proteinase K). The following day, the genomic DNA was purified by Phenol-chloroform extraction and precipitated in 95% ethanol. After washing with 70% ethanol, the DNA pellet was dried at room temperature and resuspended in 300 µl milliQ H<sub>2</sub>O.

### **2.2.2 RNA extraction**

Dissected mouse tissues (100mg) were placed in 1 ml of TRIZOL reagent (Invitrogen), homogenized and RNA extraction was performed. Tissue samples were homogenized in 1 ml of TRIZOL® reagent per 50-100 mg of tissue using power homogenizer. Homogenized samples were incubated for 5 minutes at room temperature (RT) to permit the complete dissociation of nucleoprotein complexes. After homogenization, 0.2 ml of chloroform per 1 ml of TRIZOL initially used were added followed by vigorous shaking for 15 seconds and 2 to 3 minutes incubation at RT. Samples were then centrifuged at 12,000 × g for 15 minutes at 4°C. Following centrifugation, the mixture separates into a lower red, phenol-chloroform phase, an interphase, and a colorless upper aqueous phase. RNA remains exclusively in the aqueous phase. The aqueous phase was transferred to a clean tube, and precipitation of the RNA from the aqueous phase was performed by mixing with 0.5 ml of isopropyl alcohol per 1 ml of TRIZOL. Samples were incubated at RT for 10 minutes and centrifuged at 12,000 × g for 10 minutes at 4°C. After removal of the supernatant, the RNA pellet was washed once with 1 ml of 75% ethanol per 1 ml of TRIZOL reagent

used for the initial homogenization. The samples were mixed by vortexing and centrifuged at  $7,500 \times g$  for 5 minutes at  $4^{\circ}\text{C}$ . The RNA pellet was briefly air-dried and the RNA was dissolved in RNase-free water followed by 10 minutes incubation at  $65^{\circ}\text{C}$ , cooled in the ice for 10 minutes and stored at  $-80^{\circ}\text{C}$ . Total RNA samples from human tissues were purchased from Clontech.

### 2.2.3 Synthesis of cDNA

Total RNA was reverse transcribed into cDNA by using the SuperScript™ First Strand Synthesis System (Invitrogen). RNA/primer mixtures were prepared in sterile 0.2 tubes as follows:

<u>Component</u>	<u>Sample</u>	<u>No RT Control</u>	<u>Control RNA</u>
1 $\mu\text{g}$ total RNA	$n \mu\text{l}$	$n \mu\text{l}$	—
Control RNA (50 ng/ $\mu\text{l}$ )	—	—	1 $\mu\text{l}$
10 mM dNTP mix	1 $\mu\text{l}$	1 $\mu\text{l}$	1 $\mu\text{l}$
Oligo(dT) <sub>12-18</sub> (0.5 $\mu\text{g}/\mu\text{l}$ )	1 $\mu\text{l}$	1 $\mu\text{l}$	1 $\mu\text{l}$
DEPC-treated water	to 10 $\mu\text{l}$	to 10 $\mu\text{l}$	to 10 $\mu\text{l}$

Each sample was incubated at  $65^{\circ}\text{C}$  for 5 min, and then placed on ice for at least 1 min. To each RNA/primer mixture 9  $\mu\text{l}$  of following reaction mixture was added, mixed gently, and collected by brief centrifugation.

<u>Reaction mixture</u>	<u>Sample</u>	<u>Final concentration</u>
10X RT buffer*	2 $\mu\text{l}$	1X
*(200mM Tris-HCl pH 8.4, 500mM KCl)		
25 mM $\text{MgCl}_2$	4 $\mu\text{l}$	5mM
0.1 M DTT	2 $\mu\text{l}$	0.01M
RNaseOUT™ Recombinant		
RNase Inhibitor	1 $\mu\text{l}$	40 units



Each sample was incubated at 42°C for 2 min. Following incubation 50 units of SuperScript™ II RT was added to each tube except the no RT control, mixed, and incubated at 42°C for 50 min. The reactions were terminated by incubation at 70°C for 15 min, chilled on ice and collected by brief centrifugation. Finally 2 units of RNase H was added to each tube and incubated for 20 min at 37°C before proceeding to PCR.

#### **2.2.4 Treatment of human and mouse eye bulbs**

Human eye bulbs were obtained from cornea donors (Table 1) collected by the Italian Eye bank (Fondazione Banca degli Occhi del Veneto, Venice, Italy).

**Table 1. Information about eye donors**

<b>INDIVIDUAL</b>	<b>AGE</b>	<b>CAUSE OF DEATH</b>	<b>POSTMORTEM TIME before eye removal (HOURS:MINUTES)</b>
<b>43427/43428</b>	30	Trauma	19:45
<b>50608/50609</b>	48	Tumor	6:45
<b>52493</b>	37	Trauma	5:45
<b>53041</b>	48	Cardiovascular	5:45
<b>60933</b>	48	Tumor	5:10
<b>60935</b>	41	Cardiovascular	8:45
<b>62135</b>	58	Cardiovascular	22:15
<b>62658/62659</b>	56	Tumor	19:40

Eye bulbs were dipped in 4% paraformaldehyde (PFA) right after cornea removal. Then, after removal of the lens, eye bulbs were fixed for an extra 48 hours at 4°C with 4% PFA in phosphate-buffered saline (PBS), followed by cryoprotective treatment with 30% sucrose in PBS and embedded in 7.5% gelatin. Mouse CD1 adult eyes were fixed only 24 hours and then treated in the

same way. Twenty-micrometer cryosections were collected on Superfrost Plus slides, air dried and stored at -80°C.

### **2.2.5 Hematoxylin/Eosin Staining**

Cryosections were thawed at RT, followed by 10 minutes fixation in 4%PFA and extensive washes with water 3 times for 5 minutes. Hematoxylin staining was performed for 1 minute at RT, followed by washes with tap water. Eosin staining was performed for 30 second. Sections were washed extensively with tap water, dehydrated with ethanol series for 1 minute each (30%-50%-70%-95%-100% ethanol), immersed twice in xylene for 1 minute, air dried and mounted with Eokitt.

## **2.3 EXPRESSION STUDIES**

### **2.3.1 Reverse Transcriptase Polymerase Chain Reaction RT-PCR**

The PCR reactions were set up as follow:

Final concentration in PCR mix:

milliQ H<sub>2</sub>O

1X PCR buffer

1.5 mM MgCl<sub>2</sub>

300 μM dNTPs

0.4 μM forward primer

0.4 μM reverse primer

1U AmpliTaq Gold (Roche)

100-500 ng cDNA

Sequences of oligonucleotide primers used and annealing temperatures are listed in Table 2.

**Table 2. List of the primers used for RT-PCR analysis, annealing temperatures for each primer pair and size of the obtained products.**

		Forward primer	Reverse primer	Annealing temperature °C	Product size bp
1.	Hs.40814	ATCACACCAGGCAGGAGTTT	AGGCACATTTTCTTGCCAGA	58	250
2.	Hs.441592	TGAACCCAGGTGACTTGACTC	CCAAACTCTGTCTTTCCCTGA	58	240
3.	Hs.532691	GATGTGTACAGCCGTGAGGAG	AGAGCCTGTGCATGTTCCCTT	58	374
4.	Hs.354243	TTCCCTCAGGAGGACAGCTTCT	GGACACTTGGCTGTCACACTT	60	372
5.	Hs.131130	CTGCCTGCTGCTCTTCATC	CGTTGAGAATGATCCCAAAG	57	221
6.	Hs.433492	CAACTACTATGTGGCCCTGGA	GTAGTGCTGGCTAAGCTGCTC	60	223
7.	Hs.154140	ATCAGACCAAGCCAAACACAC	CAGGCAGATGCCTCTTTTATG	57	213
8.	Hs.433493	CAGGGGACGAAGTGTATGTG	CTGGATGAAAGGAGGAGGAG	58	388
9.	Hs.473495	TGCCTAGGAAGAGGAATGGA	CATTTCACCAAGCACCTTTTT	55	228
10.	Hs.493589	CAAGGGAAGATAGCTTCAAGTCA	CCAAGGAGTCGTCTGGTAG	61	360
11.	Hs.69749	CCAAATTCTTCCCCATACCA	CCTAAGCAGCCCAGAGAATG	61	357
12.	Hs.21162	GTCCTCTCGGCCTTCTGTAA	CTGGCGTACCCCAATAG	56	222
13.	Hs.247888	CAAATGCACCATCCTGTGAG	ATGGTCTTGGACGCCATCT	61	263
14.	Hs.124010	TCTCGGAGGTCTAGACTCG	GTCCTTGGCCACTTGCAT	56	232
15.	Hs.171485	GACCCAGGTGTGAAAACCTT	CTTACCCGGTCTCCGCTCT	58	213
16.	Hs.240053	GGTGGCCACATGATGTATT	CAGTTCGGGTTTTCTTGAA	55	222
17.	Hs.386402	TCGCATGAAAAATGGAGCTT	CCATCCAATGTGTCTGGGTA	56	215
18.	Hs.295015	AGGTCTCATCGCCATAGCAGT	CCCCCATGCCACACTTATC	57	362
19.	Hs.221513	CTGGCTCCTCACCAACTCT	AACCTGGGCTCCTTTTCAAC	58	210
20.	Hs.32766	CGCAGTCTCAAAGGGTAAG	GCTCAGAACAGGCCTCAGTC	55	209
21.	Hs.527819	CTGGTGTCTTCCCGAGTGT	ACCACAGGCCTTCTCTTCT	58	258
22.	Hs.444181	CCCGACACATCTCATTAGGG	ACATGCTGTGGTCTCTCAG	58	600
23.	Hs.503113	GATTTTGTGGGAGGCAAGA	AGGAGTGGGCATCTGTAGGA	58	210
24.	Hs.148427	GCAGTATTTCCGCAACATGA	CATGCTCCAGGGAGAAGTTG	57	218
25.	Hs.131342	AACCTGAGAAGGGCCTGATT	AAGCGTCTCGGATGAAAAT	58	340
26.	Hs.549054	TTTGCCACATACGACGAGAG	CGGGGGAAGAGAAGAAAGTC	58	230
27.	Hs.185777	TGACCAAGGAGACAGTGGTG	TGGCCTCATTCTTCTCATCC	58	315
28.	Hs.40808	CGGCCATCAAGTACCACTTT	AACCATGTTCCACATCAGCA	56	350
29.	Hs.33102	GGAGATCTTTGCGAGAAAGG	GTGCGTGATGAGGCTGAAGT	58	370
30.	Hs.149585	CGCCTCCAGTTTGTACGATT	GCCCATGGCAAACCTCTAAA	56	236
31.	Hs.449884	GGCATGCCTCAGAGTTTCATC	CGCTGTCTGCTTGATTCAG	58	250

PCRs were performed under the following cycling parameters: denaturation 95°C/1 min, annealing (temperatures listed in Table 2)/1 min and extension 72°C/1 min for 35 cycles. The PCR products were analyzed by electrophoresis in 1% agarose gel (0.5µg/ml ethidium bromide) in TAE buffer (40mM Tris-Acetate pH7.5, 1mM EDTA).

### 2.3.2 RNA in situ hybridization

#### 2.3.2.1 Synthesis of cRNA probes

Antisense and sense cDNA templates were obtained using a variety of approaches including the use of public Expressed Sequence Tag (ESTs) clones, PCR amplification of human/mouse genomic DNA or cDNA prepared

from human/mouse total retina RNA with the specific primers tailed by sequences recognized by the RNA polymerases (T3, T7 or SP6). Finally, some of them were generous gifts of external investigators, as listed in Table 3.

**Table 3. Information about the source used to obtain cDNA templates, template size and RNA ISH hybridization temperature used for each analyzed gene.**

Probe	Source	Restriction enzymes for plasmid linearization	Product size (bp)	Hybridization temperature °C
Hs.354243	PCR on genomic DNA T7 CGAGGAGAGCCCTAAGAAGG T3 ATTGATTTCTGACTCCAGCAGA		1251	60
Hs.131130	PCR on genomic DNA T7 CGAAGACGGCGAGGAGGAGG T3 ACGCCAGCTTGAGGATGCGGA		1000	60
Hs.433492	PCR on genomic DNA T7 ACCTGACAGCAGTGGACCCT T3 GAATACACTGTAGAGTATGCTCTG		985	60
Hs.69749	PCR on genomic DNA T7 GGCTCCAATGTATCCAGGTC T3 ACAGTATCATAAGCATTCACTGT		1050	60
Hs.21162	EST clone (IMAGE:397588)		1145	60
Hs.240053	PCR on genomic DNA T7 CGAACTGCCTACCCATCAC T3 AGGTACATTTCTCAGAAGGGATGA		989	60
Hs.295015	EST clone (IMAGE:5182276)	EcoRI NotI	529	60
Hs.444181	EST clone (IMAGE:753760)		758	60
Hs.148427	RT-PCR T7 GGCAACTTCTCCCTGGAGCA T3 AAGAAGGGGCGCCAGGCATTT		994	60
Hs.171485	EST clone (IMAGE:40963)		1574	60
Hs.221513	EST clone (IMAGE:5296173)	EcoRI BamHI	1728	60
Hs.131342	EST clone (IMAGE:2010188)		1500	60
Hs.33102	EST clone (IMAGE:4745989)	NotI EcoRI	2033	60
Hs.449884	PCR on genomic DNA T7 TGAAGATCTCCGAAAATGG T3 AATGGGAAGGGACAGGAGAAG		1095	60
hABCA4	EST clone (IMAGE ID:2504257)		2000	65
mABCA4	EST clone (IMAGE ID:5400135)		781	65
hAIPL1	PCR on genomic DNA T7 GGCCAAGGCGGACCTCCAGA T3 CTTTCTGGGGGAGGCCAAG		860	65
mAIPL1	EST clone (IMAGE ID:6489895)		732	65
hCA4	EST clone kindly provided by William S. Sly		558	60
mCA4	EST clone (IMAGE ID:H3095H12)		736	60
hCERKL	RT-PCR T7 AGGAAGCATGGAAGAAATGA T3 TTACATTTGGTTCTTTCTTA		962	60
mCERKL	PCR on genomic DNA T7 TGTGTAAATCTCCATCCCA T3 AGCTAGGTGGGGTGTCTTAA		814	60
hCNGA1	EST clone (IMAGE ID:357046)		1000	65
mCNGA1	PCR on genomic DNA T7 GGCAGAATTTCAATCAAGAG		1041	65

	T3 ATCCCAGGAGAAGATGATACT			
<b>hCNGB1</b>	<i>PCR on genomic DNA</i> T7 CTCCGCCGCCCCAGACCAGC T3 CGGCTTCCCAAAGCACTGGG		753	65
<b>mCNGB1</b>	<i>PCR on genomic DNA</i> T7 GGAGGGCTCTGGGGCCACAG T3 GTGGCTTCTGGTGGGGACCC		570	65
<b>hCRB1</b>	<i>EST clone kindly provided by Anneke den Hollander</i>		1000	60
<b>mCRB1</b>	<i>PCR on genomic DNA</i> T7 ACTGCACCCTTGCCATAATG T3 AGGCCTGTCACATTCACACTG		898	60
<b>hCRX</b>	<i>EST clone kindly provided by Rod McInnes</i>		1600	60
<b>mCRX</b>	<i>RT-PCR</i> T7ATCCAGGAGAGTCCCCATTT T3 GACAGCCTGGTGCATCAGG		1284	60
<b>hFSCN2</b>	<i>PCR on genomic DNA</i> T7 CCCGGCCAGCCTGAAGATGC T3 GTGACTCTCCTCCAGATCAA		790	65
<b>mFSCN2</b>	<i>EST clone kindly provided by Pierre D. McCrea</i>		751	65
<b>hGUCA1B</b>	<i>PCR on genomic DNA</i> T7 GAGGGGCGTTCATGGGGAGG T3 GTGACCCAGGGCACTGGTTT		630	65
<b>mGUCA1B</b>	<i>PCR on genomic DNA</i> T7 GGGTAATGAAGATGCTACAA T3 ATGTGACACTGGTCTACTTA		961	65
<b>hIMPDH1</b>	<i>PCR on genomic DNA</i> T7 ATGCACCCCAAGTGTCCACTT T3 AACTGTGATCCCAAGTGTGC		641	65
<b>mIMPDH1</b>	<i>PCR on genomic DNA</i> T7 TCTAGGAACAGCCTCCCTCC T3 AACACAATTGTGACCCCAAAG		666	65
<b>hLRAT</b>	<i>EST clone kindly provided by Dean Bok</i>		700	65
<b>hLRAT-1</b>	<i>EST clone kindly provided by Dean Bok</i>		728	65
<b>mLRAT</b>	<i>EST clone kindly provided by Dean Bok</i>		2500	60
<b>hMERTK</b>	<i>EST clone kindly provided by Douglas Vollrath</i>		796	60
<b>mMERTK</b>	<i>PCR on genomic DNA</i> T7 TACTCTTGCTGGAGTGCTGA T3 ATTTACCTGGTGCTGTCCGG		979	60
<b>hNR2E3</b>	<i>EST clone kindly provided by Anand Swaroop</i>		742	65
<b>mNR2E3</b>	<i>EST clone kindly provided by Jeremy Nathans</i>		1188	65
<b>hNRL</b>	<i>PCR on genomic DNA</i> T7 CAGAGCGGTTTTCCGACGCG T3 CAACCCCAAGAGCTCACTCT		910	65
<b>mNRL</b>	<i>PCR on genomic DNA</i> T7 CGACCACACACCTCTTCC T3 AGGGGGCCACTTAGGCAGTAC		921	65
<b>hPAP1</b>	<i>EST clone kindly provided by Chris Inglehearn</i>		592	60
<b>mPAP1</b>	<i>EST clone kindly provided by Hiroyoshi Ariga</i>		1108	60
<b>hPDE6A</b>	<i>PCR on genomic DNA</i> T7 TGCAGACAAGACCCAGAGAA T3 GTGTTGGGGACGTTAGCAAT		578	65
<b>mPDE6A</b>	<i>PCR on genomic DNA</i> T7 CAGGGGGTGCACCTGCATCT T3 ATTTCCCTTGAGGTTTGGTC		1041	65
<b>hPDE6B</b>	<i>EST clone kindly provided by Jean Bennett</i>		1000	65
<b>mPDE6B</b>	<i>EST clone kindly provided by Jean Bennett</i>		1061	65
<b>hPRPF3</b>	<i>EST clone kindly provided by Shomi</i>		1016	60

	<i>Bhattacharya</i>			
mPRPF3	EST clone (IMAGE ID:5344086)		821	60
hPRPF31	EST clone kindly provided by Shomi Bhattacharya		970	60
mPRPF31	EST clone (IMAGE ID:5347609)		1800	60
hPRPF8	EST clone (IMAGE ID:341060)		678	60
mPRPF8	EST clone (IMAGE ID:5353944)		712	60
hRDH12	PCR on genomic DNA T7 AAGAGGACCTGGGTGTCTCC T3 ATTGAAAGGCAAACGGA ACTC		667	60
mRDH12	PCR on genomic DNA T7 ATCCTCAAGGGCCCGGAACA T3 ATTTGGGGAGGGGGAAATCT		613	60
hRDS	EST clone (IMAGE ID:2299889)		700	65
mRDS	EST clone kindly provided by Muna Naash		858	65
hRGR	EST clone (IMAGE ID:2110323)		876	65
hRGR-1	RT-PCR T7 CAGCCTCAATACCCTGACCA T3 CCTTCTCCCTCTTCTGCGGT		765	65
mRGR	PCR on genomic DNA T7 CATGCCACAATCAACGCCA T3 ATGGTCAGGGGACACCTAACC		731	65
hRHO	EST clone (IMAGE ID:212541)		1000	65
mRHO	EST clone (IMAGE ID:212541)		1000	65
hRLBP1	PCR on genomic DNA T7 CTTTGTCCACGGGGATGACC T3 TTTAACCCGGGCTCCTTGCC		520	65
hRLBP1-1	RT-PCR T7ATCTCACAGCCTGCAAGTGG T3 TTCTCAATGATGCAGAAGCC		808	65
mRLBP1	PCR on genomic DNA T7 GAGATGACCTGGATGGCTTC T3 ACCCAGCACCAAGGATCACAT		715	65
hRP1	PCR on genomic DNA T7 CAGTTGAGATGAAAGTTCTGA T3 TTTTGCTGGCAACAGATGAC		1020	60
mRP1	PCR on genomic DNA T7 ACTCTTTGGATAAACTCTAT T3 AGTTTAAAGTTACATTTACCC		1081	60
hRP2	PCR on genomic DNA T7 CTGGAGATGTAGACAGCTTC T3 TACTTGCCAAGCTGGTTATC		653	60
mRP2	PCR on genomic DNA T7 GATGTTGATAGCTTCTATAA T3 ACTGGAAGTTACTATTATCAA		1317	60
hRPE65	EST clone kindly provided by Enrico Surace		846	65
hRPE65-1	EST clone kindly provided by Enrico Surace		710	65
mRPE65	PCR on genomic DNA T7 CTATCACCTGTTTGATGGAC T3 AGTTGTATGGGGCAGTGTGA		992	65
hRPGR	PCR on genomic DNA T7 TGTTCAAAGAGTCCCCTCA T3 AAATATGTTTATTATAAACA		630	60
hRPGR-ORF15	PCR on genomic DNA T7 AAAGGATCTGTGAAATATGG T3 AAATTAATTTTAAAGTGTA		1080	60
mRPGR	PCR on genomic DNA T7 GATGTCATTGACAGGTCAGA T3 AACAGCAGAACCAACAGACA		641	60
mRPGR-ORF15	EST clone kindly provided by Alan Wright		1484	60
hRPGRIP	EST clone kindly provided by Alan Wright		3000	60
mRPGRIP	PCR on genomic DNA T7 GCCCTAGAAACCAGGCCATC T3 ATAGAGGGAGGCTTAAAGGAG		711	60
hSAG	EST clone (IMAGE ID:360579)		700	65
mSAG	EST clone (IMAGE ID:5401150)		1200	65
hTULP1	EST clone (IMAGE ID:221670)		758	65
mTULP1	EST clone (IMAGE ID:1533494)		535	65
hUSH2A	PCR on genomic DNA T7 AGGATTCAGCTCAGTGA CT		1040	60

	T3 GGTATAGTCTTGTCTCTACA			
mUSH2A	PCR on genomic DNA T7 TCCAGTCTGTGGGGCCCACC T3 ACAAGACACTGCCCGGCTGT		1071	60

### 2.3.2.2 Transformation of *E.coli* with plasmid DNA

*E.coli* DH5 $\alpha$  cells were prepared for transformation as follows: cells were grown to mid-log phase ( $A_{600}=0.6$ ) in Luria Broth (LB: 1% bactotryptone, 1% NaCl and 0.5% Bacto-yeast extract) at 37°C with shaking. Cells were harvested by centrifugation at 2000 x g at 4°C, resuspended into 100ml (for each 100ml of culture) of ice cold 10% glycerol solution. This suspension was then centrifuged at 5000 x g for 15 min at 4°C. The resulting pellet was resuspended into 100ml (for each 100ml of culture) of ice cold 10% glycerol solution and centrifuged again. The pellet was resuspended in 2.5 ml (for each 100 ml of culture) of ice cold 10% glycerol solution and centrifuged again as above. The cells were resuspended in 3 ml of ice cold 10% glycerol solution, aliquoted and stored at -80°C. For each transformation, DNA was added to 50  $\mu$ l of competent cells, and incubated in ice for 20 min; then cells were subjected to heat shock at 42°C for 2 min and successively incubated on ice for 10 min. Cells were recovered in 1 ml of LB and incubated for 40 min at 37°C, before plating on LB-agar containing appropriate antibiotics. Plates were incubated at 37°C overnight to allow bacterial colonies to grow.

### 2.3.2.3 Isolation of plasmid DNA from *E.coli*

Mini-preps plasmid DNA preparations were carried out using the QIAGEN MINI prep kits. Procedure is based on the alkaline lysis method<sup>105</sup>, but using a support column to purify isolated plasmid DNA. One aliquot of plasmid DNA

was diluted in 1:200 in milliQ water, and the concentration was determined according to the following formula: absorbance of one  $A_{260}$  unit indicates a DNA concentration of 50  $\mu\text{g/ml}$ .

#### **2.3.2.4 Linearization of the plasmids**

10 $\mu\text{g}$  of plasmid DNA were linearized using 20 units of the appropriate restriction enzyme (New England Biolabs) in 50 $\mu\text{l}$  of buffer provided by the manufacturer with the enzyme. The reaction was incubated for 1 hour at 37°C. Enzyme digestion was then controlled by agarose gel analysis. The reaction product was then purified by extraction with phenol/chlorophorm and precipitated with 70% ethanol. The linearized plasmid was then resuspended at the concentration of 0.2 $\mu\text{g}/\mu\text{l}$  in DEPC H<sub>2</sub>O to be used as template for cRNA transcription.

#### **2.3.2.4 In vitro cRNA transcription**

To synthesise cRNA probes the reaction mix was set up as follow:

- 5  $\mu\text{l}$  of linearized plasmid/PCR product (1 $\mu\text{g}$ )
- 2  $\mu\text{l}$  of 10X transcription buffer (Roche)
- 2  $\mu\text{l}$  of DIG-labelling mix (Roche)
- 2  $\mu\text{l}$  of appropriate RNA polymerase (T3, T7, SP6)-40 Units (Roche)
- 0.5  $\mu\text{l}$  of RNase inhibitor
- 8.5  $\mu\text{l}$  DEPC H<sub>2</sub>O

The reaction mix was incubated for two hours at 37°C, after which 2  $\mu\text{l}$  (20 Units) of DNase-RNase free was added to the reaction mix and incubated for 15 minutes at 37°C to degrade template DNA. 80  $\mu\text{l}$  of H<sub>2</sub>O were added to the reaction followed by precipitation with 0.1 volume 4M LiCl and 3x volume



absolute ethanol at -20°C for two hours. The probe was then centrifuged at 2000 x g for 30 minutes at 4°C, washed with 70% ethanol, air-dried, dissolved in 40 µl of DEPC H<sub>2</sub>O and stored at -20°C.

### **2.3.2.5 RNA in situ hybridization on cryostat sections**

Sections were thawed after removal from -80°C, fixed with 4% PFA in PBS for 15 minutes at room temperature. The slides were washed twice in PBT (1X PBS+0.1% Tween-20), followed by bleaching with 6% H<sub>2</sub>O<sub>2</sub> in PBT for 5 min at room temperature. The sections were washed 3 times for 5 min in PBT, and the tissue was treated with either 1 µg/ml (mouse tissue) or 10 µg/ml (human tissue) proteinase K for 15 min to permeabilise the tissue. Proteinase K activity was blocked by incubation with 2 mg/ml glycine solution in PBT for 10 min, followed by extensive washes with PBT. Post-fixation was performed with 0.2% glutaraldehyde / 4% PFA solution for 15 min at room temperature. After 3 washes with PBT for 5 minutes sections were prehybridized with pre warmed hybridization buffer (50% formamide, 5X SSC pH4.5, 50 µg/ml Yeast RNA, 1% SDS, 50 µg/ml Heparin) in humidified chamber (5X SSC, 50% formamide) for at least one hour at the appropriate hybridization temperature. The slides were overlaid with 200 µl of hybridization solution containing 200-400 ng/ml of DIG labelled cRNA probe, heated to 65°C for 10 minutes and then kept on ice to prevent re-naturation. The individual slides were covered with parafilm, placed into a humidified chamber and incubated over night at hybridization temperature as indicated in Table 3. Post-hybridization washes were performed 3 times for 15 minutes with prewarmed post-hybridization solution 1 (50% formamide, 4X SSC, 1% SDS) at hybridization temperature; 3 times for 15 min with prewarmed post-hybridization solution 2 (50% formamide, 2X SSC) at temperature 5°C

lower than the hybridization temperature and finally 3 washes for 10 minutes with TBST (1X TBS, 2mM Levamisole, 0.1% Tween-20) at room temperature. The sections were incubated for 1 hour at room temperature with blocking solution (10% sheep serum in 100mM Maleic acid, 150mM NaCl, 0.1% Tween-20). Alkaline phosphatase conjugated anti-DIG antibody was diluted 1:2000 in blocking solution and 200  $\mu$ l were used to overlay each slide. Incubation was performed at 4°C overnight in a humidified chamber. The following day sections were washed 4 times for 15 minutes with TBST followed by 3 washes for 10 min with NTMT (100mM NaCl, 100mM TrisCl pH 9.5, 50mM MgCl<sub>2</sub>, 0.1% Tween-20, 2mM Levamisole). After extensive washes sections were exposed to the substrate for alkaline phosphatase, nitroblue tetrazolium and 5-bromo-4-chloro-3-indoyl phosphate (NBT-BCIP; Sigma). Reaction was blocked by washes with PBS, pH 5.5, followed by postfixation in 4% PFA for 20 min. Slides were coverslipped with 70% glycerol in PBS or dehydrated and mounted with Eokitt.

### **2.3.3 Immunofluorescence**

The slides were fixed with 2% PFA, washed briefly in PBS and blocked for one-two hours in blocking solution (10% Goat serum, NGS in PBT) at room temperature in a humidified chamber. The primary antibodies were diluted in blocking solution (3% NGS in PBT) at the appropriate concentration:

rabbit anti-RGR antibody (kindly provided by Henry Fong<sup>106</sup>) 1:200

mouse anti-RLBP1 antibody (Abcam) 1:200.

The sections were overlaid with 200  $\mu$ l antibodies solution, covered with parafilm, placed into a humidified chamber and incubated overnight at 4°C. The slides were washed three times with PBT at room temperature for 10 minutes. Florescent secondary antibodies (Alexafluor anti-rabbit and anti-mouse,

Molecular probes) were diluted 1:1000 in blocking solution together with Fluorescein labelled peanut agglutinin-PNA (Vector) diluted 1:100. Incubation was performed for one hour at room temperature. Slides were extensively washed and mounted in Vectashield mounting medium (Vector).

## 2.4 MUTATION ANALYSIS

### 2.4.1 Sample preparation for DHPLC analysis

Genomic DNA amplifications of all the exons as well as exon-intron junctions were performed by polymerase chain reaction (PCR) using the specific oligonucleotide primer pairs listed below (Table 4). In order to obtain PCR products of the appropriate size (<500bp) for DHPLC analysis, the first exon of the analyzed gene (*KCNV2*) was divided into four overlapping segments. PCR reaction was performed under the conditions described in Chapter 2.3.1. Mutation analysis was performed on a collection of 120 Italian Leber congenital amaurosis (LCA), 96 retinitis pigmentosa (RP) and 4 cone dystrophies (CD) patient samples obtained in collaboration with the Ophthalmology department at the Seconda Università di Napoli, Naples, Italy.

**Table 4. List of the oligonucleotide primer pairs for the *KCNV2* mutation analysis.**

	Forward primer	Reverse primer	Annealing temperature °C
<i>KCNV2 first-1</i>	CCCTACCACAGCCAGGAGGA	TCTGTCTGCTCCTCGTAGTC	58
<i>KCNV2 first-2</i>	AGCTAAGCCTGTGCGACGAC	GAGTGCTGCTGCATCTCCTC	58
<i>KCNV2 first-3</i>	TCCGTGGTGGCGCTGGCGCT	GCGTTGGTGGCCCTCGCCCG	58
<i>KCNV2 first-4</i>	CCTGGTGGCCATCCTGCCGC	GGGCTGGGAAGAGGATGGG	58
<i>KCNV2 second</i>	GTGCTAACCAATCCATCCTG	ATCTACCAGCCACATGTCTT	50

### **2.4.2 DHPLC analysis**

In order to detect both homozygous and heterozygous changes, the PCR product obtained from each patient was mixed in a 1:1 ratio with the corresponding amplified sequence of healthy individuals. Amplified and mixed products underwent denaturing high performance liquid chromatography (DHPLC) analysis. DHPLC profiles from patients were compared to matching healthy individual profiles. Samples showing abnormal DHPLC profiles were re-analyzed by direct sequencing to identify putative mutations.

### **2.4.3 DNA sequence analysis**

For DNA sequence analysis PCR products were processed using the ABI-PRISM 3100 genetic analyzer (Applied Biosystems, Foster City, California, USA).

---

### **3.1 IDENTIFICATION OF PUTATIVE NOVEL HUMAN GENES WITH PREDOMINANT RETINAL EXPRESSION**

My PhD project started with the identification of novel human retinal expressed genes. The rationale behind this part of the project was based on consideration that a high percentage of genes underlying RP have a specific expression in the retina. Therefore, identification of new genes transcribed either uniquely or prevalently in the retinal tissue will provide candidates to be tested for mutations in patients for which previous mutation analyses did not reveal the presence of mutations in already known retinal dystrophy genes. I would like to emphasize again, at this point, the importance of identifying genes involved in retinal diseases since the elucidation of the molecular events leading to the failure of retinal function is the first step towards the development of effective therapeutic interventions. A schematic outline of the strategy I applied to identify novel retinal-expressed genes is shown in Figure 11.

#### **3.1.1 *In silico* identification of human EST clusters predominantly expressed in retina**

Gene expression data already available in public databases were utilized to identify a list of putative eye-expressed transcripts for which no or little information is available regarding their precise expression profiles in the human retina. *In silico* prediction was based on the analysis of the Unigene database of Expressed Sequence Tags (ESTs). ESTs are sequences obtained by performing single, automated sequencing reads from one or both ends of cDNA clones inserts<sup>87</sup>.

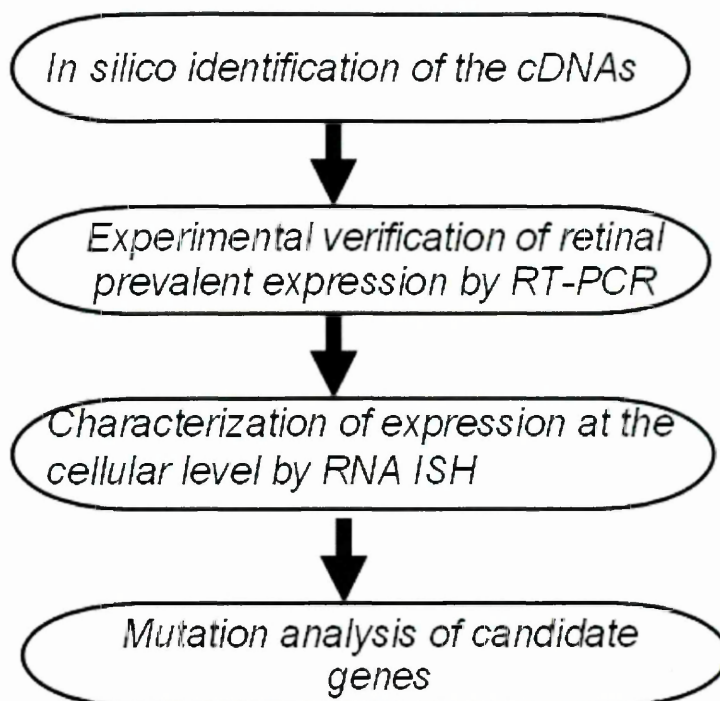


**Figure 11. Schematic outline of the strategy undertaken to identify new candidate genes for human retinal dystrophies.**

They represented, in the past fifteen years, an invaluable resource for both the discovery of new genes, including those involved in human disease processes<sup>88</sup> and for a better definition of the general features of mammalian transcriptomes. The Unigene database (<http://www.ncbi.nlm.nih.gov/entrez/query.fcgi?db=unigene>) represents one of the most valuable resources to analyze EST data in order to identify genes and to determine their predicted expression patterns. Currently, over 7,000,000 high quality human and 4,000,000 mouse ESTs are annotated in this database. By means of multiple sequence alignment analysis, Unigene groups the ESTs of a given organism in cDNA clusters, which are obtained by establishing relations between overlapping ESTs. The assignment of ESTs to cDNA clusters allows the database users to obtain *in silico* expression data for each given cluster through the analysis of the tissue origin of the ESTs belonging to it. For

example, by comparing the number of ESTs derived from eye libraries in a particular cluster with the number of ESTs from libraries derived from non-eye tissues, it is possible to select, using statistical analysis, Unigene clusters with a predicted eye-predominant expression. The Unigene database provides a very user friendly interface to perform such kind of queries. By using this interface, I retrieved 104 human cDNA clusters of Expressed Sequence Tags predicted to have predominant expression in the eye when compared to other tissues. The selection of transcripts with exclusive or predominant expression in the eye was performed using the database option to select for clusters enriched in ESTs derived from a given tissue of interest (see chapter *Materials and methods* and Figure 12), and subsequently download (in FASTA format) all the sequences belonging to the selected clusters.

The screenshot shows the UniGene database interface. At the top, there is a search bar with the query "9606[txcd] AND eye[restricted]". Below the search bar, there are tabs for "Limits", "Preview/Index", "History", "Clipboard", and "Details". The "Display" dropdown is set to "Summary", and "Show" is set to "20". The "Sort by" dropdown is set to "Send to". The results are displayed in a table with columns for item number, UniGene ID, description, number of sequences, and links.

Item	UniGene ID	Description	Sequences	Links
1	<a href="#">Hs.700881</a>	Transcribed locus, moderately similar to XP_001108532.1 similar to Zinc finger protein 593 (Zinc finger protein T86) isoform 2 [Macaca mulatta]	20 sequences	<a href="#">Links</a>
2	<a href="#">Hs.700312</a>	Transcribed locus	12 sequences	<a href="#">Links</a>
3	<a href="#">Hs.695289</a>	FAM57B	52 sequences	<a href="#">Links</a>
4	<a href="#">Hs.694925</a>	Family with sequence similarity 57, member B	14 sequences	<a href="#">Links</a>

**Figure 12. Example of a Unigene query for EST clusters with restricted expression in human eye cDNA libraries.**

Even though the Unigene database identifies the ESTs that should belong to the same transcript and groups them together in a single cluster, it does not provide a consensus sequence for each cluster but only the sequences of all the ESTs belonging to it. Therefore, to obtain the consensus sequences of a given Unigene cluster, the EST sequences must be independently assembled. This was achieved by using the CAP software, which performs multiple sequence alignment of nucleotide sequences ([http://www.infobiogen.fr/services/analyseseq/cgi-bin/cap\\_in.pl](http://www.infobiogen.fr/services/analyseseq/cgi-bin/cap_in.pl)). Once the candidate clusters were identified, it was necessary to carry out sequence analysis on all of them to define their identity. To this purpose, I first mapped each cluster-specific consensus on the human genome using the May 2004 release of the Human Genome Browser at University of California Santa Cruz (UCSC) at <http://genome.ucsc.edu/cgi-bin/hgBlat>. By BLAT analysis, I could determine the genomic locations of all clusters and their possible correspondence to already known genes. This analysis revealed that 60 out of the starting 104 cDNAs corresponded to either known genes with an already well-documented retinal expression profile or with an already reported functional role in eye development. All these clusters were therefore excluded from further analysis. Examples of the discarded clusters (see also Table 5) are represented by cluster Hs.517978, which maps to chromosome 3 and corresponds to the well studied *GNAT1* gene, already known to cause congenital stationary night blindness, and cluster Hs.162754, mapping to chromosome 19 and corresponding to the *LIM2* gene, which is an already known lens intrinsic membrane protein. The remaining 44 cDNAs did not correspond to well characterize genes and no information was available in terms of their expression profile at the time of this analysis (spring 2005.) Due to the constant



update of the databases used in this study, a revised analysis, performed in 2007, showed slight differences in the current status of the selected EST clusters (see Table 5, column *Notes*).

**Table 5. List of all the EST clusters retrieved from the Unigene database.**

	<b>EST cluster</b>	<b>Corresponding gene</b>	<b>In silico expression (number of ESTs for each tissue)</b>	<b>Function</b>	<b>Notes</b>
1.	Hs.117694	<i>CABP5</i>	Eye(13) Muscle(1)	The product of this gene belongs to a subfamily of calcium binding proteins, which share similarity to calmodulin. Calcium binding proteins are an important component of calcium mediated cellular signal transduction.	
2.	Hs.31746	<i>SCRT</i>	Eye(8) Brain(12) Pancreas(1) Testis(1)	It codes for a neural-specific transcriptional repressor that binds to E-box motifs. The protein may promote neural differentiation and may be involved in cancers with neuroendocrine features.	
3.	Hs.288655	<i>OTX2</i>	Eye(44) Brain(6)	Plays a role in the development of the brain and the sense organs.	
4.	Hs.114762	<i>IRBP</i>	Eye(64) Brain(10) Blood(1) Muscle(1)	IRBP shuttles 11-cis and all trans retinoids between the retinol isomerase in the pigment epithelium and the visual pigments in the photoreceptor cells of the retina.	
5.	Hs.309958	<i>GUCY2D</i>	Eye(4) Lung(2) Prostate(2)	Plays a key role in the phototransduction cascade by controlling intracellular calcium concentration via the influence on cation channels of its	

				enzymatic product, guanosine 3', 5'-cyclic monophosphate (cGMP).	
6.	Hs.307096	<i>LACRT</i>	Eye(82) Mammary gland(1)	Function in augmenting lachrymal cell secretion.	
7.	Hs.194756	<i>SIX6</i>	Eye(11)	Involved in eye development.	
8.	Hs.139263	<i>CACNA1F</i>	Eye(16) Lung(3) Muscle(2)	Voltage-sensitive calcium channel mediate the entry of calcium ions into excitable cells.	
9.	Hs.118555	<i>FSCN2</i>	Eye(11) Ovary(1) Lymph node(1)	Acts as an actin bundling protein. May play a pivotal role in photoreceptor cell-specific events, such as disk morphogenesis.	
10.	Hs.60843	<i>KCNA1</i>	Eye(4) Brain(2) Lung(5)	Mediates voltage-dependent potassium ion permeability of excitable membranes; causes episodic ataxia without myokymia.	
11.	Hs.33538	<i>RP1L1</i>	Eye(21)	Retinal-specific; expressed in photoreceptor.	
12.	Hs.2133	<i>RPE65</i>	Eye(18) Brain(7)	Plays important roles in the production of 11-cis retinal and in visual pigment regeneration.	
13.	Hs.546247	<i>CRYGD</i>	Eye(17) Ovary(2)	Crystallins are the dominant structural components of the vertebrate eye lens.	
14.	Hs.534315	<i>GNB3</i>	Eye(106) Brain(9) Muscle(4) Pituitary gland(11)	Guanine nucleotide-binding proteins (G proteins) are involved as a modulator or transducer in various transmembrane signaling systems.	
15.	Hs.533022	<i>CRYBB3</i>	Eye(18)	Crystallins are the dominant structural components of the vertebrate eye lens	
16.	Hs.530311	<i>LCN1</i>	Eye(220)	Member of human tear prealbumin.	
17.	Hs.517978	<i>GNAT1</i>	Eye(109) Brain(10)	Transducin is a 3-subunit guanine nucleotide-binding protein (G protein)	

				which stimulates the coupling of rhodopsin and cGMP-phosphodiesterase during visual impulses. The transducin alpha subunits in rods and cones are encoded by separate genes. This gene encodes the alpha subunit in rods.	
18.	Hs.479905	<i>PRL1</i>	Eye (114)	This gene encodes a member of the proline-rich protein family. The protein may provide a protective function at the eye surface	
19.	Hs.467538	<i>OPTC</i>	Eye(55) Brain(11)	Opticin is present in significant quantities in the vitreous of the eye and also localizes to the cornea, iris, ciliary body, optic nerve, choroid, retina, and fetal liver. Opticin may noncovalently bind collagen fibrils and regulate fibril morphology, spacing, and organization.	
20.	Hs.449771	<i>CHX10</i>	Eye(14) Brain(2)	CHX10 may control retinal bipolar cell specification or differentiation by repressing genes required for the development of other cell types.	
21.	Hs.435845	<i>ESRRB</i>	Eye(14) Colon(1) Kidney(2) Liver(2) Lung(1) Muscle(2) Pancreas(1)	This gene encodes a protein with similarity to the estrogen receptor. Its function is unknown; however, a similar protein in mouse plays an essential role in placental development.	
22.	Hs.416707	<i>ABCA4</i>	Eye(16) Lung(1) Muscle(1) Placenta(2)	Retinoids, and most likely retinal, are the natural substrates for transport by ABCA4 in rod outer segments.	
23.	Hs.415790	<i>CRYBA2</i>	Eye(88) Pancreas(19) Placenta(3)	Crystallins are the dominant structural components of the	

				vertebrate eye lens.	
24.	Hs.410397	<i>KRT3</i>	Eye(25)	This type II cyokeratin is specifically expressed in the corneal epithelium with family member KRT12 and mutations in these genes have been associated with Meesmanns Corneal Dystrophy.	
25.	Hs.376209	<i>CRYGS</i>	Eye(183) Brain(8) Blood(2)	This gene encodes the most significant gamma-crystallin in adult eye lens tissue.	
26.	Hs.373074	<i>CRYBB2</i>	Eye(309) Lung (1)	This gene encodes crystallin in adult eye lens tissue.	
27.	Hs.279887	<i>AIPL1</i>	Eye(133) Brain(6) Muscle(6)	The photoreceptor/pineal-expressed gene, AIPL1, encoding aryl-hydrocarbon interacting protein-like 1, was mapped within the LCA4 candidate region. The protein contains three tetratricopeptide motifs, consistent with nuclear transport or chaperone activity.	
28.	Hs.251687	<i>RP1</i>	Eye(14) Trachea(12) Muscle(6)	Mutations in this gene cause autosomal dominant RP, and the encoded protein has an important but unknown role in photoreceptor biology.	
29.	Hs.249186	<i>CRX</i>	Eye(66) Muscle(2)	The protein encoded by this gene is a photoreceptor-specific transcription factor, which plays a role in the differentiation of photoreceptor cells. This homeodomain protein is necessary for the maintenance of normal cone and rod function.	
30.	Hs.247565	<i>RHO</i>	Eye(439) Brain(10) Muscle(40)	This is the transmembrane protein which, when	

				photoexcited, initiates the visual transduction cascade.	
31.	Hs.233363	<i>GUCA1C</i>	Eye(15)	This Ca(2+)-sensitive regulation of guanylyl cyclase (GC) is a key event in recovery of the dark state of rod photoreceptors following light exposure.	
32.	Hs.184085	<i>CRYAA</i>	Eye(281) Kidney(23) Liver(1) Placenta(1) Thymus(1)	This gene encodes crystallin in adult eye lens tissue.	
33.	Hs.162754	<i>LIM2</i>	Eye(32)	LIM2 functions in some way as a junctional component, possibly involved with lens cell communication.	
34.	Hs.151710	<i>PDE6A</i>	Eye(69) Muscle(20) Brain(6)	PDE6A encodes the cyclic-GMP (cGMP) specific phosphodiesterase 6A alpha subunit, expressed in cells of the retinal rod outer segment.	
35.	Hs.129702	<i>BFSP1</i>	Eye(92) Liver(10) Mammary gland(2) Skin(2) Bone(2)	More than 99% of the vertebrate ocular lens is comprised of terminally differentiated lens fiber cells. Lens-specific intermediate filament-like protein BFSP1 is expressed only after fiber cell differentiation has begun.	
36.	Hs.125750	<i>KERA</i>	Eye(30) Intestine(2)	Important to the transparency of the cornea.	
37.	Hs.120090	<i>C1ORF36 (RD3)</i>	Eye(21) Brain(10) Lung(1)	The retinopathy-associated RD3 protein is part of subnuclear protein complexes involved in diverse processes, such as transcription and splicing.	
38.	Hs.104637	<i>SLC1A7</i>	Eye(25) Brain(5) Muscle(2)	Sodium:dicarboxylate symporter activity.	
39.	Hs.92858	<i>GUCA1A</i>	Eye(84) Testis(38) Brain(3)	Stimulates guanylyl cyclase 1 (GC1) when free calcium	

				ions concentration is low and inhibits GC1 when free calcium ions concentration is elevated. This Ca(2+)-sensitive regulation of GC is a key event in recovery of the dark state of rod photoreceptors following light exposure.	
40.	Hs.89606	<i>NRL</i>	Eye(57) Brain(8)	This gene encodes a basic motif-leucine zipper transcription factor of the Maf subfamily. The encoded protein is conserved among vertebrates and is a critical intrinsic regulator of photoreceptors development and function.	
41.	Hs.80539	<i>RCV1</i>	Eye(134) Brain(6) Muscle(5)	This gene encodes a member of the recoverin family of neuronal calcium sensors. The encoded protein prolongs the termination of the phototransduction cascade in the retina by blocking the phosphorylation of photo-activated rhodopsin.	
42.	Hs.72981	<i>NEUROD1</i>	Eye(32) Brain(10) Lung(1) Muscle(13) Pancreas(33)	Differentiation factor required for dendrite morphogenesis and maintenance in the cerebellar cortex. Transcriptional activator.	
43.	Hs.66739	<i>KRT12</i>	Eye(325) Brain(1)	KRT12 encodes the type I intermediate filament chain keratin 12, expressed in corneal epithelia. Mutations in this gene lead to Meesmann corneal dystrophy.	
44.	Hs.63085	<i>MPP4</i>	Eye(31) Brain(1) Liver(1) Muscle(9)	Play a role in retinal photoreceptors development.	
45.	Hs.57690	<i>CRYBA4</i>	Eye(201)	This gene encodes crystallin in adult eye	

				lens tissue.	
46.	Hs.54471	<i>PDE6H</i>	Eye(13) Brain(8)	PDE6H encodes the cyclic-GMP (cGMP) specific phosphodiesterase 6H expressed in cells of the retinal cone outer segment.	
47.	Hs.37135	<i>CRYBB1</i>	Eye(88) Connective tissue(33) Lung(4)	This gene encodes crystallin in adult eye lens tissue.	
48.	Hs.32721	<i>SAG</i>	Eye(117) Muscle(20) Brain(4)	S-arrestin, also known as S-antigen, is a major soluble photoreceptor protein that is involved in desensitization of the photoactivated transduction cascade.	
49.	Hs.1933	<i>RLBP1</i>	Eye(56) Skin(16)	The protein encoded by this gene is a 36-kD water-soluble protein which carries 11-cis-retinaldehyde or 11-cis-retinal as physiologic ligands. It is a functional component of the visual cycle.	
50.	Hs.1892	<i>PNMT</i>	Eye(5) Brain(6)	The product of this gene catalyzes the last step of the catecholamine biosynthesis pathway, which methylates norepinephrine to form epinephrine (adrenaline). The enzyme also has beta-carboline 2N-methyltransferase activity. This gene is thought to play a key step in regulating epinephrine production.	
51.	Hs.1857	<i>PDE6G</i>	Eye(224) Connective tissue(17) Muscle(7)	PDE6G encodes the cyclic-GMP (cGMP) specific phosphodiesterase 6G gamma subunit, expressed in cells of the retinal rod outer segment.	
52.	Hs.1544	<i>RGR</i>	Eye(24) Brain(15) Muscle(5)	The protein acts as a photoisomerase to catalyze the conversion of all-	

				trans-retinal to 11-cis-retinal. The reverse isomerization occurs with rhodopsin in retinal photoreceptor cells.	
53.	Hs.308	<i>ARR3</i>	Eye(24) Lymph node(1) Muscle(2)	May play a role in an as yet undefined retina-specific signal transduction. Could bind to photoactivated-phosphorylated red/green opsins.	
54.	Hs.278957	<i>RAX</i>	Eye(14) Hart(1)	The Rax homeobox gene (also known as Rx, with the human gene designated RAX or RX) is expressed very early in retinal development and appears to direct the initial specification of retinal cell fate and the subsequent proliferation of retinal stem cells.	
55.	Hs.131010	<i>NEUROD4</i>	Eye(17) Brain(1) Testis(2)	Appears to mediate neuronal differentiation.	
56.	Hs.72910	<i>CRYGC</i>	Eye(23) Placenta(1)	This gene encodes crystallin in adult eye lens tissue.	
57.	Hs.46275	<i>CRYBA1</i>	Eye(123)	This gene encodes crystallin in adult eye lens tissue.	
58.	Hs.209249	<i>IMPG2</i>	Eye(13) Brain(6)	Interphotoreceptor matrix proteoglycan-2 is part of an extracellular complex occupying the interface between photoreceptors and the retinal pigment epithelium in the fundus of the eye.	
59.	Hs.290856	<i>SSBP2</i>	Brain(8) Eye(7) Lung(3) Pancreas(3)	Single-stranded DNA-binding protein 2 involved in regulation of transcription.	
60.	Hs.440417	<i>GRIA4</i>	Eye(23) Brain(83) Ear(1) Testis(2)	Ionotropic glutamate receptor. L-glutamate acts as an excitatory neurotransmitter at many synapses in the central nervous system.	
61.	Hs.185777	<i>TMIE</i>	Eye(10) Colon(1)	Transmembrane inner ear protein -	



			Kidney(2) Muscle(1) Testis(1)	may play some role in a cellular membrane location. May reside within an internal membrane compartment and function in pathways such as those involved in protein and/or vesicle trafficking.	
62.	Hs.465612	<i>none</i>	Brain(9) Eye(5) Lung(2)	unknown	This cluster was retired in the 2007 version of Unigene
63.	Hs.444805	<i>none</i>	Eye(28) Brain(7) Liver(1) Muscle(1)	unknown	This cluster was retired in the 2007 version of Unigene
64.	Hs.446662	<i>none</i>	Eye(9) Brain(2) Kidney(1) Placenta(1)	unknown	This cluster was retired in the 2007 version of Unigene
65.	Hs.62813	<i>INSM2</i>	Brain(11) Eye(4)	unknown	
66.	Hs.546732	<i>none</i>	Eye(10) Brain(5) Muscle(1)	unknown	
67.	Hs.445613	<i>none</i>	Eye(12)	unknown	
68.	Hs.154140	<i>OSAP</i>	Eye(16) Mammary gland(1) Prostate(1) Skin(2) Uterus(4)	unknown	
69.	Hs.149585	<i>GLULD1</i>	Eye(10) Tongue(1)	Glutamate-ammonia ligase (glutamine synthase) domain containing 1	
70.	Hs.131130	<i>KCNV2</i>	Eye(19) Brain(2) Muscle(1) Testis(4)	Modulates channel activity by shifting the threshold and the half-maximal activation to more negative values	
71.	Hs.354243	<i>none</i>	Eye(18) Brain(1) Prostate(1)	unknown	
72.	Hs.240053	<i>GSG1</i>	Eye(64) Brain(42) Bone(1) Muscle(1) Ovary(4) Placenta(1) Testis(19)	unknown	
73.	Hs.40808	<i>none</i>	Eye(26) Brain(17) Kidney(5)	unknown	

			Placenta(6)		
74.	Hs.33102	<i>TFAP2B</i>	Eye(147) Brain(14) Heart(11) Kidney(23) Lung(2) Mammary gland(45) Muscle(9) Skin(4)	AP-2 activate genes involved in a large spectrum of important biological functions including proper eye, face, body wall, limbs and neural tube development.	
75.	Hs.444181	<i>ZNF536</i>	Eye(12) Colon(1) Brain(9) Lung(1)	unknown	
76.	Hs.21162	<i>RTBDN</i>	Eye(35) Brain(24) Bone(1) Liver(1) Lung(3) Skin(1)	C1q-domain containing protein.	
77.	Hs.503113	<i>SIX3OS</i>	Eye(5) Lung(7)	unknown	
78.	Hs.441592	<i>OTX2OS</i>	Eye(12)	unknown	
79.	Hs.386402	<i>none</i>	Eye(10) Colon(1) Bone(1)	unknown	
80.	Hs.493589	<i>C1orf32</i>	Eye(9) Brain(4) Placenta(2) Testis(3)	Transmembrane and immunoglobulin domain-containing protein.	
81.	Hs.295015	<i>none</i>	Eye(6) Brain(7) Pancreas(11)	unknown	
82.	Hs.40814	<i>none</i>	Eye(13)	unknown	
83.	Hs.532691	<i>none</i>	Eye(22)	unknown	Novel QRX transcript
84.	Hs.433492	<i>ANKRD33</i>	Eye(8) Placenta(7)	The function of ankyrin repeat domains is to mediate protein-protein interactions.	
85.	Hs.433493	<i>C1QL2</i>	Eye(3) Brain(6) Lung(1)	C1q-domain containing protein - subunit of the C1 enzyme complex that activates the serum complement system.	
86.	Hs.473495	<i>none</i>	Eye(5) Brain(2) Kidney(2) Pancreas(2) Stomach(1) Testis(2)	unknown	
87.	Hs.69749	<i>none</i>	Eye(13) Brain(6) Blood(1) Kidney(1) Prostate(2)	unknown	
88.	Hs.247888	<i>GNG13</i>	Eye(41) Brain(3)	Guanine nucleotide-binding proteins (G proteins) are	

				involved as a modulator or transducer in various transmembrane signaling systems. The beta and gamma chains are required for the GTPase activity, for replacement of GDP by GTP, and for G protein-effector interaction.	
89.	Hs.124010	<i>none</i>	Eye(9) Brain(2) Lung(1) Mammary gland(1) Ovary(1) Prostate(1) Skin(1) Testis(1)	unknown	
90.	Hs.171485	<i>none</i>	Eye(4) Brain(5) Pancreas(5) Uterus(1)	unknown	
91.	Hs.221513	<i>none</i>	Eye(14) Testis(1)	unknown	
92.	Hs.527819	<i>none</i>	Eye(12) Lung(1) Muscle(1)	unknown	
93.	Hs.148427	<i>LHX3</i>	Eye(10) Brain(4)	Transcription factor that is required for pituitary development and motor neuron specification.	
94.	Hs.131342	<i>CCL26</i>	Eye(8) Colon(2) Hart(1) Kidney(1) Lung(2)	Chemokine (C-C motif) ligand 2)- may contribute to the eosinophil accumulation in atopic diseases.	
95.	Hs.549054	<i>MIP</i>	Eye(13) Brain(1)	Major intrinsic protein of lens fiber.	
96.	Hs.449884	<i>CPLX4</i>	Eye(129) Brain(1) Muscle(1)	Complexin IV - positively regulates a late step in synaptic vesicle exocytosis.	
97.	Hs.493947	<i>none</i>	Eye(5) Brain(5) Uterus(1)	unknown	
98.	Hs.283661	<i>none</i>	Eye(12) Brain(6) Lung(1) Pancreas(3)	unknown	
99.	Hs.271783	<i>none</i>	Eye(10) Brain(2) Spleen(1)	unknown	This cluster was retired in the 2007 version of Unigene
100.	Hs.245886	<i>none</i>	Eye(8)	unknown	This cluster

			Mammary gland(2)		was retired in the 2007 version of Unigene
101.	Hs.193876	<i>none</i>	Eye(7) Lung(2) Testis(1)	unknown	
102.	Hs.32766	<i>none</i>	Eye(8) Brain(3) Lung(2) Ovary(1) Uterus(1)	unknown	
103.	Hs.130348	<i>none</i>	Eye(27) Brain(11) Muscle(3) Ovary(1)	unknown	
104.	Hs.435710	<i>none</i>	Eye (52)	unknown	

### 3.1.2 Expression studies of selected human cDNA clusters by RT-PCR

The newly-identified transcripts underwent experimental procedures aimed at validating their *in silico* predicted retinal expression. As a first step in this verification, reverse-transcriptase polymerase chain reaction (RT-PCR) was performed. This type of analysis was essential to validate the exclusive or predominant retinal expression of the *in silico* selected genes, i.e. only genes confirmed by RT-PCR were considered for further expression studies by RNA *in situ* hybridization. Out of forty-four cDNAs showing no correspondence with already characterized eye genes, thirty were selected for RT-PCR analysis (Table 6). The remaining fourteen clusters were excluded from the analysis as they were either mostly composed by repeated sequences (such as Alu, LINE and other kinds of repeats) or were present in more than one copy in the human genome, which prevented the design of specific oligonucleotide primers and a reliable RT-PCR analysis. The RT-PCR experiments were performed on RNA purified from six different adult human tissues (kidney, lung, liver, skeletal muscle, brain, and retina). Each RT-PCR experiment included several controls: no template control, genomic DNA and RT– control (sample treated in the same way as the others except that no reverse transcriptase enzyme was added). Amplification of the house keeping gene *GAPDH* was used to normalize cDNA amounts among the different samples. Out of the thirty analyzed cDNAs, six were expressed exclusively in the retina (an example is shown in Figure 13A), five were expressed in retina and brain (Figure 13B), and the remaining ones were expressed in retina but also in a few other tissues (Figure 13C). The RT-PCR results of all the clusters analyzed are summarized in Table 6. Two clusters failed to amplify even after several attempts with different oligonucleotide pairs.

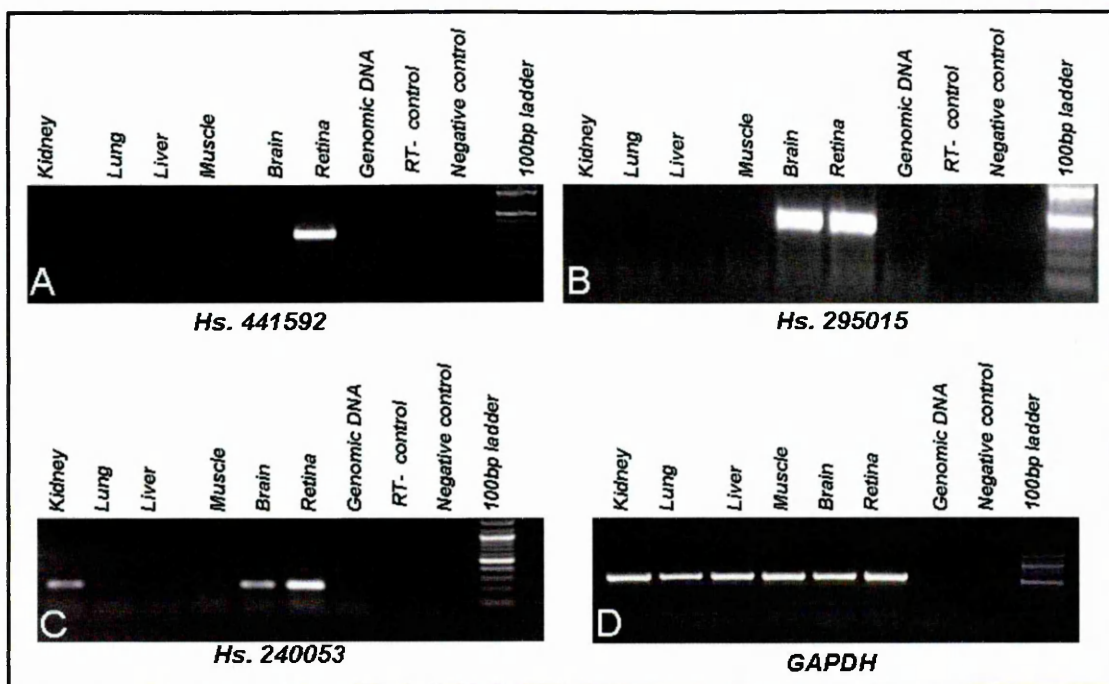


**Figure 13. Examples of the RT-PCR analysis performed for the selected thirty cDNA clusters.**

A- example of a cDNA cluster showing the exclusive RT-PCR expression in the retina (Hs.441592), B- example of a cluster with expression in both retina and brain (Hs.295015), C- example of a cluster with expression in the retina and few other tissues, D- *GAPDH* amplification control

Concomitantly to the RT-PCR analysis, I performed additional, sequence analysis of all the selected clusters, which was aimed at the recognition of protein functional domains that could shed light on the possible function of these genes within the human retina. For this analysis, I exploited the web-based tool Simple Modular Architecture Research Tool-SMART (<http://smart.embl-heidelberg.de/>), which allows to identify and annotate protein domains and to reconstruct complex protein domain architectures. Results of this analysis are also reported in Table 6.

**Table 6. cDNAs selected for experimental validation of predominant retinal expression by RT-PCR.**

	<b>cDNA cluster</b>	<b>Gene symbol</b>	<b>Function</b>	<b>Protein domains prediction by SMART</b>	<b>RT-PCR expression</b>
1.	Hs.40814	<i>none</i>	unknown		Retina Brain Kidney
2.	Hs.441592	<i>OTX2OS</i>	unknown		Retina
3.	Hs.532691	<i>none</i>	unknown		Retina
4.	Hs.354243	<i>none</i>	unknown		Retina Brain Muscle
5.	Hs.131130	<i>KCNV2</i>	Modulates channel activity by shifting the threshold and the half-maximal activation to more negative values	Signal peptide, K <sup>+</sup> channel tetramerisation domain, coiled coil region, transmembrane domain, ion transport protein domain	Retina Kidney
6.	Hs.433492	<i>ANKRD33</i>	The function of ankyrin repeat domains is to mediate protein-protein interactions	2 ankyrin repeat domains	Retina
7.	Hs.154140	<i>OSAP</i>	Corneal endothelium specific protein 1-unknown function		Retina Kidney Lung Liver Muscle Brain
8.	Hs.433493	<i>C1QL2</i>	C1q-domain containing protein - subunit of the C1 enzyme complex that activates the serum complement system		Retina Kidney Lung Liver Muscle Brain
9.	Hs.473495	<i>none</i>	unknown		Retina Kidney Lung Liver Muscle Brain
10.	Hs.493589	<i>C1orf32</i>	Transmembrane and immunoglobulin domain-containing protein		Retina Kidney Lung Liver Muscle Brain
11.	Hs.69749	<i>none</i>	unknown		Retina Brain
12.	Hs.21162	<i>RTBDN</i>	C1q-domain containing protein	Complement component C1q domain	Retina
13.	Hs.247888	<i>GNG13</i>	Guanine nucleotide binding protein		Retina Brain

14.	Hs.124010	<i>none</i>	unknown		No amplification
15.	Hs.171485	<i>none</i>	unknown		Retina Brain Muscle Kidney Liver
16.	Hs.240053	<i>GSG1</i>	Germ cell specific gene 1-unknown function	GSG1-like protein	Retina Kidney Brain
17.	Hs.386402	<i>none</i>	unknown		Retina Kidney Lung Liver Muscle Brain
18.	Hs.295015	<i>none</i>	unknown		Retina Brain
19.	Hs.221513	<i>none</i>	unknown		Retina Brain
20.	Hs.527819	<i>none</i>	unknown		No amplification
21.	Hs.444181	<i>ZNF536</i>	May be involved in transcriptional regulation	ZnF C2H2 domain	Retina Brain
22.	Hs.503113	<i>SIX3OS</i>	unknown		Retina
23.	Hs.148427	<i>LHX3</i>	Transcription factor that is required for pituitary development and motor neuron specification	2 LIM domains and HOX homeodomain	Retina
24.	Hs.131342	<i>CCL26</i>	Chemokine (C-C motif) ligand 2)- may contribute to the eosinophil accumulation in atopic diseases.	SCY- Intercrine alpha family (small cytokine C-X-C) (chemokine CXC)	Retina Lung Kidney
25.	Hs.549054	<i>MIP</i>	Major intrinsic protein of lens fiber		Retina Kidney Lung Liver Muscle Brain
26.	Hs.185777	<i>TMIE</i>	Transmembrane inner ear protein - may play some role in a cellular membrane location. May reside within an internal membrane compartment and function in pathways such as those involved in protein and/or vesicle trafficking.		Retina Kidney Lung Liver Muscle Brain
27.	Hs.40808	<i>none</i>	unknown		Retina



					Kidney Lung Liver Muscle Brain
28.	Hs.33102	<i>TFAP2B</i>	Transcription factor AP-2 beta- activate genes involved in a large spectrum of important biological functions including proper eye, face, body wall, limbs and neural tube development	Transcription factor AP-2	Kidney Brain Retina
29.	Hs.149585	<i>GLULD1</i>	Glutamate-ammonia ligase (glutamine synthase) domain containing 1		Kidney Lung Muscle Retina
30.	Hs.449884	<i>CPLX4</i>	Complexin IV - positively regulates a late step in synaptic vesicle exocytosis	2 LIM domains and HOX homeodomain	Retina Kidney Lung Liver Brain

This analysis was instrumental in identifying several interesting putative candidate genes for retinal disorders. For example, EST clusters Hs.21162 and Hs.433493 showed interesting RT-PCR expression patterns and predicted protein domains. Cluster Hs.21162 was expressed exclusively in retina (Figure 15). On the other hand, cluster Hs.433493 showed weak expression in kidney, lung, liver, skeletal muscle and very strong expression in brain and retina. Both clusters, as assessed by SMART analysis, presented open reading frames (ORFs) that are predicted to contain *complement component C1q domains*. These observations are very intriguing considering the recent findings<sup>98, 107</sup> that in many cases age-related macular degeneration (AMD) is caused by a sequence variation in one of the members of the complement system- *complement factor H*, which is one of the inhibitors of the complement system. Due to the fact that the *C1q domain* triggers the complement pathway<sup>108</sup>,

---

clusters Hs.21162 and Hs.433493, may represent new candidate genes for age-related macular degeneration.

Based on the results of the above described *in silico* and experimental integrated analysis, I was able to restrict my interest to a more confined number of genes to be further analyzed; namely fifteen cDNA clusters were selected for further expression analysis by RNA *in situ* hybridization in human retina. The fifteen clusters were selected based on their expression patterns assessed by RT-PCR analysis and protein domain prediction (see Table 6).

### ***3.1.3 Expression studies of the selected human cDNA clusters by RNA in situ hybridization***

To test the expression of the selected retina-specific transcripts in different retinal cell types, I performed RNA *in situ* hybridization (RNA ISH) on human eye sections. RNA ISH is a powerful and sensitive technique that allows to define tissue expression patterns almost at a cellular level. Therefore, by using this technique, it is possible to determine the retinal cell layer and make assumptions on the retinal cell type expressing the gene under analysis. This is possible because the retina is characterized by a well-organized distribution of seven types of cells in histologically distinguishable layers (see *Introduction*). Determination of the precise cells expressing the genes of interest can be crucial in defining candidate genes for different eye diseases and therefore selecting the appropriate panel of patients to be screened for mutation in a given gene.

Eye bulbs used in this study were obtained from cornea donors (kindly provided by Italian Eye Bank in Venice), with different background in terms of age, sex, cause of death, postmortem time or possible therapeutic treatment, as

---

reported in the *Material and methods* section. Unevenness in human samples from cornea donors can be seen as a positive variable since in this way I was able to assess expression of selected genes in different genetic and physiological background. In order to establish the best protocol for successful handling of human eye tissues for RNA *in situ* hybridization, I applied different conditions of tissue fixation and embedding. The priority was to achieve a balance between a good histological preservation and the prevention of mRNA degradation. Both features are fundamental for a successful RNA ISH experiment: abundant mRNA allows an efficient labeling and therefore detectable signal and a good histology permit a correct interpretation of the identity of positive cells.

Several human eye bulbs were treated differentially after cornea excision in order to set up the procedure. In the first pair of eye bulbs, the lens and part of the vitreous had been removed following cornea excision. After sectioning, a hematoxylin/eosin staining was performed to check the quality of the retina. Although the retina was histologically well-preserved, it appeared folded and completely detached from the retinal pigment epithelium (Figure 14A). To avoid the collapse of the retina, I used two different approaches. The first one was to keep the bulbs in fixative solution before dissecting the lens while the second consisted in making small excisions in the sclera to allow better fixative penetration. Both approaches allowed better histological preservation, however the retina was still partially detached from the retinal pigment epithelium (Figure 14B). During the course of this study, I noticed that the status of the retina mainly depends on the postmortem time, i.e. shorter postmortem time guarantees better histological preservation of the retina.

When the most appropriate protocol for histological preservation of the retina was established (see *Material and methods*), I optimized the RNA *in situ* hybridization experiment by assessment of one of the key steps in this procedure that is permeabilization of the tissue. I therefore tested different concentrations of Proteinase K (5, 10, 15 and 20  $\mu\text{g}/\mu\text{l}$ ) to establish the optimal concentration needed to permit probe accessibility while maintaining the integrity of the tissue. The concentration of 10  $\mu\text{g}/\mu\text{l}$  turned out to give the best results. In order to test mRNA preservation after fixation and embedding, I performed RNA ISH with a specific cRNA antisense probe complementary to the highly abundant *Rhodopsin* gene mRNA. This experiment showed specificity of hybridization in the photoreceptor cell layer and demonstrated a good sensitivity of this technique both with histochemical or fluorescent substrates (as shown in Figure 14C and D).

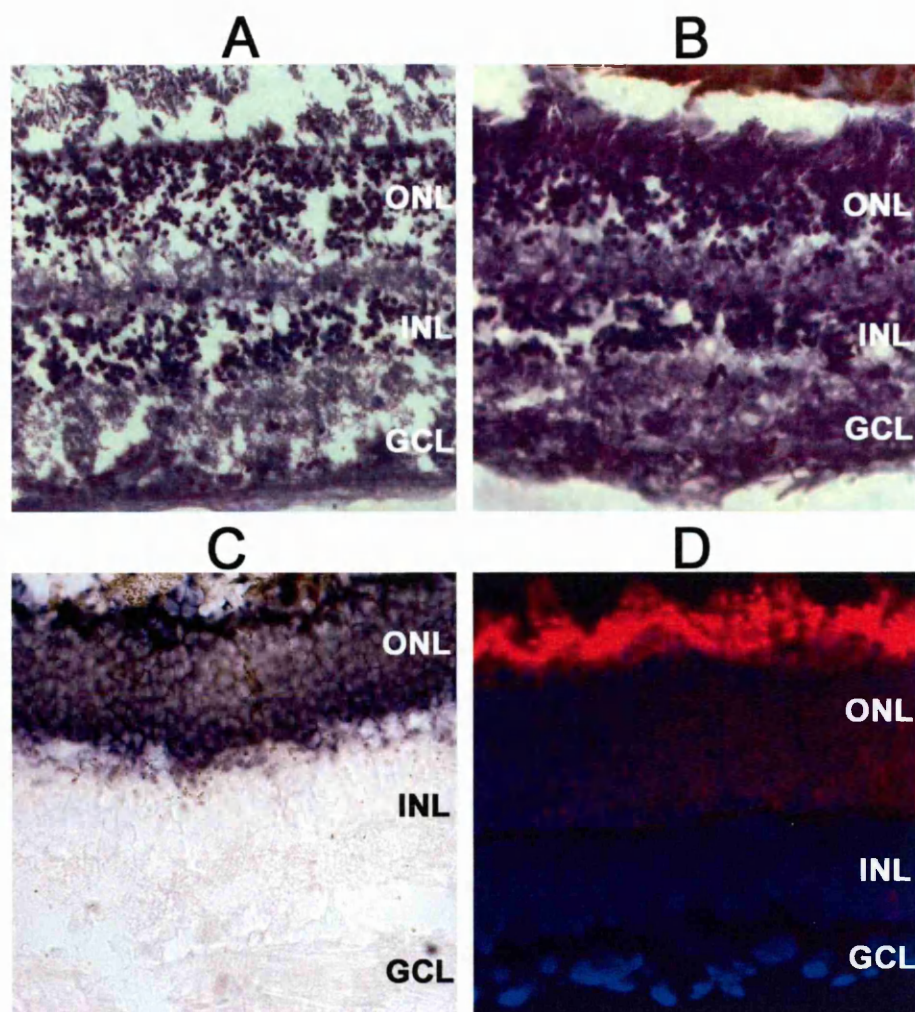


**Figure 14. Optimization of the procedure for the handling of human eye sections for RNA in situ hybridization experiments.**

A- hematoxylin/eosin staining of the retina with the lens removed before fixation;  
B-hematoxylin/eosin staining of the retina with the lens removed after fixation;  
RNA ISH on human retina using the digoxigenin-labeled RNA probe for human rhodopsin developed with histochemical (C) and fluorescence (D) substrate.  
ONL-outer nuclear layer, INL-inner nuclear layer, GCL-ganglion cell layer

After establishing the appropriate experimental protocol for RNA ISH in the human eye, I carried on the expression analysis for the selected cDNA clusters. Out of the fifteen selected cDNA clusters, two, namely Hs.240053 and Hs.444181, analyzed with two independent cRNA probes, showed no detectable expression in the retina. The remaining thirteen clusters showed specific and distinct expression in retinal cells (Table 7).

**Table 7. RT-PCR and RNA ISH expression analysis of the selected fifteen cDNA clusters in human retina.**

<b>Cluster</b>	<b>Corresponding gene</b>	<b>RT-PCR</b>	<b>RNA ISH EXPRESSION</b>
<b>Hs.131130</b>	<i>KCNV2</i>	Retina Kidney	PR
<b>Hs.433492</b>	<i>ANKRD33</i>	Retina	PR INL GCL
<b>Hs.21162</b>	<i>RTBDN</i>	Retina	PR INL GCL
<b>Hs.240053</b>	<i>GSG1</i>	Retina Kidney Brain	no expression
<b>Hs.148427</b>	<i>LHX3</i>	Retina	PR INL GCL
<b>Hs.433493</b>	<i>C1QL2</i>	Retina Kidney Lung Liver Muscle Brain	PR INL GCL
<b>Hs.131342</b>	<i>CCL26</i>	Retina Lung Kidney	PR INL GCL
<b>Hs.33102</b>	<i>TFAP2B</i>	Kidney Brain Retina	PR INL GCL

<b>Hs.354243</b>	<i>none</i>	Retina Brain Muscle	PR INL GCL
<b>Hs.69749</b>	<i>none</i>	Retina Brain	PR INL
<b>Hs.295015</b>	<i>none</i>	Retina Brain	PR INL GCL
<b>Hs.444181</b>	<i>ZNF536</i>	Retina Brain	no expression
<b>Hs.171485</b>	<i>none</i>	Retina Brain Muscle Kidney Liver	PR INL GCL
<b>Hs.221513</b>	<i>none</i>	Retina Brain	PR INL GCL
<b>Hs.449884</b>	<i>CPLX4</i>	Retina Brain Kidney	PR INL GCL

Abbreviations: PR-photoreceptors, INL-inner nuclear layer, GCL-ganglion cell layer

The majority of the analyzed clusters showed mRNA transcription in all the layers of retina, as shown in Table 7. Cluster Hs.21162 (corresponding to the *RTBDN* gene) mapped to chromosome 19p13.13, was exclusively expressed in the retina, as shown by RT-PCR analysis, and sequence analysis suggested that the predicted protein product contains a domain similar to the complement component C1q. RNA *in situ* hybridization experiments were performed on four retinas derived from different individuals and this analysis confirmed, in all the different samples, the same expression throughout the entire retina, i.e. in photoreceptors, inner nuclear layer and ganglion cell layer (Figure 15). Cluster Hs.433492 mapped to chromosome 12q13.13, by RT-PCR analysis was expressed exclusively in retina, and highly transcribed in ganglion cells (GCL), in some cells of the inner nuclear layer (INL) and in the photoreceptors inner segment, while in other parts of the retina the signal was less intense (Figure 15).

Similarly, clusters Hs.449884 and Hs.33102 were expressed in all the layers of the retina, as defined by RNA ISH analysis, in different individuals (Figure 16). Hs.449884 corresponds to the complexin IV (*CPLX4*) gene and showed expression in retina, brain, kidney and liver, while cluster Hs.33102, which corresponds to the transcription factor AP-2 beta (*TFAP2B*), showed expression exclusively in retina, brain and kidney.



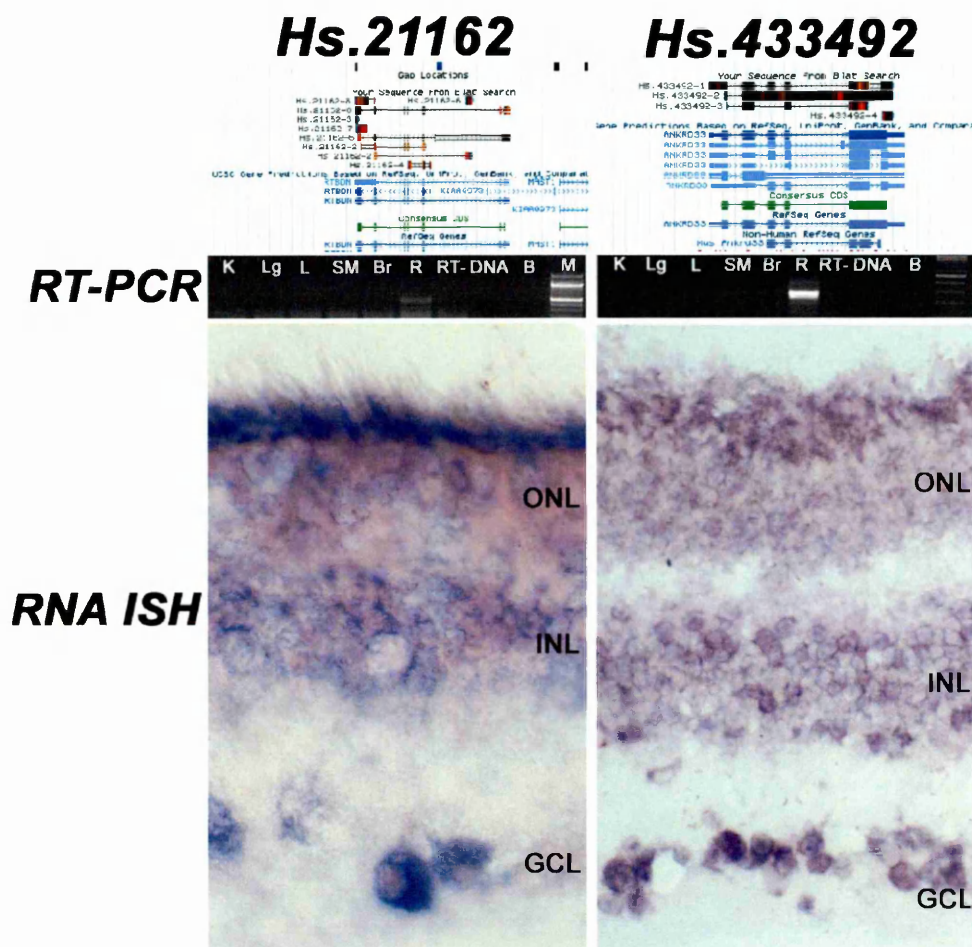


**Figure 15. Expression analysis of clusters Hs.21162 and Hs.433492.**

Cluster Hs.21162 corresponds to the *RTBDN* gene while cluster Hs.433492 corresponds to the *ANKRD33* transcript, as assessed by BLAT analysis on the Human Genome Browser web server at UCSC; RT-PCR analysis showed that both Hs.21162 and Hs.433492 are expressed exclusively in the retina; RNA ISH analysis shows expression of both cDNA clusters in all the retinal layers.

K-kidney, Lg-lung, L-liver, SM-skeletal muscle, Br-brain, R-retina, RT-RT-control, DNA-genomic DNA, B-no template control, M-100bp ladder, ONL-outer nuclear layer, INL-inner nuclear layer, GCL-ganglion cell layer.

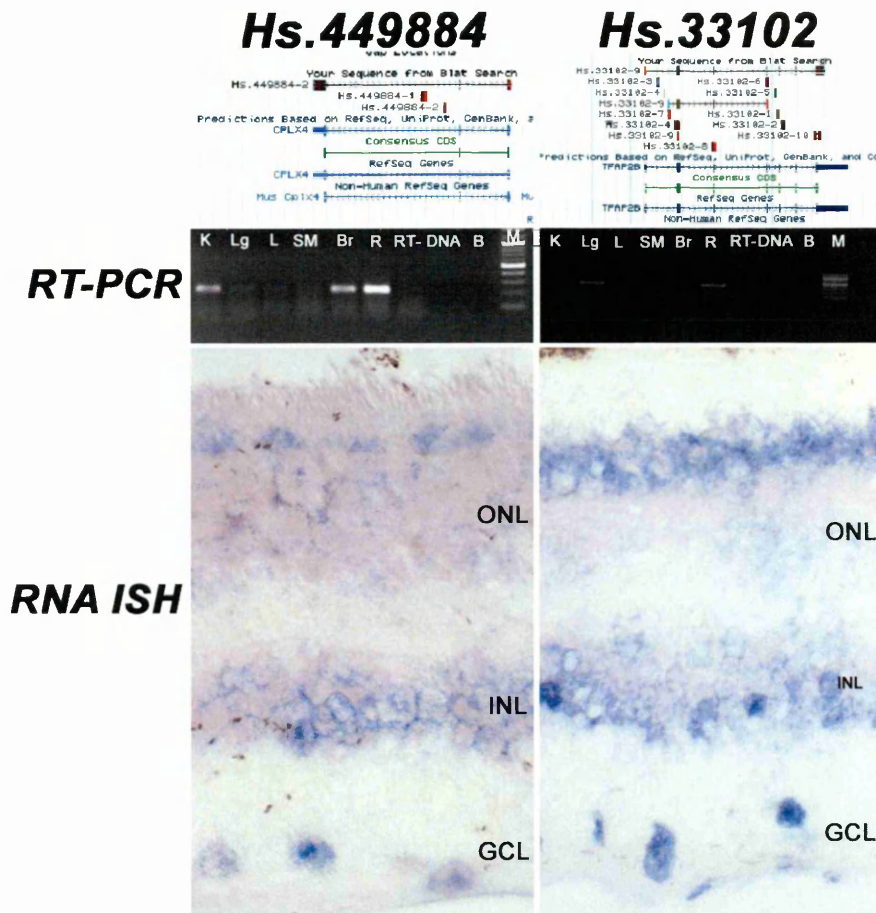


**Figure 16. Expression analysis of clusters Hs.449884 and Hs.33102.**

Clusters Hs.449884 and Hs.33102 correspond to the *Complexin IV* and the transcription factor *AP-2 beta* genes, respectively, as assessed by BLAT analysis; RT-PCR analysis showed expression of the Hs.449884 in kidney, lung, liver, brain and retina while Hs.33102 was expressed in kidney, lung and retina; RNA ISH analysis of the Hs.449884 showed expression in few cells in the outer nuclear layer, inner nuclear layer and in some ganglion cells. Hs.33102 mRNA is more strongly expressed in photoreceptors, while less spread signal is detectable also in the inner nuclear layer and ganglion cell layer. K-kidney, Lg-lung, L-liver, SM-skeletal muscle, Br-brain, R-retina, RT-RT-control, DNA-DNA, B-no template control, M-100bp ladder, ONL-outer nuclear layer, INL-inner nuclear layer, GCL-ganglion cell layer.

Even though the majority of the analyzed clusters were expressed throughout the retina, two clusters showed a more restricted expression. cDNA cluster Hs.131130, as assessed by RT-PCR analysis, was detected in retina and kidney, and RNA *in situ* hybridization, in four different individuals, revealed transcription of this gene exclusively in photoreceptors (Figure 17). Weak expression in the photoreceptor layer and in the inner nuclear layer was observed with the antisense cRNA probe for cluster Hs.69749. Interestingly, this cDNA cluster showed no sequence similarity to any annotated transcript in the genome and RNA was present only in retina and brain, as determined by RT-PCR (Figure 17).

Among the fifteen cDNA clusters selected for RNA *in situ* hybridization analysis, six did not present sequence similarity to known genes (see Table 7). Interestingly, RT-PCR analysis revealed that four of these clusters (Hs. 69749, Hs.295015, Hs.444181 and Hs.221513) have a restricted transcription in the nervous system, i.e. retina and brain. When I carried out the RNA ISH studies in the human eye, I found that clusters Hs.295015 and Hs.221513 did not show restricted expression profile at the cellular level, as in the case of Hs.69749, but cells in all the retinal layers transcribed the mRNA of these unknown transcripts (Figure 18). It would be very interesting to further investigate the function of these clusters in the retina, since exclusive expression in retina and brain suggests a specific role of these genes in neurons. Such preferential expression of Hs. 69749, Hs.295015, Hs.444181 and Hs.221513 in the retina makes these clusters good candidates for retinal disorders.

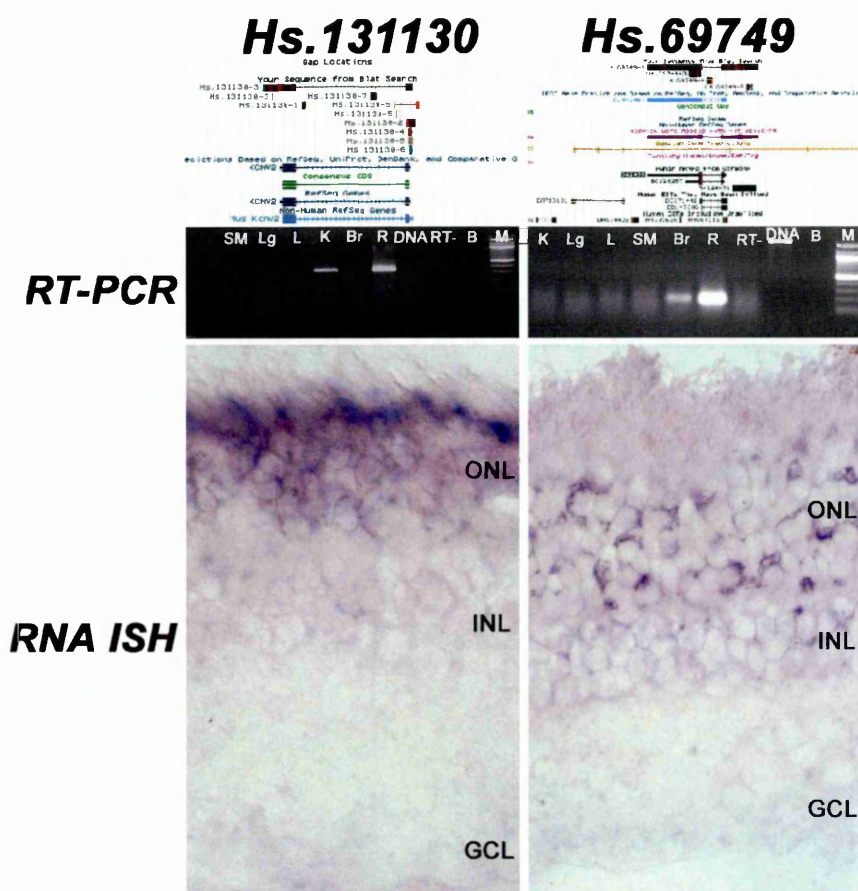


**Figure 17. Expression analysis of clusters Hs.131130 and Hs.69749.**

Cluster Hs.131130 corresponds to the *KCNV2* gene, while Hs.69749 does not share any sequence similarity to already known gene, as assessed by BLAT analysis; RT-PCR analysis showed restricted expression of *KCNV2* in kidney and retina while Hs.69749 is expressed in brain and retina. RNA ISH analysis of the *KCNV2* shows expression exclusively in the outer nuclear layer, while cluster Hs.69749 mRNA is weakly expressed in photoreceptors, and in the inner nuclear layer.

K-kidney, Lg-lung, L-liver, SM-skeletal muscle, Br-brain, R-retina, RT-RT-control, DNA-DNA, B-no template control, M-100bp ladder, ONL-outer nuclear layer, INL-inner nuclear layer, GCL-ganglion cell layer .

It is worth mentioning that all the RNA *in situ* hybridization experiments were performed not only with antisense probes specifically detecting the endogenous mRNA but also with the corresponding sense probes, which acted as controls, for each selected cDNA cluster in four different individuals. Conclusions about the mRNA expression profile of each clusters was made only when no signal was observed with the sense probe and when the expression profile was highly similar in the different individuals analyzed. It is important to underline that out of the fifteen cDNAs selected as putative novel disease genes, only cluster Hs.148427, corresponding to the *LHX3* gene, mapped within the critical region, defined by linkage analysis, of a human disease locus, namely the locus for a form of Joubert syndrome whose corresponding gene has not been identified yet. Joubert syndrome is an autosomal recessive disease, characterized by aplasia/hypoplasia of the cerebellar vermis, abnormal eye movements, ataxia, and mental retardation<sup>109</sup>.

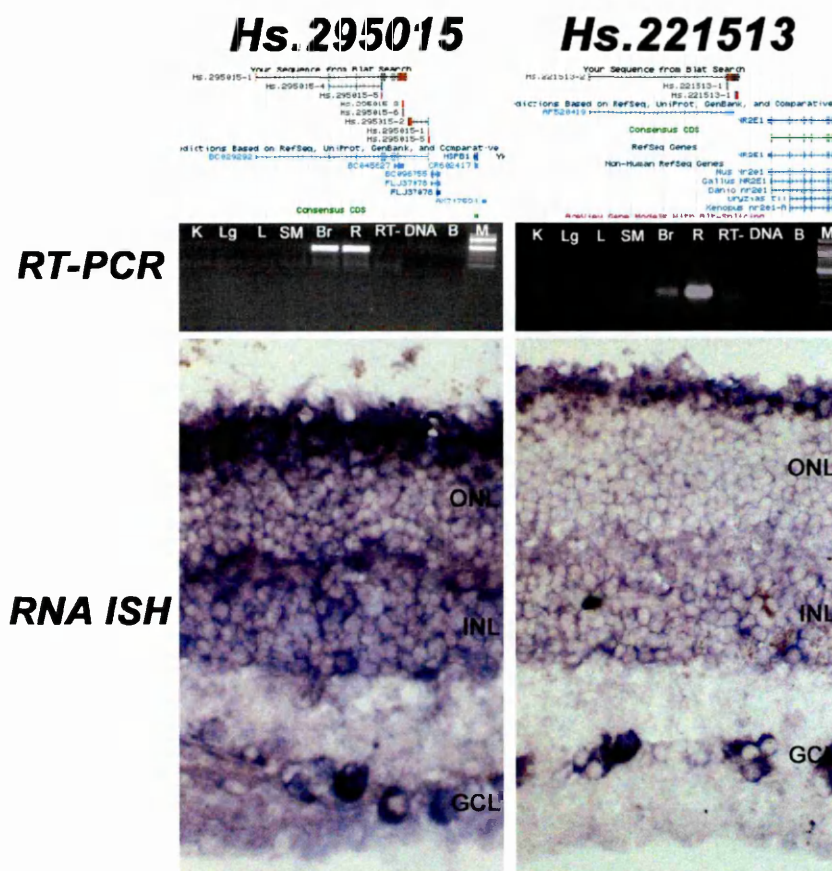


**Figure 18. Expression analysis of clusters Hs.295015 and Hs.221513.**

Clusters Hs.295015 and Hs.221513 share no sequence similarity with any known gene, as assessed by BLAT analysis; RT-PCR analysis showed restricted expression of Hs.295015 and Hs.221513 in brain and retina; RNA ISH signal with cRNA probes for both clusters is detectable in all the layers of the retina.

K-kidney, Lg-lung, L-liver, SM-skeletal muscle, Br-brain, R-retina, RT-RT-control, DNA-DNA, B-no template control, M-100bp ladder, ONL-outer nuclear layer, INL-inner nuclear layer, GCL-ganglion cell layer.

### **3.1.4 Mutation analysis of the cDNA cluster Hs.131130 (*KCNV2*)**

Out of the fifteen cDNA clusters analyzed by RNA *in situ* hybridization only cluster Hs.131130 showed mRNA expression restricted to photoreceptors. Such an expression profile and the fact that the Hs.131130 cluster corresponds to the potassium channel, subfamily V, member 2 (*KCNV2*) gene known to control excitability in neuronal and various other tissues<sup>110</sup> made this cluster a good candidate gene for retinal dystrophies. In order to test whether *KCNV2* was involved in some retinal disorders, mutation analysis was performed on a collection of Italian Leber congenital amaurosis (LCA), retinitis pigmentosa (RP) and cone dystrophy (CD) patients. Screening of 120 LCA, 96 recessive RP and 4 CD patients was performed using DHPLC analysis. All products displaying a DHPLC pattern different from controls were sequenced by direct sequencing. I did not detect any sequence variants in any of the patients available for this study. While this work was in progress, I learned that mutations in the *KCNV2* gene were found by another group in “cone dystrophy with supernormal rod electroretinogram” patients<sup>111, 112</sup>.

### **3.2 GENERATION OF AN RP GENE EXPRESSION ATLAS**

The second part of my PhD project was to generate an expression atlas in human and mouse retinas of all the genes known to cause retinitis pigmentosa (RP). The motivation for this project lies in the fact that RP is one of the leading causes of blindness in world population and even though a number of genes causing RP have been identified there is a significant lack of information regarding the expression of RP genes in the human retina. This limitation may hamper development of proper therapeutic approaches that are normally based on the information gained by the analysis of murine models for this disease. To provide this important information I applied the RNA *in situ* hybridization technique to analyze the expression of all retinitis pigmentosa genes in the human retina and compared this pattern of expression to the localization of the transcripts of the homologous genes in the mouse.

In order to generate an expression atlas representing the RP genes, I performed RNA *in situ* hybridization for 34 known genes involved in the pathogenesis of non-syndromic forms of RP both in human and mouse retinas (Table 8).



**Table 8. Summary of the RNA in situ hybridization expressions in human and mouse retinas.**

<b>GENE</b>	<b>RNA LOCALIZATION IN HUMAN</b>	<b>RNA LOCALIZATION IN MOUSE</b>
<b>ABCA4</b>	PR	PR
<b>AIPL1</b>	PR	PR
<b>CA4</b>	PR, INL, GCL	nd
<b>CERKL</b>	PR, INL, GCL	PR, INL, GCL
<b>CNGA1</b>	PR	PR
<b>CNGB1</b>	PR, INL, GCL	PR, INL, GCL
<b>CRB1</b>	PR, INL	PR, INL
<b>CRX</b>	PR, INL	PR, INL
<b>FSCN2</b>	PR, INL, GCL	PR, INL, GCL
<b>GUCA1B</b>	PR	PR
<b>IMPDH1</b>	PR, INL, GCL	PR, INL, GCL
<b>LRAT</b>	RPE	RPE
<b>MERTK</b>	nd	nd
<b>NR2E3</b>	PR	PR
<b>NRL</b>	PR, INL, GCL	PR, INL, GCL
<b>PAP1</b>	PR, INL, GCL	PR, INL, GCL
<b>PDE6A</b>	PR	PR
<b>PDE6B</b>	PR	PR
<b>PRPF3</b>	PR, INL, GCL	PR, INL, GCL
<b>PRPF31</b>	PR, INL, GCL	PR, INL, GCL
<b>PRPF8</b>	PR, INL, GCL	PR, INL, GCL
<b>RDH12</b>	PR	PR
<b>RDS</b>	PR	PR
<b>RGR</b>	RPE, PR, INL	RPE
<b>RHO</b>	PR	PR
<b>RLBP1</b>	RPE, PR, INL, GCL	RPE, INL, GCL
<b>RP1</b>	PR	PR
<b>RP2</b>	PR, INL, GCL	PR, INL, GCL
<b>RPE65</b>	RPE	RPE
<b>RPGR</b>	PR, INL	PR
<b>RPGR-ORF15</b>	PR	PR, INL, GCL
<b>RPGRIP</b>	PR	PR
<b>SAG</b>	PR	PR
<b>TULP1</b>	PR, INL, GCL	PR, INL, GCL
<b>USH2A</b>	PR, INL, GCL	PR, INL, GCL

Abbreviations: PR-photoreceptors, INL-inner nuclear layer containing bipolar cells, horizontal cells, amacrine cells and Müller glia cells, GCL-ganglion cell layer, RPE-retinal pigment epithelium, nd-not detectable

To retrieve appropriate human and murine templates for this study, a variety of approaches were used including the use of public Expressed Sequence Tag (ESTs) clones, PCR amplification of human/mouse genomic DNA or cDNA prepared from human/mouse total retina RNA with the specific oligonucleotide primers tailed by sequences recognized by the RNA polymerases (T3, T7 or SP6). Finally, some of templates were obtained through generous gifts of external investigators. For more detailed information about each template please refer to Chapter 2.3.2.1 in the *Materials and methods* section.

For the human transcripts, all the experiments were performed on eye sections obtained from more than one individual. As already mentioned in Chapter 3.1.2, eye bulbs were obtained from several individuals with different age, cause of death, post-mortem time before eye removal or possible therapeutic treatment. Information about eye donors is shown in Table 1 in section Materials and methods.

To understand if human samples heterogeneity may interfere with the detected expression patterns, I tested the majority of the genes in individuals 53041 and 62659. Individual 53041 was selected as representative of the samples with short post-mortem time before eye bulbs were removed and fixed, while post-mortem time for the eye sample obtained from individual 62659 was considerably longer. Additionally, individual 62659 suffered from cancer so it is very likely that was under some therapeutic treatment. I confirmed that both samples were appropriate for RNA ISH analysis because, as shown in Figure 19, most genes have highly similar expression profiles in these two individuals, suggesting that no significant differences between diverse eye samples could be observed.

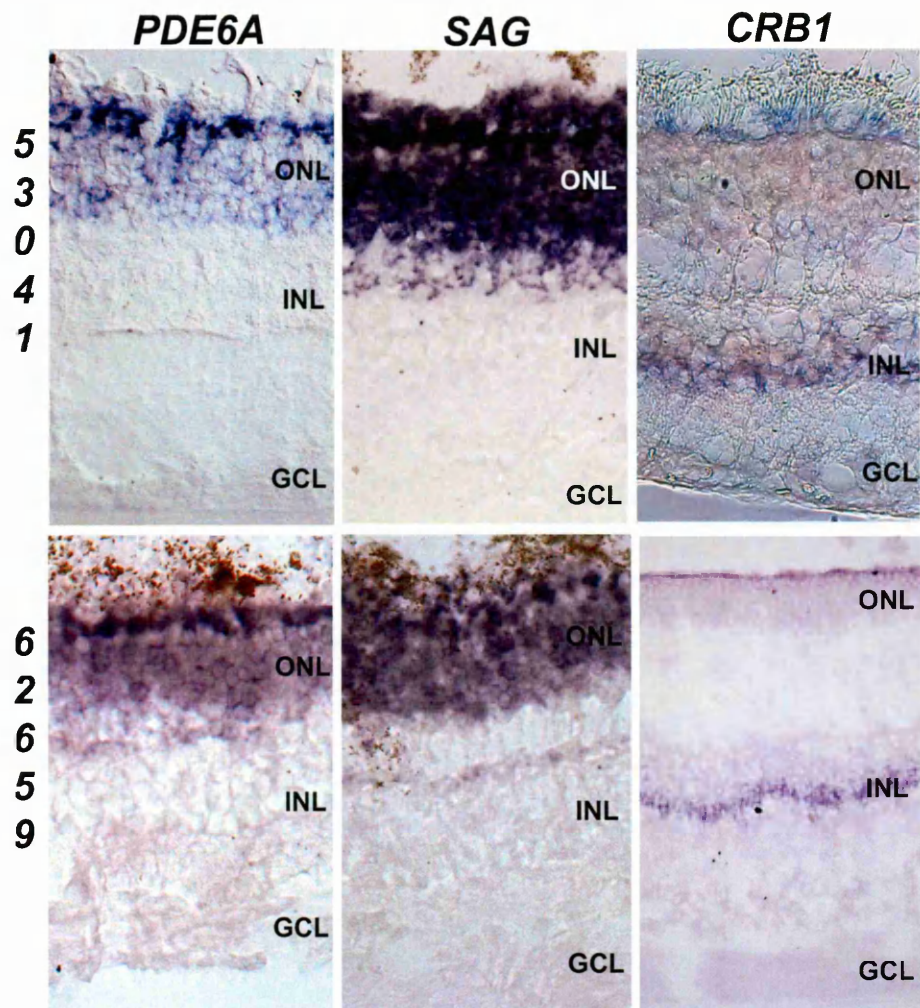


**Figure 19. Evaluation of the possible influence of post-mortem time on RNA ISH findings in the human eye.**

The *PDE6A*, *SAG* and *CRB1* genes showed very similar RNA ISH expression patterns in both the 53041 and 62659 individuals, characterized by different post-mortem times (see the text for details). *PDE6A* and *SAG* showed restricted expression in photoreceptors (ONL) while *CRB1* was expressed in ONL and INL.

ONL-outer nuclear layer, INL-inner nuclear layer, GCL-ganglion cell layer.

Out of the 34 analyzed genes, only one gene (*MERTK*) failed to show a signal both in human and mouse eye sections, even though RT-PCR experiments confirmed the expression of *MERTK* in both human and mouse eyes (Figure 20). As expected, the majority of the analyzed genes (29 out of 34) showed identical expression patterns in human and mouse eyes (Table 8). Examples of similar expression patterns are shown in Figure 21.



**Figure 20. RT-PCR analysis of *MERTK* expression.**

*MERTK* expression is detected in human retinal pigment epithelium, retina and muscle RNAs, as well as in mouse retina RNA by RT-PCR (A). *HPRT* control is shown in (B).

RPE-retinal pigment epithelium, R-retina, M-muscle, DNA-genomic DNA, B-negative control, L-100bp ladder.

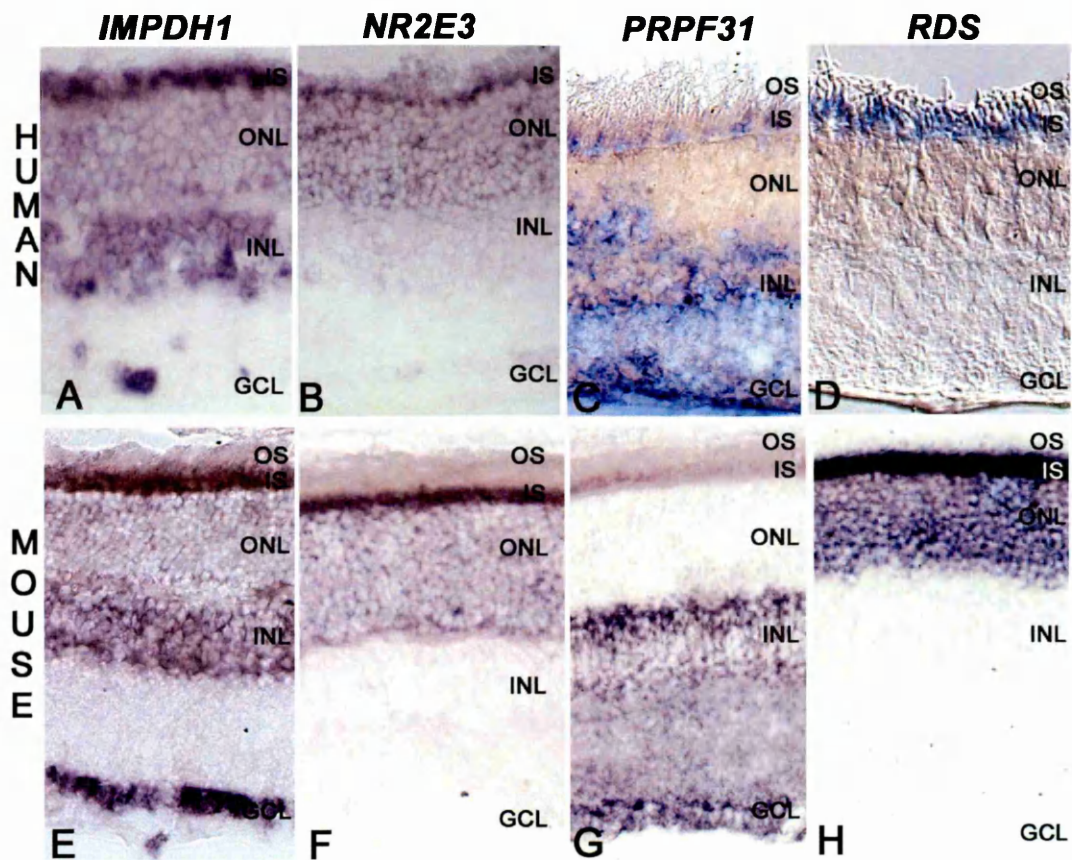


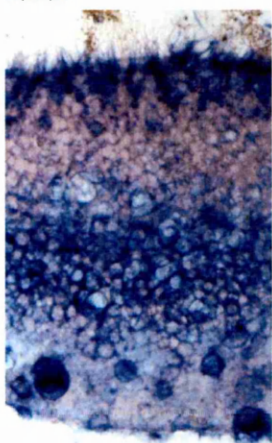

**Figure 21. Examples of genes with similar RNA ISH expression patterns in human and murine eyes.**

RNA expression patterns of the *IMPDH1* (A, E), *NR2E3* (B, F), *PRPF31* (C, G) and *RDS* (D, H) genes in human (A-D) and mouse (E-H) adult retina sections. The strong signal in the inner segment of photoreceptors (IS) reflects the distribution of the cytoplasmatic space where RNA accumulates in photoreceptors.

ONL-outer nuclear layer, INL-inner nuclear layer, GCL-ganglion cell layer.

Since the main aim of this part of my PhD project was to provide publicly available information on expression patterns of the retinitis pigmentosa genes, all the data generated during this work have been collected into an ad-hoc developed on-line database, the RP gene expression atlas database (available

at <http://www.tigem.it/RPexp/>). The database was designed to allow data mining in a user-friendly manner. For each analyzed RP gene, it contains all the expression data obtained on the eye samples from at least two different individuals and information regarding age, cause of death and postmortem time of all eye samples used. Additionally, the database also contains expression data obtained with the sense control probes for all the genes analyzed and expression profiles obtained with additional cRNA probes recognizing a specific gene, when applicable (Figure 22).

<p>Human</p>  <p>Click on the picture to see a full view View expression in a second eye sample View Additional Template For This Gene View Additional Template 2 For This Gene View Additional Template 3 For This Gene</p> <p>More Informations About This Gene View Sense Control Template Source: genomic PCR product obtained by using: Primer-F: CAGAGCGGTTTTCCGACGCG Primer-R: CAACCCAGAGCTCACTCT Template Size (bp): 910 View Template Sequence</p> <p>Polymerase used to generate antisense riboprobe: T3 Polymerase used to generate sense riboprobe: T7 Hybridization Temperature: 65</p>	<p>Mouse</p>  <p>Click on the picture to see a full view</p> <p>More Informations About This Gene View Sense Control Template Source: genomic PCR product obtained by using: Primer-F: CGACCACACACACCTCTTCC Primer-R: AGGGGGCCACTTAGGCAGTAC Template Size (bp): 921 View Template Sequence</p> <p>Polymerase used to generate antisense riboprobe: T3 Polymerase used to generate sense riboprobe: T7 Hybridization Temperature: 65</p>
--	--

**Figure 22. Schematic view of the information accessible from the RP gene expression atlas database (<http://www.tigem.it/RPexp/>) for each analyzed gene.**

### **3.2.1 *CNGB1*, *USH2A* and *FSCN2* are expressed across all retinal cell layers**

Among the above mentioned 29 genes showing identical expression patterns in human and murine retinas, I observed interesting mRNA localization for the following genes: *CNGB1*, *USH2A* and *FSCN2*. The observed expression data for these genes are not concordant with previously reported findings. According to the literature, *CNGB1*, *USH2A* and *FSCN2* are all exclusively expressed in photoreceptors<sup>55, 77, 113-115</sup>, whereas I obtained more widespread expression profiles. As shown in Figure 23A, the mRNA of the rod cGMP-gated channel beta subunit protein (*CNGB1*) is detectable in all retinal cell layers both in human and in mouse retinas (Figures 23A, 23D). A similar result was observed when *Usherin-2A* mRNA (*USH2A*) was analyzed, as shown in Figure 23B and 23E. The *USH2A* is characterized by the presence of two main isoform, a shorter one spanning twenty-one exons and a longer one spanning seventy-two exons. In order to confirm this unusual expression pattern and to exclude the possibility that this pattern was due to differential expression of the two *USH2A* isoforms, I designed an additional RNA probe for *USH2A*. Since the first RNA ISH expression data for the *USH2A* were obtained with a template specific for the long form, I designed a template also for the short form of *USH2A*. By performing RNA ISH with these two probes, one spanning the last exon and the 3'UTR (corresponding to the *USH2A* long isoform) and a second covering the 5'-UTR and the first exon of the *USH2A* (recognizing both isoforms), the possibility of unspecific signal is likely to be avoided. Expression in all the retinal layers was confirmed also with the second probe suggesting that indeed *USH2A* is not expressed exclusively in photoreceptors (the results of the

*USH2A* expression analysis with both probes are accessible in the on-line database).

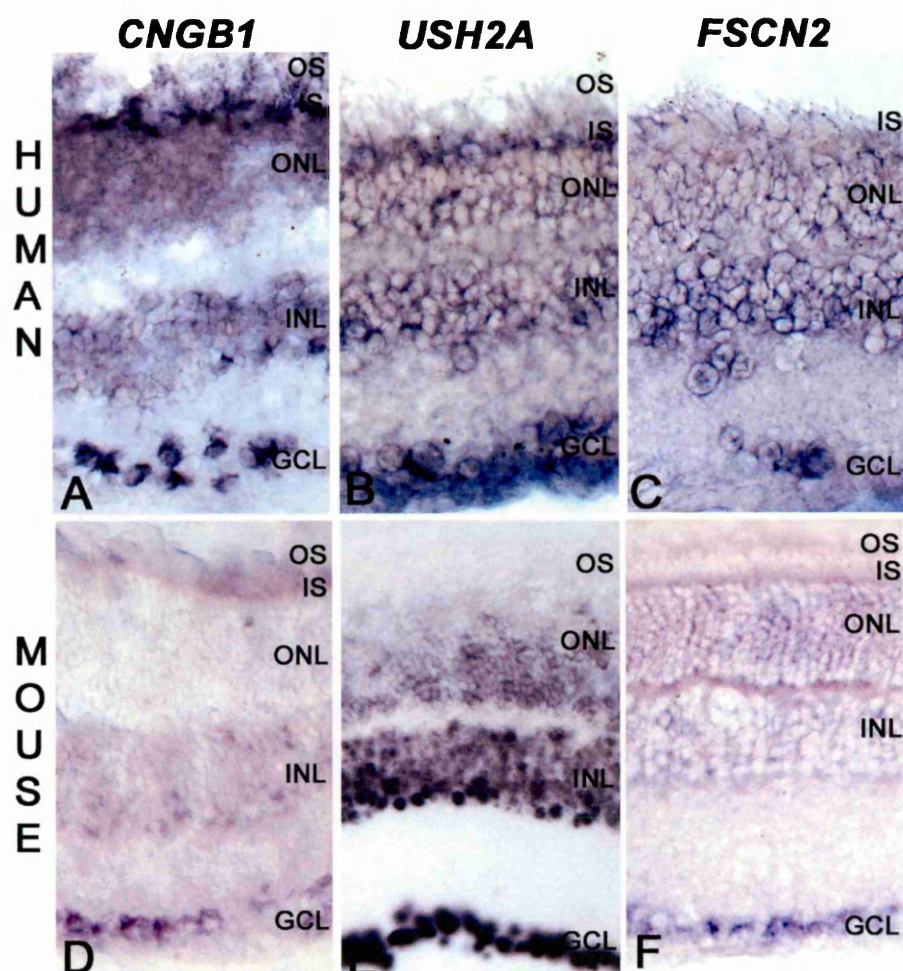


**Figure 23. Localization of *CNGB1*, *USH2A*, and *FSCN2* mRNA in human and mouse retinas.**

Hybridization of human retinas (A-C) and murine retinas (D-F) with RNA probes for: *CNGB1* (A and D), *USH2A* (B and E), *FSCN2* (C and F). In the human and in the mouse retina they are widely transcribed in IS, ONL, INL and GCL.

OS, photoreceptors outer segment; IS, photoreceptors inner segment; ONL, outer nuclear layer; INL, inner nuclear layer; GCL, ganglion cell layer.



Finally, homogeneous expression in human and mouse retinas with more intense staining in the ganglion cell layer was also detectable with RNA probes for the retinal fascin homolog 2 (*FSCN2*) gene (Figures 23C and 23F). Interestingly, also the Neural retina leucine zipper (*NRL*) transcript was detected throughout all the layers both in human and mouse retina. These results were unexpected due to fact that *NRL* has been described as a photoreceptor-specific gene<sup>116-118</sup>. Similarly to the *USH2A* gene, I generated two highly specific riboprobes spanning the opposite sides of the both the mouse and human *NRL* transcript. I also generated two additional probes recognizing different *NRL* splice isoforms annotated in the UCSC Human Genome Browser in order to define whether the obtained widespread signal was due to the different expression profiles of different isoforms (Figure 24). Nevertheless, the four specific probes of the human *NRL* and the two specific probes for the mouse *Nrl* transcript showed identical expression patterns (data accessible at <http://www.tigem.it/RPexp/> and Figure 24). Additionally, the expression of the *Nrl*, *Cngb1*, *Ush2A* and *Fscn2* mRNAs was also present in the INL and GCL of the *Aip11*<sup>-/-</sup> mouse model, which lacks photoreceptors<sup>119</sup> as assessed by the absence of *Rhodopsin* transcripts (Figures 24 and 25).

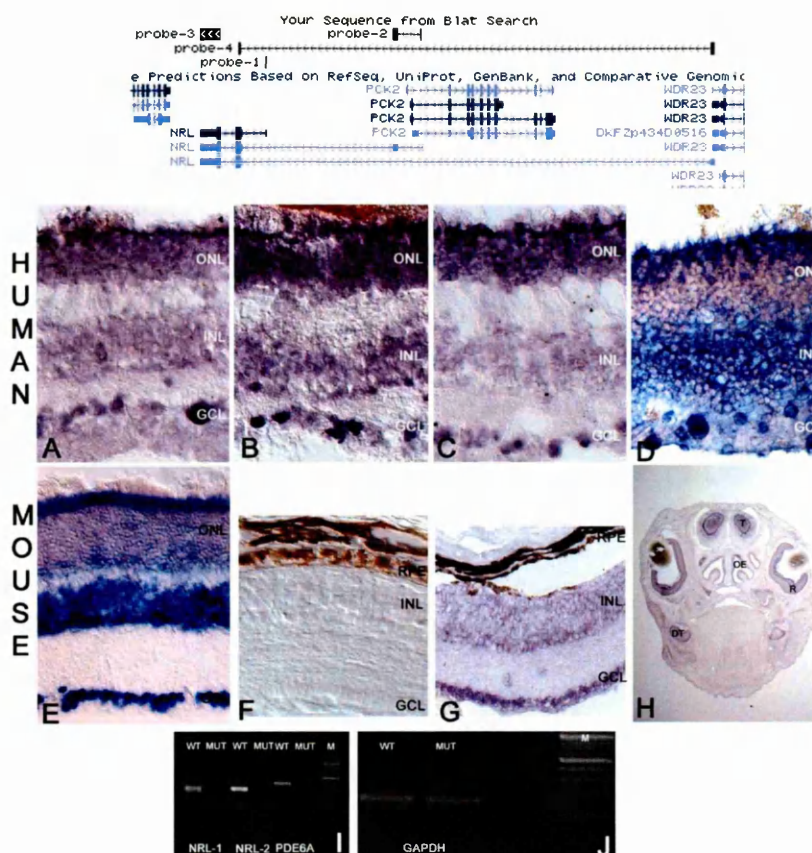


**Figure 24. NRL expression profile.**

Four different and specific RNA probes (respectively, probes 1, 2, 3 and 4) recognizing different *NRL* isoforms, as shown by BLAT analysis (diagram on top), show strong expression of the *NRL* in all the layers in human retina (A-D). The same expression pattern can be observed also in the mouse wild type retina (E). RNA ISH with the *Rhodopsin* probe shows no staining in the *Aipl1*<sup>-/-</sup> mouse eye sections (F), while the *Nrl* probe labels INL and GCL (G). In the head section of wild type mouse postnatal day 1.5 *Nrl* is detectable in retina, telencephalon, olfactory epithelium, cerebellum and in developing tooth (H). RT-PCR analysis of wild type (WT) and *Aipl1*<sup>-/-</sup> mouse (MUT) showed the expression of *Pde6A* and *Nrl* only in wild type mouse. NRL-1 represents an RT-PCR product obtained with oligonucleotide primers spanning the first and second exons, while the NRL-2 product was obtained with oligonucleotide primers spanning the second and third exons of *Nrl* (I). *GAPDH* control is shown in (J).

ONL-outer nuclear layer, INL-inner nuclear layer, GCL-ganglion cell layer, T-telencephalon, OE-olfactory epithelium, R-retina, DT-developing tooth, WT-wild type mouse, MUT-*Aipl1*<sup>-/-</sup> mouse, M-100bp ladder.

To test the specificity of the *Nrl* probes used on the mouse eye sections, I also performed RNA ISH experiments on postnatal day 1.5 (P1.5) mouse head sections. As shown in Figure 24H, RNA ISH signal is present not only in the developing eye but also in other parts of the head (olfactory epithelium, developing tooth and telecephalon). The detection of signal in non-eye tissues suggested that the observed signal might not be specific for the *NRL* transcript since there is no evidence whatsoever that this gene is transcribed anywhere outside the retina. For these reasons, I decided to investigate *Nrl* mRNA expression using a different method such as RT-PCR on RNA extracted from the same photoreceptor deficient mouse *Aip1*<sup>-/-</sup> (Figure 24I). *Nrl* expression is detectable only in the wild type retina while no amplification can be observed in *Aip1*<sup>-/-</sup> retina suggesting that indeed *Nrl* is a photoreceptor-specific gene and that RNA ISH is not a proper method for the analysis of the expression of this gene. Similarly, I wanted to test the specificity of the obtained RNA ISH data for all the genes whose expression pattern diverged from previously reported data. To this purpose, I performed RT-PCR analysis on RNA purified from three months-old *Aip1*<sup>-/-</sup> and wild type retinas using oligonucleotide primers specific for *Cngb1*, *Ush2A* and *Fscn2*. To confirm the absence of photoreceptors in 3 months old *Aip1*<sup>-/-</sup> mice, I evaluated the expression of a photoreceptor-specific marker (*PDE6A*) and no expression could be detected, as shown in Figure 25G. On the other hand, *Cngb1*, *Ush2A* and *Fscn2* amplification was observed both in the wild type and *Aip1*<sup>-/-</sup> retinas, as assessed both by RT-PCR and RNA ISH experiments, confirming the expression of these genes also outside photoreceptor cells (Figure 25).

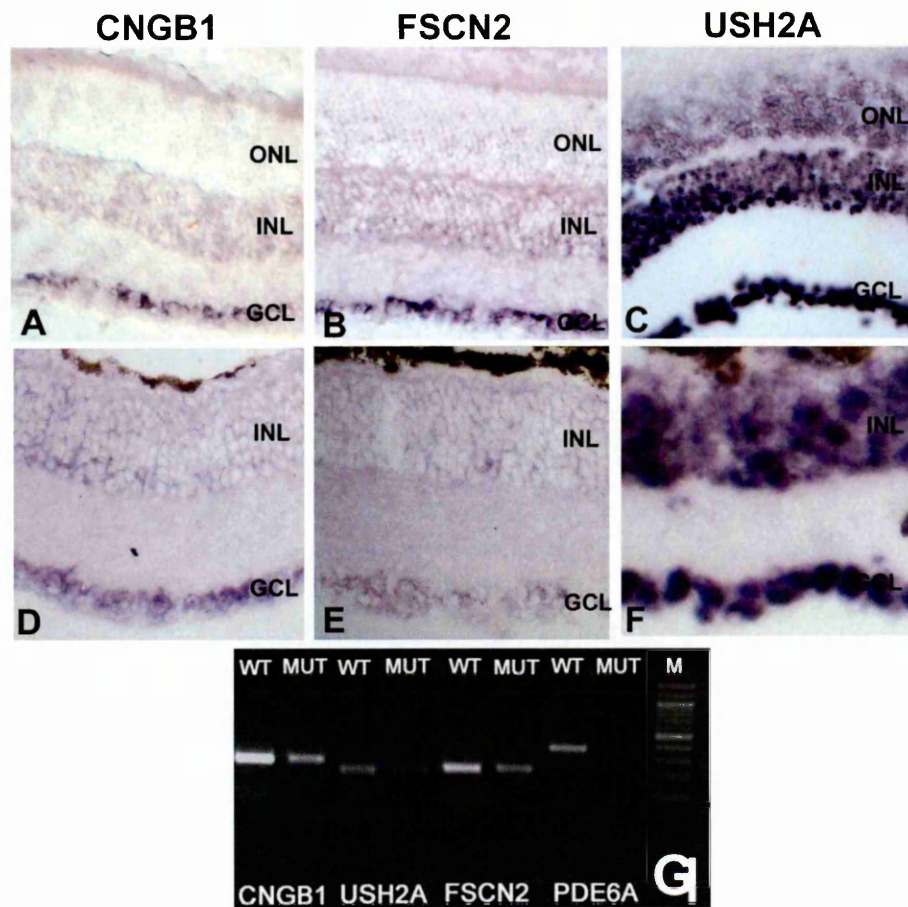


**Figure 25. Expression profiles of *Cngb1*, *Fscn2* and *Ush2A* genes in wild type and mutant mouse retinas.**

Hybridization of wild type (A-C) and *Aip1*<sup>-/-</sup> murine retinas (D-F) with RNA probes for: *Cngb1* (A and D), *Ush2A* (B and E), *Fscn2* (C and F). In the wild type and in the mutant mouse retina, they are transcribed in IS, ONL, INL and GCL. RT-PCR analysis of wild type (WT) and *Aip1*<sup>-/-</sup> mouse (MUT) showed expression of *Cngb1*, *Fscn2* and *Ush2A* in both retinas (G).

WT-wild type mouse, MUT-*Aip1*<sup>-/-</sup> mouse, M-100bp ladder, ONL-outer nuclear layer, INL-inner nuclear layer, GCL-ganglion cell layer.

### **3.2.2 RNA in situ hybridization expression profiles of the RGR, RLBP1 and CA4 genes**

During the course of this study, I found some notable differences between the expression profiles in human and mouse adult eye sections for the *RGR*, *RLBP1* and *CA4* genes (Figure 26). *RGR* and *RLBP1* are members of the visual cycle with a reported expression in the mouse retina in RPE, Müller cells and in the case of *RLBP1* also in the ganglion cells<sup>106, 120-122</sup>. Regarding the *RGR* and *RLBP1* mRNA expression in human retina, no data were available so far, while protein localization is similar to that reported in the murine retina. In agreement with previous reports, I observed that in the murine retina both *Rgr* and *Rlbp1* were expressed in the RPE and *Rlbp1* transcripts were also detectable in the INL and in the GCL (Figure 26D and E). Surprisingly, in the human retina, besides the expected expression in the RPE and INL<sup>106, 120</sup>, the *RGR* transcript was detectable also in photoreceptors and *RLBP1* was distributed in all the different cell types of the retina including the photoreceptors (Figure 26B). mRNA localization for each of these genes in human photoreceptors was confirmed with a second, non-overlapping probe on sections obtained from at least two individuals (see <http://www.tigem.it/RPexp/>).

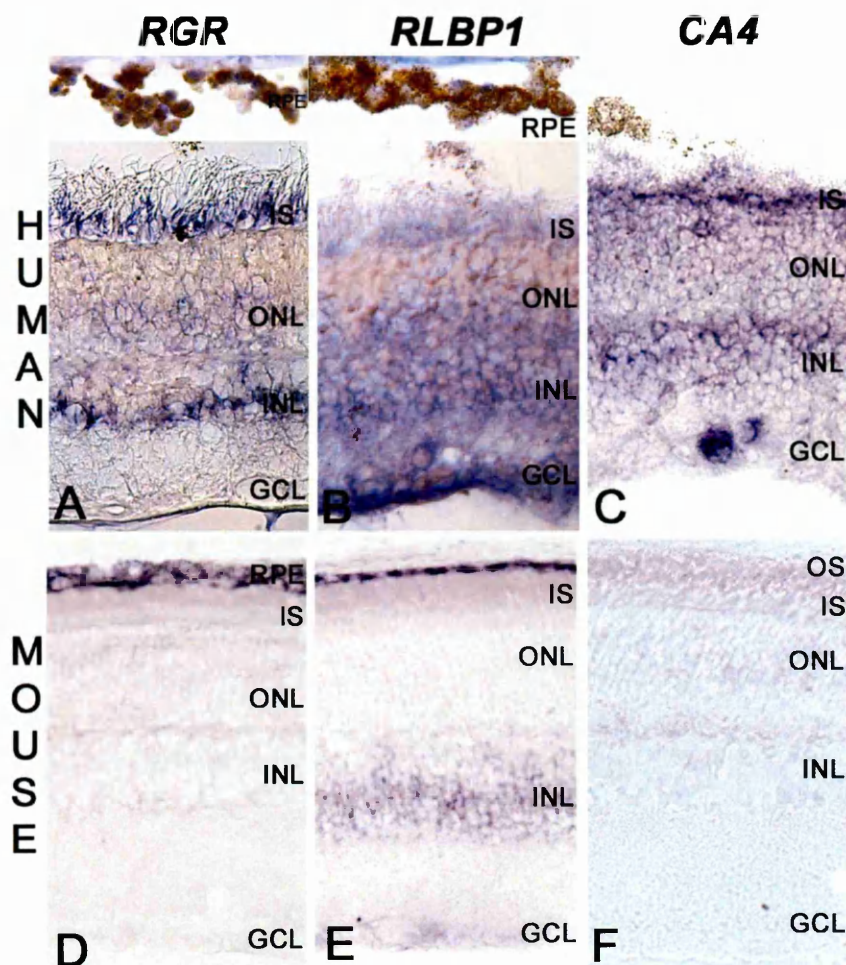


**Figure 26. Expression profiles of *RGR*, *RLBP1* and *CA4* genes.**

*RGR* is expressed in RPE, photoreceptors and weak signal can also be observed in the INL of the human retina (A). In the mouse retina, signal is detectable only in the RPE (D). *RLBP1* mRNA is ubiquitously detectable in the human retina and RPE (B) while in the mouse retina it is visible in the RPE, INL and weakly in the GCL (E). *CA4* mRNA is present in photoreceptors, INL and GCL in the human retina (C). No staining can be observed in the mouse retina (F).

RPE-retinal pigment epithelium, IS-photoreceptors inner segment, ONL-outer nuclear layer, INL-inner nuclear layer, GCL-ganglion cell layer.

I also detected major differences in the expression of the *CA4* gene between the human and mouse retinas. *CA4* is the only gene underlying RP that has not been reported to be expressed in the retina, as the *CA4* protein was shown to be localized in the choriocapillaris surrounding the retina<sup>83, 123</sup>. My studies revealed an expression of *CA4* in all the retinal cell layers. Similar to the previously described cases in which an unexpected expression pattern was observed, I designed an additional RNA probe for the *CA4* gene to validate these results. The same expression profile was also observed with the second independent probe suggesting that *CA4* was indeed expressed in all the retinal layers of the human retina (Figure 26C and on-line database). Conversely, by RNA ISH, I could not detect any signal in the mouse retina (Figure 26F).

In order to understand if *RGR* and *RLBP1* proteins are indeed translated in the human photoreceptor cells as suggested by mRNA localization, I performed double immunofluorescence experiments on human eye sections using the *RGR* and *RLBP1* antibodies followed by rods staining with *RHO* antibody or cones staining with FITC labeled peanut-agglutinin (PNA). No staining could be observed with the *RGR* antibody suggesting that the antibody used was not appropriate for the experiments in human retina. On the other hand, the *RLBP1* protein was detected in photoreceptors, INL and GCL (Figure 27A). Colocalization experiment with antibodies directed against *RLBP1* and *RHO* showed partial co-localization suggesting that *RLBP1* is probably expressed in rods (C), while no co-localization could be detected with the cone-specific marker PNA (D).

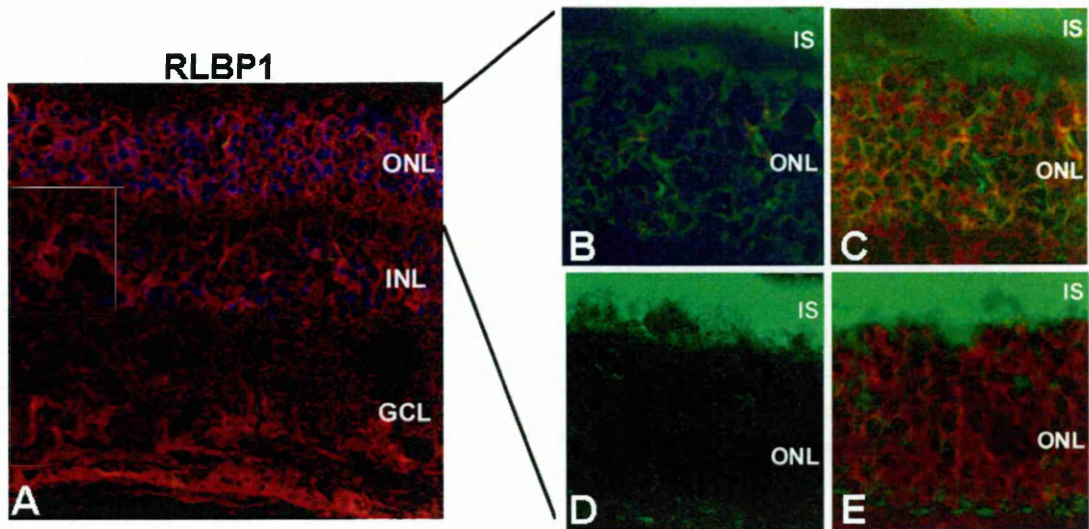


**Figure 27. RLBP1 protein localization in human retina.**

Confocal microscopy of human adult eye sections stained with antibody directed against RLBP1 in red (A). Staining with anti-RHO antibody (B) and with p-agglutinin (D). Merged staining of RLBP1 in red and RHO as a rod-specific marker in green (C) and RLBP1 red and p-agglutinin as a cone-specific marker in green (E).

IS-photoreceptors inner segment, ONL-outer nuclear layer, INL-inner nuclear layer, GCL-ganglion cell layer.



### 3.2.3 *RPGR* and *PAP1* genes show prevalent expression in human photoreceptors

Unlike the above-described genes, which display significant difference in expression between human and mouse eye sections, *RPGR* and *PAP1* showed less evident discrepancy in the retinal expression patterns between these two species. The *RPGR* gene is characterized by the presence of 2 main isoforms, a “default variant” which consists of 19 exons and the so-called “ORF15 variant” with a terminal exon within intron 15 of the default variant<sup>75</sup>. So far, the *RPGR* protein was shown to be localized in the photoreceptor connecting cilia or photoreceptor outer segments depending on the species analyzed<sup>75, 76, 124</sup>. However, there are no high-resolution expression data at the RNA level for this gene in either the human or mouse retinas and no comparative analysis of the expression pattern of the two main isoforms. I detected the *RPGR* “default variant” mRNA in human photoreceptors and in the INL, while in the mouse retina weak staining could be observed only in photoreceptors (Figure 28A, D). Interestingly, the *RPGR-ORF15* splice variant is specifically transcribed in human photoreceptors, while two independent probes for mouse *RPGR-ORF15* showed mRNA localization in all retinal cells with a more intense staining in the GCL (Figure 28B, E).

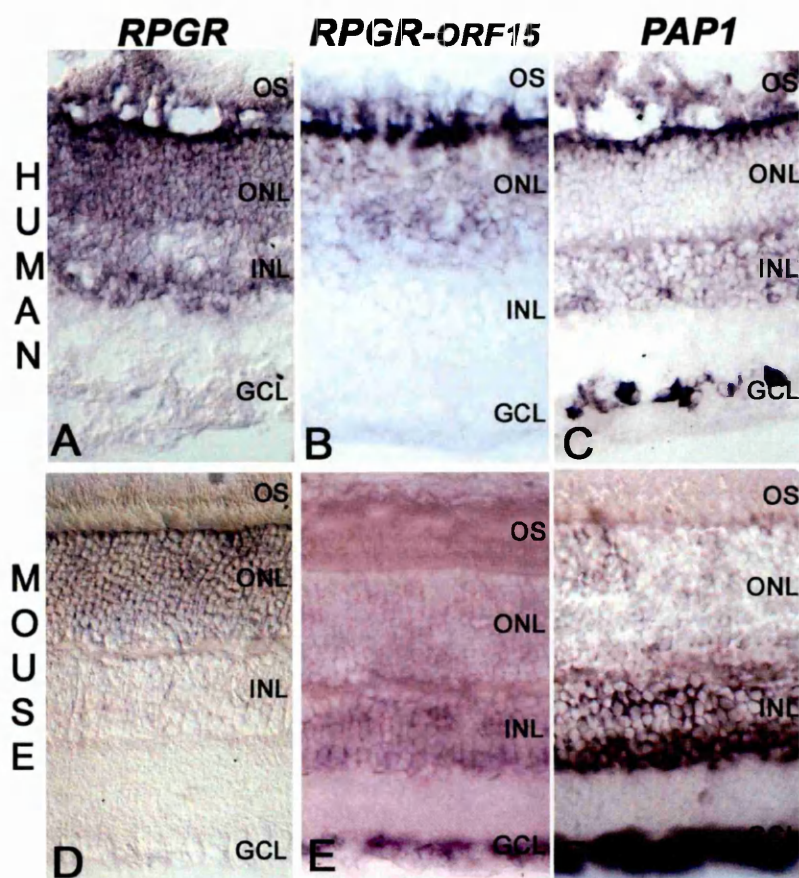


**Figure 28. *RPGR* and *PAP1* mRNA distribution.**

The *RPGR* “default” variant is expressed in ONL and INL in the human retina (A), while in the mouse retina (D) a faint signal can be observed only in ONL. *RPGR-ORF15* variant shows intense staining in photoreceptors of the human retina (B), whereas in the mouse retina the signal is present in ONL, INL and GCL (E). *PAP1* in the human retina is strongly expressed in ONL while a weaker expression is also detectable in INL and GCL (C). On the other hand, in the mouse retina signal is prevalent in the GCL and INL, while staining of the ONL is at the limit of detection (F).

OS-outer segment, ONL-outer nuclear layer, INL-inner nuclear layer, GCL-ganglion cell layer.

*PAP1* (*RP9*) is one of the four splicing factors (*PRPF3*, *PRPF31*, *PRPF8*, *PAP1*) linked to autosomal dominant RP<sup>70, 125</sup>. There is almost no information available regarding the RNA expression of these splicing factors in the retina. RNA expression patterns for *PRPF3*, *PRPF31* and *PRPF8* obtained in this study suggest that these genes are ubiquitously expressed in all the layers of the retina but seem to present an expression gradient with a stronger level in GCL and a lower one in photoreceptors, similarly to what previously reported for the murine *Prpf3* and the human protein<sup>72</sup> (data available at <http://www.tigem.it/RPexp/>). Similar expression was also observed for *Pap1* in the mouse retina where signal intensity in ONL is much lower compared to INL and GCL (Figure 28F). On the other hand, in human retina, a specific 100bp-long cRNA probe showed a predominant transcription in the ONL when compared to INL and GCL (Figure 28C and <http://www.tigem.it/RPexp/>). When a second riboprobe was used, the expression was detectable only in photoreceptors. It is worth noticing that the second RNA probe used may potentially cross-react also with a *PAP1* pseudogene<sup>126</sup>.

---

#### **4.1 IDENTIFICATION OF HUMAN GENES WITH PREDOMINANT RETINAL EXPRESSION**

Eye is the window of the brain and therefore eye diseases leading to blindness represent one of the most devastating conditions affecting the quality of life. The final goal of all the research efforts on eye diseases is to find an efficient treatment to restore vision. However, the obvious prerequisite for the treatment of any kind of disease is represented by the elucidation of molecular causes and pathogenetic events that lead to its onset. More specifically, a considerable effort has been devoted to the determination of all the genetic causes of inherited retinal disorders. In particular, an important step forward was made, during the last decades, in elucidating the molecular events of several diseases affecting retina functionality. As a result, over 160 genes have been identified to date as responsible for different forms of inherited retinal disorders. Nevertheless, it is widely believed that the total number of retinal disease genes is higher than what is currently known<sup>3</sup>. So far, the majority of retinal disease genes have been identified thanks to an efficient but laborious procedure, such as positional cloning, which rely on the establishment of the chromosomal mapping assignment of a genetic locus, usually by linkage analysis or by the recognition of cytogenetic abnormalities. This was followed by the isolation, mainly by experimental and time-consuming approaches, of genes localized within the genetic interval and these had to be tested by mutation analysis in patients<sup>127</sup>. However, the outcome of the Human Genome Project effort has revolutionized and largely facilitated the approaches aimed at disease gene identification not only by providing more easily the list of genes to be analyzed in positional cloning efforts but also by providing alternative avenues, for instance by improving the *ab initio* candidate gene approach<sup>127</sup>. It has already

been recognized that the integration of genome sequence and gene expression data holds great promise for the identification of retinal disease genes<sup>89, 90, 94, 95</sup>. Some functional genomic approaches aimed at the *in silico* identification of genes with a preferential expression in the murine retina have already been carried out in order to identify candidate genes for human inherited eye disorders. Animal models are highly beneficial for human disease studies: however, in some cases, the translation to humans of the knowledge gained from the use of animal models, and above all the mouse, requires additional information on the function of the same gene in the human tissue. Additionally, there are no reported examples of a strategy combining *in silico* identification of candidate genes for human eye inherited disorders and experimental determination of their cellular distribution in the human retina.

The rationale behind this part of my PhD project was to overcome such a lack of information by identifying new candidate genes for retinal disorders in humans. To this purpose, I carried out a combined approach, including the use of bioinformatics tools and of expression studies in the human retina. The human genome project provided a valuable source of information regarding the genomic sequence and enabled the identification of a complete set of genes. However, one of the ultimate goals of this effort was aimed at the understanding of when, where, and how a gene is expressed. To achieve this goal, the Expressed Sequence Tags (ESTs) project was used, which provides a quick and inexpensive route for discovering new genes, for obtaining data on gene expression and regulation, and for constructing transcript maps. By exploiting the ESTs database, I was able to retrieve a set of putative retina-specific or predominant transcripts. Briefly, *in silico* prediction was based on the analysis of the Unigene database in order to identify a set of cDNAs (Unigene clusters)

that, based on EST counts, were predicted to show an exclusive or predominant retinal expression in humans. Mapping of each cluster-specific consensus sequence to the human genome enabled identification of cDNAs for which no connection to the pathogenesis of retinal disease or to a defined role in retina biology was previously established. To validate the *in silico* predicted retinal expression, I performed experimental studies. By RT-PCR validation of the exclusive or predominant expression in the retina of the selected EST clusters, I was able to restrict the number of transcripts to be further analyzed at the cellular level by RNA *in situ* hybridization. Confirmation of retinal expression by RT-PCR is not sufficient to reliably predict the type of disease in which a particular cDNA may be involved, if mutated. To that purpose, it is essential, for each selected cDNA, to have more precise information about which cell type within the retina expresses it and therefore to infer the cellular functionality that may be affected by mutations in that specific gene. This led me to perform RNA ISH experiments in order to determine the specific retinal cell types expressing the gene of interest. One of the major advantages of this study is in the fact that all the data are collected for the human retina, both as far as the *in silico* and the experimental analyses are concerned. Additionally, by performing RNA ISH experiments on the eye samples obtained from different individuals I was able to exclude inter-individual variations that could have been misleading. Out of fifteen selected cDNA clusters analyzed by RNA *in situ* hybridization, thirteen showed specific expression patterns, as assessed by lack of signal when RNA ISH experiments were performed with the control sense probes and by the fact that patterns were highly similar in different eye samples. This study allowed me to identify some interesting candidate genes for retinal disorders.

Cluster Hs.21162, which corresponds to the *Retbindin* (*RTBDN*) gene, was exclusively expressed in the retina. A protein prediction analysis, by the SMART software, suggested that it contains a complement component C1q domain. I found that the *RTBDN* mRNA was present in all the layers of the retina as assessed by RNA *in situ* hybridization experiments. Wistow et al.<sup>128</sup> in 2002 described *Retbindin* as a highly abundant retinal transcript that matches (27% identity over 135 residues) with riboflavin binding proteins, and potentially binds a number of ligands, including retinoids and other carotenoids (such as lutein) or may exert a protective roles against the toxic free radicals generated by flavinoids. *C1q* is a member of the complement system and acts as a trigger of the system<sup>108</sup> the key player of innate immunity by mediating immune control against infectious agents. Recent findings<sup>98, 107, 129</sup> demonstrated that, in many cases, age-related macular degeneration (AMD) is associated to a sequence variation in one of the members of the complement system, complement factor H (*CFH*), which has an established role in complement system inhibition. AMD is a major cause of blindness in the elderly<sup>98</sup>. It is a highly complex disease probably caused by both genetic and environmental components and the pathogenetic mechanisms underlying development of the disease are still obscure<sup>130</sup>. A key feature of AMD is the formation of extracellular deposits called drusen concentrated in and around the macula behind the retina, between the retinal pigment epithelium (RPE) and the choroid<sup>130</sup>. Complement system components are present in the drusen, suggesting that AMD involves at least partially an aberrant inflammation process<sup>131, 132</sup>. In light of the observation that a sequence variation in a complement system inhibitor, i.e., *CFH*, is associated with AMD, it is reasonable to assume that, similarly, changes in the function of other components of the complement system such as the activator

*C1q* may contribute to the onset of AMD. Indeed, it has been demonstrated that variants in other activators of the complement system, such as complement factor B and complement C3 genes influence susceptibility to age-related macular degeneration<sup>133, 134</sup>. Additionally, Hayward et al., showed that mutation in Complement 1q Tumor Necrosis Factor 5 gene (*C1QTNF5*) causes late-onset macular degeneration, disease similar to AMD<sup>135</sup>. Interestingly, *C1QTNF5* contains a C1q domain present also in *RTBDN*. Thus, I classified cluster Hs.21162 as a new candidate gene for age-related or late-onset macular degeneration.

The mRNAs of clusters Hs.433492, Hs.449884 and Hs.33102 were localized in all the layers of the human retina. Cluster Hs.433492 corresponds to the ankyrin repeat domain 33 (*ANKRD33*) and showed an exclusive expression in the retina. No information is available regarding the function of *ANKRD33*. In contrast, ankyrin repeats have been found in numerous proteins with very diverse functions that include cell–cell signaling, cytoskeleton integrity, transcription, cell–cycle regulation, inflammatory response, development, and various transport phenomena<sup>136</sup>. Even though a number of ankyrin repeat proteins have been linked to human diseases (such as cancer), the putative role of *ANKRD33* in retinal pathology still needs to be determined. Contrary to the above mentioned *ANKRD33*, cDNA cluster Hs.449884 was connected with retinal function by an independent study<sup>137</sup>. Analysis performed during the course of this study revealed that Hs.449884 corresponds to the Complexin IV (*CPLX4*) gene. RT-PCR analysis revealed that this transcript does not have a retina-specific expression whereas RNA ISH showed that, in the retina, it was transcribed mostly by cells of the inner nuclear layer but also by few cells of the outer nuclear layer and some ganglion cells. Complexins are proteins involved



in neurotransmitter release at the level of neuronal synapses. Two members of the complexin family (Complexin I and Complexin II) were previously linked to the onset of neurological phenotypes, including ataxia and seizures<sup>138</sup>. Two novel members (Complexin III and Complexin IV) were identified and characterized in 2005 by Reim et al.<sup>137</sup> that demonstrated their role in the formation of retinal ribbon synapses. According to authors, Complexin IV is present only in the retina but not in conventional neuronal synapses and acts as a positive regulator of synaptic exocytosis. Considering the importance of signal transmission in the functionality of the retina, Complexin IV can be considered a candidate gene for retinal dystrophy. It has already been demonstrated that impairment of retinal synapses caused by mutations in some of the synaptic structural components (*CACNA2D4*)<sup>139</sup> or in regulatory proteins of the synapses, such as *RIM1*, cause cone dystrophies<sup>140</sup>.

Cluster Hs.33102, which corresponds to the transcription factor AP-2 beta, was also expressed in all the layers of retina. Transcription factors AP-2 (*TFAP-2 alfa* and *TFAP-2 beta*) have important functions in retinoid-controlled morphogenesis and differentiation<sup>141</sup>. There are no data indicating that *TFAP-2B* is involved in pathogenesis of retinal disorders: however, it was reported that mutations in this gene cause Char syndrome, an autosomal dominant trait characterized by patent ductus arteriosus, facial dysmorphism and hand anomalies<sup>142</sup>. Data showing that AP proteins have dynamic spatial and temporal expression patterns during development of the murine eye<sup>143</sup> as well as the expression data in the human retina, provided by my study, make the *TFAP-2B* an interesting candidate gene for retinal disorders particularly considering the fact that mutation in other transcription factors important for the retinal development cause retinal disorders like retinitis pigmentosa (e.g. *NRL* and

*NR2E3* transcription factors<sup>59, 60</sup>) or Leber congenital amaurosis that can be caused by *CRX* mutations<sup>64</sup>.

Unlike the majority of the clusters analyzed in this project which were expressed throughout the retina, cDNA clusters Hs.69749 and Hs.131130 showed a more restricted expression pattern. The Hs.69749 mRNA, only detected in retina and brain by RT-PCR, was transcribed mainly in photoreceptors and in a few cells within the inner nuclear layer. Hs.69749 is one of the five cDNA clusters selected for RNA *in situ* hybridization analysis that show no sequence similarity to any known gene. A restricted expression of Hs.69749 in brain and retina (mainly in photoreceptors, as assessed by RNA ISH) renders cluster Hs.69749 worth of further investigation, since this pattern of expression suggests a specific role in neuronal tissues. However, in order to define whether or not this cDNA may be responsible for any eye disorders more specific functional studies are required. The remaining clusters that show no correspondence with known genes, namely Hs.171485, Hs.354243, Hs.295015 and Hs.221513, were expressed exclusively in retina and brain but their mRNAs were distributed in all the layers of the retina (examples are shown in the *Results* section).

Cluster Hs.131130 displayed a photoreceptor-specific expression, as detected by RNA ISH. Sequence homology analysis defined that this cDNA corresponds to the potassium channel, subfamily V, member 2 (*KCNV2*), as assessed by sequence homology analyses. Voltage-gated potassium channels serve a wide range of functions including regulation of the resting membrane potential and control of the shape, duration, and frequency of action potentials<sup>110</sup>. Its photoreceptor-specific expression and the fact that *KCNV2* may play a function in excitability of neurons makes this cluster a good

candidate gene for retinal disorder. In order to test whether mutations in the *KCNV2* gene may play a pathogenetic role in retinal disorders, mutation analysis was performed on a collection of Italian patients affected by different retinal diseases. Screening for the presence of mutations was performed on one hundred and twenty Leber congenital amaurosis patients and ninety-six patients diagnosed with recessive retinitis pigmentosa. No sequence variants were detected in the analyzed patients. These data did not however exclude the possible involvement of this gene in other types of retinal dystrophies. In fact, while this study was in progress, Wu et al.<sup>111</sup> published that *KCNV2* mutations cause “cone dystrophy with supernormal rod electroretinogram”, an autosomal recessive disease of unknown etiology. The involvement of *KCNV2* in “cone dystrophy with supernormal rod electroretinogram” was also confirmed by Thiagalingam et al.<sup>112</sup>. Based on these observations, I analyzed four cone dystrophy Italian patients with a phenotype compatible to the one described in the two above mentioned papers but again I did not find any mutation. These data indicate that there is evidence for additional genes responsible for the “cone dystrophy with supernormal rod electroretinogram”, at least in the Italian population.

The process of disentangling the causes behind inherited eye diseases is greatly dependent on the availability of large families of patients and the availability of genetic markers positioned closely enough to the disease chromosome region in order to define a small as possible critical region. However, in the majority of cases, many genes reside within the two flanking markers defining the borders of the critical region identified by linkage and the final identification of the disease gene requires extensive and laborious mutation analyses if no obvious candidate gene is present in the interval.

Additionally, the importance of the identification of candidate genes is even more obvious in the sporadic cases of retinal disorders. Providing a list of genes that can be good candidate for retinal dystrophies can greatly facilitate this task. Indeed, there are several reports<sup>89-95</sup> on the identification of novel candidate genes for retinal disorders using systematic approaches as already described in Chapter 1.4. I retrospectively compared my results with those of these previous studies to evaluate whether the candidate genes selected in this study had been previously identified. This analysis revealed that even though different approaches were used to retrieve novel retinal ESTs, the average number of the identified ESTs in different studies including this one is similar. However, only one gene (*RTBDN*) identified by this study was previously recognized as a novel retinal EST cluster, putatively involved in retinal disorders<sup>92</sup>. One of the explanations for the discrepancy in the identification of novel retinal ESTs between this and previous studies can be that, in the past few years, the number of human ESTs generated from eye and retina cDNA libraries has considerably increased, which allowed me to recognize additional cDNAs that were not present in previous Unigene releases. Furthermore, not only the numbers but also the annotation of Unigene clusters is very dynamic and prone to changes in the various releases. Indeed, as I already mentioned, I recently revised all the EST clusters that were first retrieved in 2005 for this study and I could verify that the status of some of them was changed (see column "Notes" Table 5). These considerations further stress the usefulness of periodically updating such kind of analysis in order to make it more effective.

The studies performed during the course of this part of my PhD project were aimed at providing a list of genes with a preferential expression in the human retina together with information on the specific cell types expressing

---

them, in order to pinpoint candidate genes for retinal disorders. The effectiveness and the utility of this approach are confirmed by the fact that one of these genes (*KCNV2*) was shown by an independent study to cause a retinal disorder. It is reasonable to expect that making the list of these candidate genes publicly available may facilitate discovering of new retinal disease genes.

#### **4.2 GENERATION OF THE RP GENE EXPRESSION ATLAS**

Unraveling and understanding the genetic cause and the disease mechanism underlying retinitis pigmentosa is very important, because this will help in the identification of targets for therapeutic intervention. No effective approach to prevent, stabilize, or reverse the degenerative process exists for the majority of RP cases. Additionally, in spite of the characterization of a number of genes responsible for RP, the genetic causes for the majority of cases have yet to be discovered. A further limitation is the lack of information regarding the expression of already identified genes in the human retina. Ongoing research is putting most of its efforts towards two as yet elusive goals: the discovery of all the genes linked to RP in patients, and the development of therapeutic strategies to halt or reverse the loss of photoreceptor cells. Even though there are still many obstacles to be overcome in order to establish an effective treatment, there is an important progress in gene therapy treatment of retinal degeneration. The best example for this progress is the gene therapy approach for Leber congenital amaurosis, caused by mutations in the *RPE65* gene. This study is in the first phase of clinical trials, confirming that the full understanding of the causes of a certain disease can ultimately lead to the design of an efficient therapy<sup>99, 102</sup>. The eye represents an ideal system for gene therapy because of its highly specialized and compartmentalized nature, which enables

precise delivery of therapeutic agents with almost no systemic side effects. However, in order to obtain the highest benefits of such a treatment, it is necessary to deliver the therapeutic agents to specific target sites within the eye corresponding to the cells that normally express the affected gene. In order to achieve this, we need accurate and detailed information about the expression profiles of disease-causing genes in the human retina. To provide this vital information I generated a high-resolution expression atlas in the human retina of thirty-four genes responsible for RP and compared their expression to that of their mouse orthologs in the murine retina. The generation of this atlas provided novel expression data for this biologically relevant group of genes. In this study I report novel mRNA expression profiles of twenty human RP genes and of six corresponding murine orthologs, which have never been reported before. In addition, the systematic and comparative expression analysis of all known RP genes provides new insights into the putative functional activities of some of these genes.

As expected, the majority of the analyzed genes displayed identical expression patterns in the human and in the murine eye. It is important to point out that all the genes were analyzed on human eye sections obtained from at least two different individuals and these results can be retrieved from an ad-hoc generated on-line database (<http://www.tigem.it/RPexp>). I would like to emphasize again that comparison of data from two different individuals was crucial because eye bulbs used in this study were obtained from cornea donors with different background in terms of age, sex, cause of death, postmortem time. Analyzing all the genes in different individuals enabled me to verify whether differences in any of the above mentioned factors pertaining to the donor could interfere with the reliability of the results obtained. I verified a high

---

similarity in the expression patterns on eye sections from different donors suggesting that the tissue handling procedure was optimal and that the data obtained were reliable.

Within the catalog of the genes with expression patterns conserved between mouse and human, I found three genes for which I observed RNA expression profiles that are not in agreement with previously published reports. This is the case of the *CNGB1*, *USH2A* and *FSCN2* genes. All these three genes were previously reported to be expressed only in the photoreceptor layer<sup>55, 77, 113-115</sup>, while data obtained during the course of this study suggested that they have a more widespread distribution across all retinal cell layers, both in human and in mouse. The B subunit of rod cGMP-gated channel (*CNGB1*), together with subunit A, forms cyclic nucleotide gated channels that play a critical role in visual transduction<sup>113</sup>. These two subunits build heteromeric channels that localize in the outer segments of photoreceptors<sup>113, 114</sup>. In darkness, these channels are opened by cGMP, maintaining an inward current. Light induces hydrolysis of cGMP, thus resulting in closure of the channels and hyperpolarization of the cell as a final response<sup>144</sup>. The B1 subunit of the CNG channel has been previously detected not only in photoreceptor cells of the retina but also in olfactory channels<sup>145</sup>, sperm cells and other tissues<sup>146</sup>. In my study, both human and mouse specific probes show expression of *CNGB1* in all the layers of the retina. Hence, it is possible that *CNGB1* plays some role in channels assembling in the different neurons of the retina.

The *USH2A* gene is responsible for both non-syndromic RP and for Usher syndrome that is characterized by hearing loss and RP<sup>32</sup>. The *USH2A* is thought to be an extracellular matrix protein as it is composed of protein domains that are commonly seen in extracellular proteins or that are involved in

protein-protein or protein-matrix interactions<sup>77</sup>. This led to the suggestion that this gene may play a role in nerve fiber guidance<sup>147</sup>. *USH2A* mRNA expression was previously reported exclusively in the retina outer segment in various species<sup>77</sup>, while subsequent studies indicated the presence of the *USH2A* protein in basement membranes and extracellular matrix in different tissues<sup>148, 149</sup>. The *USH2A* gene encodes for two alternatively spliced isoforms, a short ~170 kDa *USH2A isoform a*, previously termed usherin, and a much longer ~580 kDa *USH2A isoform b*<sup>150</sup>. I used different probes to analyze these two different *USH2A* mRNA isoforms in order to exclude the possibility that the observed differences were related to different RNA expression patterns of the isoforms. These experiments confirmed a diffuse staining in the different retinal layers with both probes specific for the different isoforms. Similarly, I also observed ubiquitous expression in the retina of both the human and mouse *FSCN2* genes, contrary to previously published photoreceptor-specific expression data<sup>55, 115</sup>. There is only one report showing that mutation in the *FSCN2* gene cause retinitis pigmentosa<sup>54</sup>; however these findings were subsequently questioned because four independent studies showed no correlation between *FSCN2* mutation and RP<sup>56, 151-153</sup>. Particularly interesting are the findings concerning the *NRL* gene. *NRL* (neural retina leucine zipper) causes both autosomal-recessive and autosomal-dominant RP<sup>60</sup>. Initially *NRL* was reported to be a retinal-specific transcription factor<sup>154</sup>. However, intensive studies in the past years suggest that *NRL* is a rod-specific transcription factor<sup>116-118, 155</sup>. Precisely, the first reports on RNA and protein localization showed expression in all the retina layers at different developmental stages and in adults in different species<sup>118, 154, 156</sup>. However, the *NRL* cRNA full length probe and antibody used in the mentioned studies were suggested to cross-react with



sequences other than *NRL* and this led to the belief that *NRL* is rod specific based on the evidence that it regulates rod photoreceptor-specific gene expression<sup>118</sup>. In favor of this hypothesis was also the phenotype observed in *Nrl* knock out mice in which the inactivation of this gene causes functional transformation of rods into cones<sup>117</sup>. Furthermore, the *Nrl*-specific promoter drives gene expression specifically in rod photoreceptors in a transgenic mouse<sup>116</sup>. Nevertheless, data showing restricted expression of *Nrl* in photoreceptor (both at the transcript and at the protein levels) are not available in literature. *NRL* expression data obtained in my study are in agreement with the previously mentioned reports showing that *NRL* mRNA is apparently detectable in all retinal cells. In my experiments, I used four independent and highly specific human riboprobes, covering either the 3'-UTR or different alternative 5' ends of different splice isoforms belonging to this gene and two independent mouse *Nrl* probes. All the analyzed probes gave highly similar expression patterns in human and mouse eye sections. Furthermore, I detected a widespread expression across all mouse retinal cell layers also in *Aip1*<sup>-/-</sup> mouse retinas. However, RT-PCR assessment of *Nrl* expression revealed that the *Nrl* mRNA is detectable only in wild type mouse retina and not in *Aip1*<sup>-/-</sup> retina that has lost its photoreceptors, suggesting that indeed this gene is exclusively expressed in photoreceptors<sup>116-118</sup>. These findings suggest that, contrary to all the genes that I have analyzed in this study, RNA ISH is not the appropriate method for *NRL* expression analysis. This consideration is supported also by the RT-PCR analysis of the other transcripts that showed a pattern diverging from previous reports, i.e. *Cngb1*, *Ush2A* and *Fscn2* that confirmed a non-photoreceptor restricted expression demonstrated by the amplification of their transcripts in *Aip1*<sup>-/-</sup> retina. Considering the recent findings

that significant fractions of eukaryotic genomes give rise to some unannotated RNAs that may act as primary transcripts for the production of short RNAs<sup>157</sup>, the observed expression of *NRL* obtained by RNA ISH may be explained by the presence of as yet uncharacterized additional RNAs transcribed from the *NRL* genomic region.

I also detected significant differences in the expression pattern of the *CA4* gene in the human retina with respect to previous reports. *CA4* is an important regulator of pH balance because it catalyzes hydration of carbon dioxide<sup>83</sup>. Due to the fact that retina is a highly metabolic tissue with a high rate of acid production, mutations in a pH modulator, such as *CA4*, may lead to retinal cell apoptosis. Indeed, it has been shown that *CA4*, when mutated, causes retinitis pigmentosa<sup>83, 158</sup> and interestingly, it is the only RP-causing gene shown to be expressed outside the neural retina or retinal pigment epithelium: more precisely, the *CA4* protein was reported to be present in choriocapillaris<sup>83, 123</sup>. My expression analysis revealed that the human *CA4* mRNA is localized in all retina layers, as determined by using two different probes. On the other hand, I could not detect the *CA4* transcripts in the murine retina. This may be due either to the low RNA levels of *CA4* in mouse retina or indeed to a real difference in *CA4* localization in the two species.

I also detected differences in the expression patterns between the human and murine retina for the following genes: *RGR*, *RLBP1*, *RPGR* and *PAP1*. *RGR* and *RLBP1* genes are members of the visual cycle cascade, which is responsible for the regeneration of bleached visual pigments. In rods, the visual cycle initiates in the photoreceptor cells, but then it is completed in the RPE. These two genes encode enzymes very important for chromophore regeneration in the RPE<sup>106, 121, 122</sup> although both are also expressed in Müller

cells while *RLBP1* is additionally detectable in ganglion cells<sup>120, 122</sup>. I confirmed the expected expression pattern in the RPE of the *Rgr* and *Rlbp1* genes and *Rlbp1* expression in INL and GCL in the mouse eye. However, in the human retina, I observed the *RGR* mRNA not only in the RPE and INL but also in photoreceptors. Similarly, *RLBP1* is expressed in RPE and also in ONL, INL and GCL. Protein localization associated to specific markers for rods and cones showed that *RLBP1* is probably expressed in rods, whereas no colocalization was detected with a cone-specific marker. We must bear in mind that the cone marker used in this study, i.e., PNA, marks only the cone outer and inner segments, while, on the other hand, the *RLBP1* protein is not a membrane protein. Thus, we cannot definitely exclude that *RLBP1* may also be present in cones. The function of the *RGR* and *RLBP1* genes is well established in the RPE<sup>106, 121, 122</sup>; however their exact role in cells other than RPE is still not clear. The newly reported RNA localizations of *RGR* and *RLBP1* in photoreceptors in humans are worth of further investigation for a better understanding of their function outside the RPE.

The comparative RNA ISH analysis of RP genes in human and mouse retinas also revealed interesting expression patterns for the *RPGR* and *PAP1* genes. *RPGR* stands for Retinitis Pigmentosa GTPase regulator and is necessary for maintenance of photoreceptor viability<sup>75</sup>, probably by being associated with protein trafficking from inner to outer segments of photoreceptors<sup>76</sup>. Two splice-variants are present in the retina: the “default form” and the so-called “ORF15 form”, which harbors a mutation hot spot for retinitis pigmentosa<sup>76, 159</sup>. Both *RPGR* proteins were previously detected in connecting cilia or in photoreceptor outer segments depending on the species analyzed<sup>75</sup>. I performed RNA ISH analysis with probes specifically recognizing

each of the two forms in human and murine retina and found different expression profiles. Interestingly, *ORF15* shows a specific expression in human photoreceptors, i.e., the cells that are the main targets of RP while the “default form”, although predominantly expressed in photoreceptors, can be detected also in the INL. The photoreceptor-specific transcription of *RPGR-ORF15* nicely correlates with the observation that the majority of *RPGR* mutations causing the RP phenotype fall within this particular splice variant. Likewise, *PAP1* is also predominantly expressed in photoreceptors in the human retina compared to the mouse retina where it is expressed mainly in the GCL and INL. *PAP1*, together with *PRPF3*, *PRPF31* and *PRPF8*, is a pre-mRNA splicing factor involved in assembling of spliceosome U4/U6.U5 tri-snRNP complex<sup>67-70</sup>. It is very challenging to understand why mutations in ubiquitously expressed splicing factors cause such a specific phenotype as RP. Expression analysis of *PRPF3*, *PRPF31* and *PRPF8* performed in this study did not show prevalent expression of these genes in photoreceptors. Only the *PAP1* mRNA appears to be more abundant in human photoreceptors compared to other retinal cells. These observations may open new perspectives for the study of the link between pre-mRNA splicing factors and RP pathogenesis.

This study provides the first systematic comparative expression analysis in the human and in the mouse retina of all known genes responsible for RP (RP gene expression atlas, <http://www.tigem.it/RPexp/>) providing important insights into the function of these genes through expression analysis in the human retina. The differences observed in the expression patterns of some of the analyzed genes in humans and mice will shed new light on the function of these genes and their role in the disease pathogenesis and will be a

fundamental support towards the correct transfer of information obtained from animal models to human RP patients.

1. Jacobs GH. Biological Psychology. In: Gallagher MN, R. J. (ed), *Handbook of Psychology*. New York: Wiley; 2002:47–70
2. Lev S. Molecular aspects of retinal degenerative diseases. *Cellular and molecular neurobiology* 2001;21:575-589.
3. Schmitt A, Wolfrum U. Identification of novel molecular components of the photoreceptor connecting cilium by immunoscreens. *Exp Eye Res* 2001;73:837-849.
4. Nathans J. Rhodopsin: structure, function, and genetics. *Biochemistry* 1992;31:4923-4931.
5. Palczewski K. G protein-coupled receptor rhodopsin. *Annual review of biochemistry* 2006;75:743-767.
6. Lerea CL, Somers DE, Hurley JB, Klock IB, Bunt-Milam AH. Identification of specific transducin alpha subunits in retinal rod and cone photoreceptors. *Science* 1986;234:77-80.
7. Stryer L. Visual excitation and recovery. *J Biol Chem* 1991;266:10711-10714.
8. Baehr W, Devlin MJ, Applebury ML. Isolation and characterization of cGMP phosphodiesterase from bovine rod outer segments. *J Biol Chem* 1979;254:11669-11677.
9. Dhallan RS, Macke JP, Eddy RL, et al. Human rod photoreceptor cGMP-gated channel: amino acid sequence, gene structure, and functional expression. *J Neurosci* 1992;12:3248-3256.
10. Dryja TP. Retinitis pigmentosa and stationary night blindness. In: Scriver CR, Beaudet, A.L., Sly, W.S. and Valle, D. (ed), *The Metabolic and Molecular Bases of Inherited Disease, 8th edn*. New York: McGraw-Hill; 2001.:5987–6032.

11. van Soest S, Westerveld A, de Jong PT, Bleeker-Wagemakers EM, Bergen AA. Retinitis pigmentosa: defined from a molecular point of view. *Survey of ophthalmology* 1999;43:321-334.
12. Thompson DA, Gal A. Vitamin A metabolism in the retinal pigment epithelium: genes, mutations, and diseases. *Progress in retinal and eye research* 2003;22:683-703.
13. Allikmets R. A photoreceptor cell-specific ATP-binding transporter gene (ABCR) is mutated in recessive Stargardt macular dystrophy. *Nat Genet* 1997;17:122.
14. Weng J, Mata NL, Azarian SM, Tzekov RT, Birch DG, Travis GH. Insights into the function of Rim protein in photoreceptors and etiology of Stargardt's disease from the phenotype in abcr knockout mice. *Cell* 1999;98:13-23.
15. Rattner A, Smallwood PM, Nathans J. Identification and characterization of all-trans-retinol dehydrogenase from photoreceptor outer segments, the visual cycle enzyme that reduces all-trans-retinal to all-trans-retinol. *J Biol Chem* 2000;275:11034-11043.
16. Pfeffer BA, Clark VM, Flannery JG, Bok D. Membrane receptors for retinol-binding protein in cultured human retinal pigment epithelium. *Invest Ophthalmol Vis Sci* 1986;27:1031-1040.
17. Saari JC, Bredberg L, Garwin GG. Identification of the endogenous retinoids associated with three cellular retinoid-binding proteins from bovine retina and retinal pigment epithelium. *J Biol Chem* 1982;257:13329-13333.

18. Ruiz A, Winston A, Lim YH, Gilbert BA, Rando RR, Bok D. Molecular and biochemical characterization of lecithin retinol acyltransferase. *J Biol Chem* 1999;274:3834-3841.
19. Digner PS, Law WC, Canada FJ, Rando RR. Membranes as the energy source in the endergonic transformation of vitamin A to 11-cis-retinol. *Science* 1989;244:968-971.
20. Xue L, Gollapalli DR, Maiti P, Jahng WJ, Rando RR. A palmitoylation switch mechanism in the regulation of the visual cycle. *Cell* 2004;117:761-771.
21. Simon A, Hellman U, Wernstedt C, Eriksson U. The retinal pigment epithelial-specific 11-cis retinol dehydrogenase belongs to the family of short chain alcohol dehydrogenases. *J Biol Chem* 1995;270:1107-1112.
22. Saari JC, Nawrot M, Kennedy BN, et al. Visual cycle impairment in cellular retinaldehyde binding protein (CRALBP) knockout mice results in delayed dark adaptation. *Neuron* 2001;29:739-748.
23. Horsford DJ, Hanson, I., Freund, C., McInnes, R. R., van Heyningen, V. *Transcription factors in eye disease and ocular development*. 8th ed. New York: McGraw-Hill; 2001:5987-6032.
24. Gregory-Evans K, Bhattacharya SS. Genetic blindness: current concepts in the pathogenesis of human outer retinal dystrophies. *Trends Genet* 1998;14:103-108.
25. Rattner A, Sun H, Nathans J. Molecular genetics of human retinal disease. *Annual review of genetics* 1999;33:89-131.
26. Farrar GJ, Kenna PF, Humphries P. On the genetics of retinitis pigmentosa and on mutation-independent approaches to therapeutic intervention. *Embo J* 2002;21:857-864.



27. Boughman JA, Fishman GA. A genetic analysis of retinitis pigmentosa. *Br J Ophthalmol* 1983;67:449-454.
28. Hartong DT, Berson EL, Dryja TP. Retinitis pigmentosa. *Lancet* 2006;368:1795-1809.
29. Phelan JK, Bok D. A brief review of retinitis pigmentosa and the identified retinitis pigmentosa genes. *Mol Vis* 2000;6:116-124.
30. Li ZY, Possin DE, Milam AH. Histopathology of bone spicule pigmentation in retinitis pigmentosa. *Ophthalmology* 1995;102:805-816.
31. Hims MM, Diager SP, Inglehearn CF. Retinitis pigmentosa: genes, proteins and prospects. *Dev Ophthalmol* 2003;37:109-125.
32. Kremer H, van Wijk E, Marker T, Wolfrum U, Roepman R. Usher syndrome: molecular links of pathogenesis, proteins and pathways. *Hum Mol Genet* 2006;15 Spec No 2:R262-270.
33. Katsanis N. The oligogenic properties of Bardet-Biedl syndrome. *Hum Mol Genet* 2004;13 Spec No 1:R65-71.
34. Nathans J, Hogness DS. Isolation and nucleotide sequence of the gene encoding human rhodopsin. *Proc Natl Acad Sci U S A* 1984;81:4851-4855.
35. Huang SH, Pittler SJ, Huang X, Oliveira L, Berson EL, Dryja TP. Autosomal recessive retinitis pigmentosa caused by mutations in the alpha subunit of rod cGMP phosphodiesterase. *Nat Genet* 1995;11:468-471.
36. McLaughlin ME, Ehrhart TL, Berson EL, Dryja TP. Mutation spectrum of the gene encoding the beta subunit of rod phosphodiesterase among patients with autosomal recessive retinitis pigmentosa. *Proc Natl Acad Sci U S A* 1995;92:3249-3253.

37. Dryja TP, Finn JT, Peng YW, McGee TL, Berson EL, Yau KW. Mutations in the gene encoding the alpha subunit of the rod cGMP-gated channel in autosomal recessive retinitis pigmentosa. *Proc Natl Acad Sci U S A* 1995;92:10177-10181.
38. Fuchs S, Nakazawa M, Maw M, Tamai M, Oguchi Y, Gal A. A homozygous 1-base pair deletion in the arrestin gene is a frequent cause of Oguchi disease in Japanese. *Nat Genet* 1995;10:360-362.
39. Payne AM, Downes SM, Bessant DA, et al. Genetic analysis of the guanylate cyclase activator 1B (GUCA1B) gene in patients with autosomal dominant retinal dystrophies. *Journal of medical genetics* 1999;36:691-693.
40. Bowne SJ, Sullivan LS, Blanton SH, et al. Mutations in the inosine monophosphate dehydrogenase 1 gene (IMPDH1) cause the RP10 form of autosomal dominant retinitis pigmentosa. *Hum Mol Genet* 2002;11:559-568.
41. Howes K, Bronson JD, Dang YL, et al. Gene array and expression of mouse retina guanylate cyclase activating proteins 1 and 2. *Invest Ophthalmol Vis Sci* 1998;39:867-875.
42. Aherne A, Kennan A, Kenna PF, et al. On the molecular pathology of neurodegeneration in IMPDH1-based retinitis pigmentosa. *Hum Mol Genet* 2004;13:641-650.
43. Martinez-Mir A, Bayes M, Vilageliu L, et al. A new locus for autosomal recessive retinitis pigmentosa (RP19) maps to 1p13-1p21. *Genomics* 1997;40:142-146.

44. Martinez-Mir A, Paloma E, Allikmets R, et al. Retinitis pigmentosa caused by a homozygous mutation in the Stargardt disease gene ABCR. *Nat Genet* 1998;18:11-12.
45. Maw MA, Kennedy B, Knight A, et al. Mutation of the gene encoding cellular retinaldehyde-binding protein in autosomal recessive retinitis pigmentosa. *Nat Genet* 1997;17:198-200.
46. Gu SM, Thompson DA, Srikumari CR, et al. Mutations in RPE65 cause autosomal recessive childhood-onset severe retinal dystrophy. *Nat Genet* 1997;17:194-197.
47. Morimura H, Fishman GA, Grover SA, Fulton AB, Berson EL, Dryja TP. Mutations in the RPE65 gene in patients with autosomal recessive retinitis pigmentosa or leber congenital amaurosis. *Proc Natl Acad Sci U S A* 1998;95:3088-3093.
48. Morimura H, Saindelle-Ribeauveau F, Berson EL, Dryja TP. Mutations in RGR, encoding a light-sensitive opsin homologue, in patients with retinitis pigmentosa. *Nat Genet* 1999;23:393-394.
49. Thompson DA, Li Y, McHenry CL, et al. Mutations in the gene encoding lecithin retinol acyltransferase are associated with early-onset severe retinal dystrophy. *Nat Genet* 2001;28:123-124.
50. Gal A, Li Y, Thompson DA, et al. Mutations in MERTK, the human orthologue of the RCS rat retinal dystrophy gene, cause retinitis pigmentosa. *Nat Genet* 2000;26:270-271.
51. Nour M, Ding XQ, Stricker H, Fliesler SJ, Naash MI. Modulating expression of peripherin/rds in transgenic mice: critical levels and the effect of overexpression. *Invest Ophthalmol Vis Sci* 2004;45:2514-2521.

52. Dryja TP, Adams SM, Grimsby JL, et al. Null RPGRIP1 alleles in patients with Leber congenital amaurosis. *Am J Hum Genet* 2001;68:1295-1298.
53. Zhao Y, Hong DH, Pawlyk B, et al. The retinitis pigmentosa GTPase regulator (RPGR)- interacting protein: subserving RPGR function and participating in disk morphogenesis. *Proc Natl Acad Sci U S A* 2003;100:3965-3970.
54. Wada Y, Abe T, Takeshita T, Sato H, Yanashima K, Tamai M. Mutation of human retinal fascin gene (FSCN2) causes autosomal dominant retinitis pigmentosa. *Invest Ophthalmol Vis Sci* 2001;42:2395-2400.
55. Saishin Y, Shimada S, Morimura H, et al. Isolation of a cDNA encoding a photoreceptor cell-specific actin-bundling protein: retinal fascin. *FEBS Lett* 1997;414:381-386.
56. Zhang Q, Li S, Xiao X, Jia X, Guo X. The 208delG mutation in FSCN2 does not associate with retinal degeneration in Chinese individuals. *Invest Ophthalmol Vis Sci* 2007;48:530-533.
57. Freund C, Horsford DJ, McInnes RR. Transcription factor genes and the developing eye: a genetic perspective. *Hum Mol Genet* 1996;5 Spec No:1471-1488.
58. Chen S, Wang QL, Nie Z, et al. Crx, a novel Otx-like paired-homeodomain protein, binds to and transactivates photoreceptor cell-specific genes. *Neuron* 1997;19:1017-1030.
59. Sohocki MM, Sullivan LS, Mintz-Hittner HA, et al. A range of clinical phenotypes associated with mutations in CRX, a photoreceptor transcription-factor gene. *Am J Hum Genet* 1998;63:1307-1315.

60. Bessant DA, Payne AM, Mitton KP, et al. A mutation in NRL is associated with autosomal dominant retinitis pigmentosa. *Nat Genet* 1999;21:355-356.
61. Freund CL, Gregory-Evans CY, Furukawa T, et al. Cone-rod dystrophy due to mutations in a novel photoreceptor-specific homeobox gene (CRX) essential for maintenance of the photoreceptor. *Cell* 1997;91:543-553.
62. Furukawa T, Morrow EM, Cepko CL. Crx, a novel otx-like homeobox gene, shows photoreceptor-specific expression and regulates photoreceptor differentiation. *Cell* 1997;91:531-541.
63. Swain PK, Chen S, Wang QL, et al. Mutations in the cone-rod homeobox gene are associated with the cone-rod dystrophy photoreceptor degeneration. *Neuron* 1997;19:1329-1336.
64. Swaroop A, Wang QL, Wu W, et al. Leber congenital amaurosis caused by a homozygous mutation (R90W) in the homeodomain of the retinal transcription factor CRX: direct evidence for the involvement of CRX in the development of photoreceptor function. *Hum Mol Genet* 1999;8:299-305.
65. Coppieters F, Leroy BP, Beysen D, et al. Recurrent mutation in the first zinc finger of the orphan nuclear receptor NR2E3 causes autosomal dominant retinitis pigmentosa. *Am J Hum Genet* 2007;81:147-157.
66. Cheng H, Khanna H, Oh EC, Hicks D, Mitton KP, Swaroop A. Photoreceptor-specific nuclear receptor NR2E3 functions as a transcriptional activator in rod photoreceptors. *Hum Mol Genet* 2004;13:1563-1575.

67. Vithana EN, Abu-Safieh L, Allen MJ, et al. A human homolog of yeast pre-mRNA splicing gene, PRP31, underlies autosomal dominant retinitis pigmentosa on chromosome 19q13.4 (RP11). *Molecular cell* 2001;8:375-381.
68. Chakarova CF, Hims MM, Bolz H, et al. Mutations in HPRP3, a third member of pre-mRNA splicing factor genes, implicated in autosomal dominant retinitis pigmentosa. *Hum Mol Genet* 2002;11:87-92.
69. McKie AB, McHale JC, Keen TJ, et al. Mutations in the pre-mRNA splicing factor gene PRPC8 in autosomal dominant retinitis pigmentosa (RP13). *Hum Mol Genet* 2001;10:1555-1562.
70. Keen TJ, Hims MM, McKie AB, et al. Mutations in a protein target of the Pim-1 kinase associated with the RP9 form of autosomal dominant retinitis pigmentosa. *Eur J Hum Genet* 2002;10:245-249.
71. Vithana EN, Abu-Safieh L, Pelosini L, et al. Expression of PRPF31 mRNA in patients with autosomal dominant retinitis pigmentosa: a molecular clue for incomplete penetrance? *Invest Ophthalmol Vis Sci* 2003;44:4204-4209.
72. Comitato A, Spanpanato C, Chakarova C, Sanges D, Bhattacharya SS, Marigo V. Mutations in splicing factor PRPF3, causing retinal degeneration, form detrimental aggregates in photoreceptor cells. *Hum Mol Genet* 2007;16:1699-1707.
73. van der Spuy J, Kim JH, Yu YS, et al. The expression of the Leber congenital amaurosis protein AIPL1 coincides with rod and cone photoreceptor development. *Invest Ophthalmol Vis Sci* 2003;44:5396-5403.

74. Sohocki MM, Perrault I, Leroy BP, et al. Prevalence of AIPL1 mutations in inherited retinal degenerative disease. *Molecular genetics and metabolism* 2000;70:142-150.
75. Hong DH, Pawlyk B, Sokolov M, et al. RPGR isoforms in photoreceptor connecting cilia and the transitional zone of motile cilia. *Invest Ophthalmol Vis Sci* 2003;44:2413-2421.
76. Shu X, Black GC, Rice JM, et al. RPGR mutation analysis and disease: an update. *Hum Mutat* 2007;28:322-328.
77. Huang D, Eudy JD, Uzvolgyi E, et al. Identification of the mouse and rat orthologs of the gene mutated in Usher syndrome type IIA and the cellular source of USH2A mRNA in retina, a target tissue of the disease. *Genomics* 2002;80:195-203.
78. Liu J, Huang Q, Higdon J, et al. Distinct gene expression profiles and reduced JNK signaling in retinitis pigmentosa caused by RP1 mutations. *Hum Mol Genet* 2005;14:2945-2958.
79. Grayson C, Bartolini F, Chapple JP, et al. Localization in the human retina of the X-linked retinitis pigmentosa protein RP2, its homologue cofactor C and the RP2 interacting protein Arl3. *Hum Mol Genet* 2002;11:3065-3074.
80. Tuson M, Marfany G, Gonzalez-Duarte R. Mutation of CERKL, a novel human ceramide kinase gene, causes autosomal recessive retinitis pigmentosa (RP26). *Am J Hum Genet* 2004;74:128-138.
81. den Hollander AI, Ghiani M, de Kok YJ, et al. Isolation of Crb1, a mouse homologue of Drosophila crumbs, and analysis of its expression pattern in eye and brain. *Mechanisms of development* 2002;110:203-207.

82. Xi Q, Pauer GJ, Marmorstein AD, Crabb JW, Hagstrom SA. Tubby-like protein 1 (TULP1) interacts with F-actin in photoreceptor cells. *Invest Ophthalmol Vis Sci* 2005;46:4754-4761.
83. Yang Z, Alvarez BV, Chakarova C, et al. Mutant carbonic anhydrase 4 impairs pH regulation and causes retinal photoreceptor degeneration. *Hum Mol Genet* 2005;14:255-265.
84. Rivolta C, Sharon D, DeAngelis MM, Dryja TP. Retinitis pigmentosa and allied diseases: numerous diseases, genes, and inheritance patterns. *Hum Mol Genet* 2002;11:1219-1227.
85. Wright AF, Van Heyningen V. Short cut to disease genes. *Nature* 2001;414:705-706.
86. Adams MD, Kelley JM, Gocayne JD, et al. Complementary DNA sequencing: expressed sequence tags and human genome project. *Science* 1991;252:1651-1656.
87. Boguski MS, Tolstoshev CM, Bassett DE, Jr. Gene discovery in dbEST. *Science* 1994;265:1993-1994.
88. Sikela JM, Auffray C. Finding new genes faster than ever. *Nat Genet* 1993;3:189-191.
89. Katsanis N, Worley KC, Gonzalez G, Ansley SJ, Lupski JR. A computational/functional genomics approach for the enrichment of the retinal transcriptome and the identification of positional candidate retinopathy genes. *Proc Natl Acad Sci U S A* 2002;99:14326-14331.
90. Lord-Grignon J, Tetreault N, Mears AJ, Swaroop A, Bernier G. Characterization of new transcripts enriched in the mouse retina and identification of candidate retinal disease genes. *Invest Ophthalmol Vis Sci* 2004;45:3313-3319.



91. Gieser L, Swaroop A. Expressed sequence tags and chromosomal localization of cDNA clones from a subtracted retinal pigment epithelium library. *Genomics* 1992;13:873-876.
92. Sohocki MM, Malone KA, Sullivan LS, Daiger SP. Localization of retina/pineal-expressed sequences: identification of novel candidate genes for inherited retinal disorders. *Genomics* 1999;58:29-33.
93. Malone K, Sohocki MM, Sullivan LS, Daiger SP. Identifying and mapping novel retinal-expressed ESTs from humans. *Mol Vis* 1999;5:5.
94. Sinha S, Sharma A, Agarwal N, Swaroop A, Yang-Feng TL. Expression profile and chromosomal location of cDNA clones, identified from an enriched adult retina library. *Invest Ophthalmol Vis Sci* 2000;41:24-28.
95. Blackshaw S, Fraioli RE, Furukawa T, Cepko CL. Comprehensive analysis of photoreceptor gene expression and the identification of candidate retinal disease genes. *Cell* 2001;107:579-589.
96. Dalke C, Graw J. Mouse mutants as models for congenital retinal disorders. *Exp Eye Res* 2005;81:503-512.
97. Maronpot R, Boorman, GA, Gaul, BW. *Pathology of the mouse*. Vienna, IL: Cache River Press; 1999:471-480.
98. Klein RJ, Zeiss C, Chew EY, et al. Complement factor H polymorphism in age-related macular degeneration. *Science* 2005;308:385-389.
99. Acland GM, Aguirre GD, Ray J, et al. Gene therapy restores vision in a canine model of childhood blindness. *Nat Genet* 2001;28:92-95.
100. Schlichtenbrede FC, da Cruz L, Stephens C, et al. Long-term evaluation of retinal function in Prph2Rd2/Rd2 mice following AAV-mediated gene replacement therapy. *The journal of gene medicine* 2003;5:757-764.

101. O'Reilly M, Palfi A, Chadderton N, et al. RNA interference-mediated suppression and replacement of human rhodopsin in vivo. *Am J Hum Genet* 2007;81:127-135.
102. Bainbridge JW, Tan MH, Ali RR. Gene therapy progress and prospects: the eye. *Gene therapy* 2006;13:1191-1197.
103. Reymond A, Marigo V, Yaylaoglu MB, et al. Human chromosome 21 gene expression atlas in the mouse. *Nature* 2002;420:582-586.
104. Buniello A, Montanaro D, Volinia S, Gasparini P, Marigo V. An expression atlas of connexin genes in the mouse. *Genomics* 2004;83:812-820.
105. Sambrook J, Fritsch, E.F., Maniatis, T. *Molecular Cloning: A Laboratory Manual*. . Second edition ed: CSH; 1989.
106. Fong HK, Lin MY, Pandey S. Exon-skipping variant of RGR opsin in human retina and pigment epithelium. *Exp Eye Res* 2006;83:133-140.
107. Edwards AO, Ritter R, 3rd, Abel KJ, Manning A, Panhuysen C, Farrer LA. Complement factor H polymorphism and age-related macular degeneration. *Science* 2005;308:421-424.
108. Gaboriaud C, Thielens NM, Gregory LA, Rossi V, Fontecilla-Camps JC, Arlaud GJ. Structure and activation of the C1 complex of complement: unraveling the puzzle. *Trends in immunology* 2004;25:368-373.
109. Saar K, Al-Gazali L, Sztriha L, et al. Homozygosity mapping in families with Joubert syndrome identifies a locus on chromosome 9q34.3 and evidence for genetic heterogeneity. *Am J Hum Genet* 1999;65:1666-1671.
110. Ottschytsch N, Raes A, Van Hoorick D, Snyders DJ. Obligatory heterotetramerization of three previously uncharacterized Kv channel

- alpha-subunits identified in the human genome. *Proc Natl Acad Sci U S A* 2002;99:7986-7991.
111. Wu H, Cowing JA, Michaelides M, et al. Mutations in the gene *KCNV2* encoding a voltage-gated potassium channel subunit cause "cone dystrophy with supernormal rod electroretinogram" in humans. *Am J Hum Genet* 2006;79:574-579.
112. Thiagalingam S, McGee TL, Weleber RG, et al. Novel Mutations in the *KCNV2* Gene in Patients with Cone Dystrophy and a Supernormal Rod Electroretinogram. *Ophthalmic Genet* 2007;28:135-142.
113. Huttl S, Michalakis S, Seeliger M, et al. Impaired channel targeting and retinal degeneration in mice lacking the cyclic nucleotide-gated channel subunit *CNGB1*. *J Neurosci* 2005;25:130-138.
114. Trudeau MC, Zagotta WN. An intersubunit interaction regulates trafficking of rod cyclic nucleotide-gated channels and is disrupted in an inherited form of blindness. *Neuron* 2002;34:197-207.
115. Yokokura S, Wada Y, Nakai S, et al. Targeted disruption of *FSCN2* gene induces retinopathy in mice. *Invest Ophthalmol Vis Sci* 2005;46:2905-2915.
116. Akimoto M, Cheng H, Zhu D, et al. Targeting of GFP to newborn rods by *Nrl* promoter and temporal expression profiling of flow-sorted photoreceptors. *Proc Natl Acad Sci U S A* 2006;103:3890-3895.
117. Mears AJ, Kondo M, Swain PK, et al. *Nrl* is required for rod photoreceptor development. *Nat Genet* 2001;29:447-452.
118. Swain PK, Hicks D, Mears AJ, et al. Multiple phosphorylated isoforms of *NRL* are expressed in rod photoreceptors. *J Biol Chem* 2001;276:36824-36830.

119. Dyer MA, Donovan SL, Zhang J, et al. Retinal degeneration in Aipl1-deficient mice: a new genetic model of Leber congenital amaurosis. *Brain research* 2004;132:208-220.
120. Bailey MJ, Cassone VM. Opsin photoisomerases in the chick retina and pineal gland: characterization, localization, and circadian regulation. *Invest Ophthalmol Vis Sci* 2004;45:769-775.
121. Bunt-Milam AH, Saari JC. Immunocytochemical localization of two retinoid-binding proteins in vertebrate retina. *J Cell Biol* 1983;97:703-712.
122. Kennedy BN, Li C, Ortego J, Coca-Prados M, Sarthy VP, Crabb JW. CRALBP transcriptional regulation in ciliary epithelial, retinal Muller and retinal pigment epithelial cells. *Exp Eye Res* 2003;76:257-260.
123. Nagelhus EA, Mathiesen TM, Bateman AC, et al. Carbonic anhydrase XIV is enriched in specific membrane domains of retinal pigment epithelium, Muller cells, and astrocytes. *Proc Natl Acad Sci U S A* 2005;102:8030-8035.
124. Hong DH, Yue G, Adamian M, Li T. Retinitis pigmentosa GTPase regulator (RPGR)-interacting protein is stably associated with the photoreceptor ciliary axoneme and anchors RPGR to the connecting cilium. *J Biol Chem* 2001;276:12091-12099.
125. Inglehearn CF, Carter SA, Keen TJ, et al. A new locus for autosomal dominant retinitis pigmentosa on chromosome 7p. *Nat Genet* 1993;4:51-53.
126. Bischof JM, Chiang AP, Scheetz TE, et al. Genome-wide identification of pseudogenes capable of disease-causing gene conversion. *Human mutation* 2006;27:545-552.

127. Ballabio A. The rise and fall of positional cloning? *Nat Genet* 1993;3:277-279.
128. Wistow G, Bernstein SL, Wyatt MK, et al. Expressed sequence tag analysis of human retina for the NEIBank Project: retbindin, an abundant, novel retinal cDNA and alternative splicing of other retina-preferred gene transcripts. *Mol Vis* 2002;8:196-204.
129. Haines JL, Hauser MA, Schmidt S, et al. Complement factor H variant increases the risk of age-related macular degeneration. *Science* 2005;308:419-421.
130. Tuo J, Bojanowski CM, Chan CC. Genetic factors of age-related macular degeneration. *Progress in retinal and eye research* 2004;23:229-249.
131. Ambati J, Anand A, Fernandez S, et al. An animal model of age-related macular degeneration in senescent Ccl-2- or Ccr-2-deficient mice. *Nat Med* 2003;9:1390-1397.
132. Hageman GS, Luthert PJ, Victor Chong NH, Johnson LV, Anderson DH, Mullins RF. An integrated hypothesis that considers drusen as biomarkers of immune-mediated processes at the RPE-Bruch's membrane interface in aging and age-related macular degeneration. *Progress in retinal and eye research* 2001;20:705-732.
133. Gold B, Merriam JE, Zernant J, et al. Variation in factor B (BF) and complement component 2 (C2) genes is associated with age-related macular degeneration. *Nat Genet* 2006;38:458-462.
134. Yates JR, Sepp T, Matharu BK, et al. Complement C3 variant and the risk of age-related macular degeneration. *The New England journal of medicine* 2007;357:553-561.

135. Hayward C, Shu X, Cideciyan AV, et al. Mutation in a short-chain collagen gene, CTRP5, results in extracellular deposit formation in late-onset retinal degeneration: a genetic model for age-related macular degeneration. *Hum Mol Genet* 2003;12:2657-2667.
136. Mosavi LK, Cammett TJ, Desrosiers DC, Peng ZY. The ankyrin repeat as molecular architecture for protein recognition. *Protein Sci* 2004;13:1435-1448.
137. Reim K, Wegmeyer H, Brandstatter JH, et al. Structurally and functionally unique complexins at retinal ribbon synapses. *J Cell Biol* 2005;169:669-680.
138. Reim K, Mansour M, Varoqueaux F, et al. Complexins regulate a late step in Ca<sup>2+</sup>-dependent neurotransmitter release. *Cell* 2001;104:71-81.
139. Wycisk KA, Zeitz C, Feil S, et al. Mutation in the auxiliary calcium-channel subunit CACNA2D4 causes autosomal recessive cone dystrophy. *Am J Hum Genet* 2006;79:973-977.
140. Johnson S, Halford S, Morris AG, et al. Genomic organisation and alternative splicing of human RIM1, a gene implicated in autosomal dominant cone-rod dystrophy (CORD7). *Genomics* 2003;81:304-314.
141. Moser M, Imhof A, Pscherer A, et al. Cloning and characterization of a second AP-2 transcription factor: AP-2 beta. *Development* 1995;121:2779-2788.
142. Satoda M, Zhao F, Diaz GA, et al. Mutations in TFAP2B cause Char syndrome, a familial form of patent ductus arteriosus. *Nat Genet* 2000;25:42-46.

143. West-Mays JA, Zhang J, Nottoli T, et al. AP-2alpha transcription factor is required for early morphogenesis of the lens vesicle. *Dev Biol* 1999;206:46-62.
144. Hofmann F, Biel M, Kaupp UB. International Union of Pharmacology. XLII. Compendium of voltage-gated ion channels: cyclic nucleotide-modulated channels. *Pharmacological reviews* 2003;55:587-589.
145. Sautter A, Zong X, Hofmann F, Biel M. An isoform of the rod photoreceptor cyclic nucleotide-gated channel beta subunit expressed in olfactory neurons. *Proc Natl Acad Sci U S A* 1998;95:4696-4701.
146. Biel M, Zong X, Ludwig A, Sautter A, Hofmann F. Molecular cloning and expression of the Modulatory subunit of the cyclic nucleotide-gated cation channel. *J Biol Chem* 1996;271:6349-6355.
147. Bhattacharya G, Miller C, Kimberling WJ, Jablonski MM, Cosgrove D. Localization and expression of usherin: a novel basement membrane protein defective in people with Usher's syndrome type IIa. *Hear Res* 2002;163:1-11.
148. Pearsall N, Bhattacharya G, Wisecarver J, Adams J, Cosgrove D, Kimberling W. Usherin expression is highly conserved in mouse and human tissues. *Hear Res* 2002;174:55-63.
149. Reiners J, Nagel-Wolfrum K, Jurgens K, Marker T, Wolfrum U. Molecular basis of human Usher syndrome: deciphering the meshes of the Usher protein network provides insights into the pathomechanisms of the Usher disease. *Exp Eye Res* 2006;83:97-119.
150. van Wijk E, Pennings RJ, te Brinke H, et al. Identification of 51 novel exons of the Usher syndrome type 2A (USH2A) gene that encode

- multiple conserved functional domains and that are mutated in patients with Usher syndrome type II. *Am J Hum Genet* 2004;74:738-744.
151. Gamundi MJ, Hernan I, Maseras M, et al. Sequence variations in the retinal fascin FSCN2 gene in a Spanish population with autosomal dominant retinitis pigmentosa or macular degeneration. *Mol Vis* 2005;11:922-928.
  152. Ziviello C, Simonelli F, Testa F, et al. Molecular genetics of autosomal dominant retinitis pigmentosa (ADRP): a comprehensive study of 43 Italian families. *Journal of medical genetics* 2005;42:e47.
  153. Sullivan LS, Bowne SJ, Birch DG, et al. Prevalence of disease-causing mutations in families with autosomal dominant retinitis pigmentosa: a screen of known genes in 200 families. *Invest Ophthalmol Vis Sci* 2006;47:3052-3064.
  154. Swaroop A, Xu JZ, Pawar H, Jackson A, Skolnick C, Agarwal N. A conserved retina-specific gene encodes a basic motif/leucine zipper domain. *Proc Natl Acad Sci U S A* 1992;89:266-270.
  155. Yoshida S, Mears AJ, Friedman JS, et al. Expression profiling of the developing and mature Nrl<sup>-/-</sup> mouse retina: identification of retinal disease candidates and transcriptional regulatory targets of Nrl. *Hum Mol Genet* 2004;13:1487-1503.
  156. He L, Campbell ML, Srivastava D, et al. Spatial and temporal expression of AP-1 responsive rod photoreceptor genes and bZIP transcription factors during development of the rat retina. *Mol Vis* 1998;4:32.
  157. Kapranov P, Cheng J, Dike S, et al. RNA maps reveal new RNA classes and a possible function for pervasive transcription. *Science* 2007;316:1484-1488.



158. Rebello G, Ramesar R, Vorster A, et al. Apoptosis-inducing signal sequence mutation in carbonic anhydrase IV identified in patients with the RP17 form of retinitis pigmentosa. *Proc Natl Acad Sci U S A* 2004;101:6617-6622.
159. Vervoort R, Lennon A, Bird AC, et al. Mutational hot spot within a new RPGR exon in X-linked retinitis pigmentosa. *Nat Genet* 2000;25:462-466.

# *Acknowledgments*

First of all I would like to thank Dr Sandro Banfi and prof. Valeria Marigo for having welcomed me in their labs and for their theoretical and practical supervision during the past three years and for enabling me to be a part of the amazing RetNet project. I am grateful to Sandro for encouraging me to always learn more and never to give up. I am grateful to Valeria for her enormous enthusiasm which kept me going and gave me strength during the hard times.

I owe my special gratefulness to my external supervisor prof. Shomi Bhattacharya for not only being the best supervisor I could ever wished for but also for being a one in a life time friend. An exclusive thanks if for all the RetNet PIs and fellows for giving me the time of my life during these three years.

I would like to thank the past and present members of Sandro's lab: Antonietta, Tiziana, Raffaella, Silvia, Marianna, Alessandro, Nicola, Ivan for their help and patience for all my errors in Italian and all my "bad" moments and for being great friends. My special thank is to Giovanna for generously sharing her amazing knowledge and for being my constant professional and personal support.

My deepest love and admiration goes to my wonderful parents for making real my every wish, for always believing in me, for their enormous love and for being the guiding light of my life. *Moja najdublja ljubav i divljenje ide mojim divnim roditeljima zato sto su omogucili ostvarenje svake moje zelje, zato sto su uvek verovali u mene, zbog njihove ogromne ljubavi I zato sto su moja zvezda vodilja. Volim vas najvise na svetu!*

To Milan, my other half, I owe all the love and support one could only dream of.

